

THE APPLICATION OF HOLOGRAPHIC INTERFEROMETRY  
TO THE DETERMINATION OF THE FLOW FIELD AROUND  
A RIGHT CIRCULAR CONE AT ANGLE OF ATTACK

By

Ravi Chandar Jagota



# United States Naval Postgraduate School



## THESIS

THE APPLICATION OF HOLOGRAPHIC INTERFEROMETRY  
TO THE DETERMINATION OF THE FLOW FIELD AROUND  
A RIGHT CIRCULAR CONE AT ANGLE OF ATTACK

by

Ravi Chandar Jagota

December 1970

*This document has been approved for public release and sale; its distribution is unlimited.*

T137682



The Application of Holographic Interferometry  
to the Determination of the Flow Field Around  
a Right Circular Cone at Angle of Attack

by

Ravi Chandar Jagota  
Lieutenant Commander, Indian Navy

Submitted in partial fulfillment of the  
requirements for the degree of

AERONAUTICAL ENGINEER

from the  
NAVAL POSTGRADUATE SCHOOL  
December 1970



## ABSTRACT

The successful application of holography to the study of three dimensional flow fields due to phase objects has been reported in the literature. The present report extends this technique to the study of density fields around opaque bodies as would normally be encountered in wind tunnel experiments. The density field around a 10 degree half-angle cone at zero and ten degree angle of attack has been investigated in the Naval Postgraduate School supersonic wind tunnel. In these experiments, the finite fringe method for the production of interferograms has, for the first time, been applied to holographic interferometry. The density field obtained from the reduction of the interferograms was found to agree with that obtained from an analytical solution of the governing equations as reported by D. J. Jones in Reference 1. The computer program used for the reduction of the interferograms has been evaluated for the effect of the presence of the cone and the shock wave and has been found to yield stable and accurate results.





## TABLE OF CONTENTS

I.	INTRODUCTION -----	5
II.	EXPERIMENTAL APPARATUS -----	9
	A. THE WIND TUNNEL -----	9
	B. THE EXPERIMENTAL SETUP FOR PRESSURE MEASUREMENT -----	10
	C. THE HOLOGRAPHIC ARRANGEMENT -----	10
	D. THE WIND TUNNEL MODEL -----	12
III.	THEORETICAL CONSIDERATIONS -----	14
	A. EVALUATION OF THE DENSITY FROM HOLOGRAPHIC INTERFEROGRAMS -----	14
	1. The Basic Equation of Interferometry ----	14
	2. The Integral Inversion -----	16
	3. The Numerical Procedure -----	19
	B. THE FLOW AROUND A RIGHT CIRCULAR CONE -----	21
	1. Axisymmetric Case -----	21
	2. Flow Around Cones with Small Yaw -----	25
IV.	DESCRIPTION OF THE EXPERIMENT -----	27
	A. NUMERICAL SIMULATION OF THE EXPERIMENT -----	27
	B. EXPERIMENTAL PROCEDURE -----	28
	1. Laboratory Techniques -----	28
	2. Photographic Techniques -----	30
	3. Data Reduction -----	31
V.	EXPERIMENTAL RESULTS AND DISCUSSION -----	34
	A. DENSITY FIELD OBTAINED EXPERIMENTALLY -----	34



1. Computer Simulation Results -----	34
2. Experimental Results -----	35
B. ERROR ANALYSIS -----	37
VI. SUMMARY -----	39
A. CONCLUSIONS -----	39
B. ACKNOWLEDGEMENTS -----	39
APPENDIX A: REDUCTION OF AN INTERFEROGRAM TO OBTAIN FRINGE SHIFTS -----	83
APPENDIX B: DESCRIPTION OF COMPUTER PROGRAM "HOLOFER" -----	86
APPENDIX C: COMPUTER PROGRAMS USED FOR INTERPOLATION -----	137
A. COMPUTER PROGRAM 1 -----	137
B. COMPUTER PROGRAM 2 -----	141
BIBLIOGRAPHY -----	146
INITIAL DISTRIBUTION LIST -----	148
FORM DD 1473 -----	149



## I. INTRODUCTION

For over three decades, the Mach-Zehnder interferometer has been widely used and has come to be accepted as a standard tool for the measurement of the flow field around bodies. Until the advent of the laser, its use required extreme stability from vibrations and precision optical components. Even with a laser as a light source, the resulting interferograms are purely two-dimensional in nature in that they provide fringe information for only one direction of view through the wind tunnel. Furthermore, due to the limit imposed by existing camera shutter speeds, the interferogram obtained does not truly represent the instantaneous flow field around the body but rather is an average over the interval of shutter opening.

The advent of holography together with the development of the high power Q-switched laser has introduced a new dimension in the field of flow measurement. Apart from removing the need for precision optical quality components in the case of double exposed holograms, the use of holography has, for the first time, enabled a three-dimensional view of the flow field to be obtained from a single hologram. The high power of the laser and the Q-switch mechanism have together enabled film exposure times in the region of 20 nano-seconds to be attained thus, in effect, "freezing" the flow during the hologram production process.



Techniques for the application of holography to interferometry have been reported in Reference 1 (Heflinger et al, 1966) and in Reference 2 (Brooks et al, 1966). Holographic interferometry has been used to determine the three-dimensional asymmetric field produced by free-jet flow (Reference 3). In this report, a series of holograms placed in a 90 degree sector around the jet were obtained simultaneously from a single exposure. Interferograms were then obtained from the holograms at suitable angular orientations within a 90 degree field of view. This provided sufficient information to determine the entire flow field since the jet was planar symmetric. Reduction of the fringe data to density information was accomplished by expressing the density in a series of orthogonal polynomials and inverting the fringe-density integral equation by a computer program using a scheme reported in References 4 and 5.

In the present report, the applicability of holography interferometry has been extended to those three-dimensional density fields produced by opaque bodies as would be encountered in wind tunnel experiments. The experiments were conducted in the Naval Postgraduate School supersonic blowdown wind tunnel at a Mach number of 2.8 using a ten degree half-angle cone at zero and ten degrees angle of attack. In this case, the multiple hologram technique was not employed. Since the flow fields investigated were steady, the procedure adopted was to obtain holograms to cover various sectors of the flow field by rotating the cone within





the wind tunnel, this being a method that would be fully applicable to any conventional wind tunnel setup.

Whereas in an infinite fringe field, the fringe information is obtained in a discontinuous manner, that is, at the points of maxima and minima, the interferogram from a finite fringe field can be evaluated at any desired point quite readily. This is of particular significance in the case of density fields where the variations in density are small. In the present case, the total variation in fringe number was generally in the region of only one to two fringes. The finite fringe method was also selected since it is less sensitive to vibrations than is the infinite fringe field, a problem encountered in Reference 3. The finite fringe field was produced by a translation of the diffusing screen in the scene beam a distance of between .0025" and .0030" between the two exposures of the hologram. A vertical fringe field, obtained by horizontal translation of the diffuser, was chosen in spite of the greater effort required to reduce the interferograms at a particular section owing to the greater uniformity and clarity of the fringes thus obtained as compared to horizontal fringes. Fringe data obtained from the interferograms was reduced to density using the same computer program as used in Reference 3. The density field obtained experimentally was compared with the analytical solution reported in Reference 6, interpolating the results therein for the actual mach number of the experiments. Good correlation was achieved, thus demonstrating



the utility of holographic interferometry for normal wind tunnel experimentation.



## II. EXPERIMENTAL APPARATUS

### A. THE WIND TUNNEL

This investigation was conducted in the Naval Postgraduate School blow-down supersonic wind tunnel. The wind tunnel is a blowdown-to-atmosphere facility which has a test section 4 inches by 4 inches in cross-section and 6 inches in length. Interchangeable nozzles are available for producing nominal test section mach numbers of 4.0, 2.8, and 1.7. The nominal run time is 5 minutes at a mach number of 2.8 with a maximum stagnation pressure of about 105 pounds per square inch. For this series of experiments, the side walls of the wind tunnel were replaced by plexiglas walls two inches thick having a refractive index of 1.49 so that a complete view of the flow in the test section could be obtained.

### B. THE EXPERIMENTAL SETUP FOR PRESSURE MEASUREMENT

Figure 1 is a schematic representation of the equipment arrangement used for pressure measurement. The static pressures on 16 out of a total of 30 orifices on the surface of the cone were measured by a Scanivalve (Model 48J4-1065 with a 0-10 psia. transducer) which was calibrated in inches of mercury vacuum. The measurements were recorded on a Honeywell 2106 twelve channel Viscicorder. The scanivalve was capable of scanning 15 ports per second. Photographs of the experimental setup are provided in Figures 2 and 3. The plexiglas side walls of the wind tunnel with the Scanivalve



mounted on top of the test section are shown in Figure 2. The power supply, control box and Viscicorder can be seen in Figure 3.

### C. THE HOLOGRAPHIC ARRANGEMENT

A schematic of the holographic arrangement employed is shown in Figure 4 and photographs thereof are in Figures 5(a) and 5(b). The equipment was mounted on a table that rested on a portion of the floor that was vibrationally isolated from the rest of the building. The monochromatic light source used was a Korad K-1 pulsed ruby laser operating at a wavelength of 6943 Angstroms together with a Pockels cell Q-switching device. The resulting effective exposure time was about 20 nanoseconds and, with a cavity length of the laser of 37 cms., a coherence length of about 2 cms. was obtained. A side band geometry was employed to obtain the holograms of the flow field around the cone. A diffuse glass in the path of the scene beam was used to produce light field holograms, which because of the diffusion of the direction of the rays in the scene beam, produced an effective field of view in a hologram of approximately 16 degrees. A continuous wave helium-neon laser was used for alignment of the Q-switched laser and the optics. A Lauda constant temperature circulator Model N controlled by an electronic relay type R-10 was used in conjunction with a Culligan de-ionizer to maintain the laser head and output etalon at a constant temperature of 28.4 degrees Centigrade.





In Figure 4, details of the side band geometry employed can be seen. The reference beam was led on top of the wind tunnel by means of the two mirrors M and the size of the beam could be adjusted by means of lenses U. The positions of the diffuser plate and the two grids, one on each of the wind tunnel side walls, are also shown therein. In Figure 5(a), the Korad K-1 laser and the smaller alignment laser are shown together with the arrangement of the optical equipment. The diffuser plate mounted on the precision X-Y slide can also be seen. The holographic table and test section was completely enclosed in a wooden box to enable the experiments to be conducted in the daytime. This is shown in Figure 5(b). Also shown therein are the Korad K-1 laser power supply and shutter control assemblies, the Culligan de-ionizer and the Lauda constant temperature circulator.

In order to be able to view the cone at angle of attack always in a direction perpendicular to its axis when it was rotated in the wind tunnel, it was necessary to construct separate grids for each rotational angle at which the holograms were taken. The front grid used for the 82.5 degree rotational position of the cone is shown in position in Figure 6. The grid lines can be seen to be parallel and perpendicular to the cone axis for this particular angular position. The orientation of the grids was designed to be at the correct angle for the particular rotational position of the cone. Since, on rotation, the axis of the cone was not in a vertical plane, it was necessary to offset the two



grids with respect to each other in such a manner that on lining up the grids, the correct viewing position perpendicular to the cone axis was automatically obtained. The method of obtaining the orientations and the relative offset of the grids is shown in Figures 7(a) and 7(b). Since the cone spindle was bent at a distance of 0.7 inches from the base of the cone, the various rotational positions of the cone tip are indicated in the end view in Figure 7(a). The corresponding positions of the cone axis in the side and bottom views are also shown therein. The orientation of the grid lines for each rotational position of the cone as shown in Figure 7(b) were obtained from the positions of the cone axis in the side view for each particular case. In order to be normal to the cone axis, lines perpendicular to the orientation of the cone axis in the bottom view were transcribed, each of these representing a line of sight. Since the distance between the grids was  $7 \frac{7}{8}$  inches, the necessary amount by which the two grids were required to be offset for each rotational position of the cone tip were obtained as shown in Figure 7(b).

#### D. THE WIND TUNNEL MODEL

The cone model used is shown in Figure 8. The 10 degree semi-apex angle cone model was fabricated out of stainless steel and had pressure ports at three cross-sections, the angular position of the ports being so arranged as to lie on a ray from the apex of the cone. Since a fixed mount was



employed, provision was made to attach the cone to spindles bent to various angles to achieve the desired angle of attack. Stainless steel tubing of .036 inches internal diameter was used from the static pressure orifices on the surface of the cone up to the base of the model, the diameter of this being adequate to provide sufficient time response of the Scanivalve. Any fifteen out of the thirty ports could be connected at a time to the Scanivalve through the hollow cone spindle and mount, this restriction being imposed by the internal diameter of the spindle.

Rotation of the model about the horizontal axis of the spindle necessitated drilling 4 holes on each side of the wind tunnel side walls through which the model spindle could be unlocked from the mount and rotated. The plexiglas side walls of the test section and the holes therein can be seen in Figure 6. The collar on the model spindle containing radial holes (also visible in the figure) was used to rotate the cone by means of a spike arrangement inserted through one of the holes in the tunnel side walls. The angle of rotation was established by lining up graduations on the spindle sleeve with a graduation on the mount. The model and spindle used for the axisymmetric case can be seen in Figure 9. The pressure ports at the three stations and one of the pressure tubes from the cone passing through the hollow spindle are visible in the photograph. After the spindle was screwed into the cone, it was locked in position by means of the setscrew shown.



### III. THEORETICAL CONSIDERATIONS

#### A. EVALUATION OF THE DENSITY FROM HOLOGRAPHIC INTERFEROGRAMS

##### 1. The Basic Equation of Interferometry

The interferometry principle is based on the fact that two originally coherent rays of light will reinforce or annul each other at a screen on which both rays are projected depending on their relative phase there. The phase difference is directly a function of the difference in the lengths of the optical paths traversed by the two rays. If the optical path is changed by an amount  $N\lambda$ , where  $\lambda$  is the wavelength of the light and  $N$  is an integer, then the order of interference changes by an amount  $N$ , that is, a shift of  $N$  fringes occurs. The change in optical path can be related to the density through the index of refraction and the Gladstone-Dale constant. If the speed of light in a medium is represented by  $\frac{c_0}{n}$  where  $c_0$  is the speed of light in vacuum and  $n$  is the index of refraction, the additional time required to traverse the test section due to a change in the index of refraction from  $n_1$  to  $n_2$  can be calculated to be equal to  $\Delta t = \frac{L}{c_0}(n_2 - n_1)$  and thus the change in optical path obtained is  $c_0 \Delta t$ , that is,  $L(n_2 - n_1)$ . The fringe shift,  $g$ , which is equal to  $\frac{\Delta L}{\lambda}$  is thus given by  $\frac{L(n_2 - n_1)}{\lambda}$ .

For a given substance and for a given wavelength of light, the index of refraction is a function of density. In the case of gases, since the speed of light varies only slightly





from that in vacuum, it can be represented very accurately by the first two terms of the Taylor series:

$$n = 1 + \beta \frac{\rho}{\rho_s} \quad (1)$$

where

$\rho_s$  = reference density at 0°C, 760 mm. Hg.

$\beta$  = dimensionless constant related to the Gladstone-Dale constant by:

$$K = \frac{\beta}{\rho_s}$$

The value of  $\beta$  for air at  $\lambda = 5893$  Angstroms is 0.000292, the variation with wavelength being small. The fringe shift relation for a fixed difference in index of refraction between the two beams becomes:

$$g = \beta \frac{L}{\lambda} \left( \frac{\rho_2 - \rho_\infty}{\rho_s} \right) \quad (2)$$

If the density is variable in the test section, the net change in optical path is the integrated effect along the ray which gives the relationship:

$$g = \frac{\beta}{\lambda \rho_s} \int_0^L (\rho - \rho_\infty) ds = Q \int_0^L f(x, y, z_c) ds \quad (3)$$

where

$$f(x, y, z_c) = \frac{\rho(x, y, z_c)}{\rho_\infty} - 1 \quad (4)$$

$$Q = \frac{\beta \rho_\infty}{\lambda \rho_s} \quad (5)$$



$ds$  = incremental distance along a ray

$z_c$  = a plane of constant  $z$ .

Equation (3) is the basic equation which has to be inverted to obtain the unknown density from the known fringe shift values obtained from an interferogram.

## 2. The Integral Inversion

The integral inversion method used was first reported by C. D. Maldonado et al in 1965 (1965; Olsen, 1968) and subsequently used by R. D. Matulka (Reference 3) to calculate the density variation in an asymmetric free jet from the fringe numbers obtained from holographic interferograms. The procedure involves the representation of the function  $f(x, y, z_c)$  by a complete set of orthogonal functions, with the unknown coefficients being evaluated by use of the orthogonality relationship between the set of functions. The set of functions employed have a region of orthogonality that covers the entire plane and have the property that they are "invariant in form" to a rotation of the co-ordinate system. The co-ordinate system used for the inversion is shown in Figure 10 where  $X$  and  $Y$  represent fixed laboratory co-ordinates and  $X'$  and  $Y'$  the co-ordinates in which the fringe number function is defined. These co-ordinates, therefore, rotate with respect to the fixed co-ordinates  $X$  and  $Y$  as the angle of view through the test section is varied.

In operator form, equation (3) can be represented as:

$$g(\xi, \eta', z_c) = T f(x, y, z_c) \quad (6)$$



and the object of the procedure is to evaluate  $f$ , that is, to obtain:

$$f(x, y, z_c) = T^{-1} g(\xi, \eta', z_c) \quad (7)$$

where  $T^{-1}$  represents the inverse of  $T$ .

This inversion is achieved by utilizing a pair of orthogonal polynomials  $U_{m+2k}^{\pm m}(\alpha x, \alpha y)$  and  $H_{m+2k}(\alpha y')$  which are related by the transform relationship:

$$T\{U_{2k}(\alpha x, \alpha y) e^{-\alpha^2 x'^2}\} = \frac{e^{\pm i m \xi}}{[k!(m+k)!]^{\frac{1}{2}}} \frac{1}{2^{m+2k}} H_{m+2k}(\alpha y') \quad (8)$$

where:

$$H_{m+2k}(\alpha y') = e^{\alpha^2 y'^2} [d^{2k} d(\alpha x)^{2k}] [e^{-\alpha^2 y'^2} H_m(\alpha y')] \quad (9)$$

and  $H_m$  are the Hermite polynomials.

The function  $f(x, y, z_c)$  is first expanded in a series of the polynomials  $U_{m+2k}$  as:

$$f(x, y, z_c) = \sum_{m=0}^{\infty} \sum_{k=0}^{\infty} \epsilon_m C_{m+2k}^{\pm m}(\alpha) U_{m+2k}^{\pm m}(\alpha x, \alpha y) e^{-(\alpha^2 x'^2 + \alpha^2 y'^2)} \quad (10)$$

where  $\epsilon_m = \frac{1}{2}$  for  $m = 0$  and 1 for  $m = 1, 2, 3, \dots$ ,  $\alpha$  is an arbitrary scale factor, and  $C_{m+2k}^{\pm m}$  are the unknown expansion coefficients. In order to evaluate these coefficients, an expression for the function  $g(\xi, \eta', z_c)$  is obtained in terms of the polynomials by transforming  $f(x, y, z_c)$  in accordance with equation (6). Using the transform relation given by equation (8), the following expression is obtained:



$$g(\xi, y' z_c) = \sum_{n=0}^{\infty} \sum_{k=0}^{\infty} \epsilon_n [k! (m+k)! 2^{2(m+2k)}]^{-\frac{1}{2}} \left[ C_{m+2k}^{\pm m}(\alpha) e^{\pm i m \xi} H_{m+2k}(\alpha y') e^{-\alpha^2 y'^2} \right] \quad (11)$$

The expansion coefficients can then be evaluated by applying the following orthogonality relationship to Equation (11):

$$\int_{-\pi}^{\pi} e^{\pm i m \xi} e^{\mp i m \xi} d\xi \int_{-\infty}^{\infty} H_{m+2k}(\alpha y') H_{n+2l}(\alpha y') e^{-\alpha^2 y'^2} dy' = \frac{2\pi}{\alpha} \left[ (m+2k)! (n+2l)! 2^{m+2k} 2^{n+2l} \delta_{mn} \delta_{m+2k, n+2l} \right] e^{\mp i m \xi} H_{m+2k}(\alpha y') \quad (12)$$

that is, by taking the scalar product of equation (11) with  $e^{\mp i m \xi} H_{m+2k}(\alpha y')$  and using equation (12), the coefficients of the series in equation (10) are obtained as:

$$C_{m+2k}^{\pm m}(\alpha) = \frac{\alpha}{2\pi} \int_{-\pi}^{\pi} \left[ \frac{k! (m+k)!}{(m+2k)!} \right]^{\frac{1}{2}} \int_{-\infty}^{\infty} g(y', \xi, z_c) H_{m+2k}(\alpha y') e^{\mp i m \xi} dy' d\xi \quad (13)$$

Substitution of equation (13) into equation (10) results

in the density variation being given by:

$$f(x, y, z_c) = \left( \frac{\alpha}{\pi} \right)^2 \sum_{n=0}^{\infty} \sum_{k=0}^{\infty} \epsilon_n \left[ \frac{k! (m+k)!}{(m+2k)!} \right]^{\frac{1}{2}} e^{-(\alpha^2 z^2 + \alpha^2 y^2)} \cdot \text{Real} \left[ \int_{-\pi}^{\pi} \int_{-\infty}^{\infty} g(y', \xi, z_c) e^{-i m \xi} H_{m+2k}(\alpha y') dy' d\xi \right] U_{m+2k}^m(\alpha x, \alpha y) \quad (14)$$

The functions  $U_{m+2k}^{\pm m}$  employed are complex polynomials

defined as:

$$U_{m+2k}^{\pm m}(\alpha x', \alpha y') = (-1)^k \left( \frac{\alpha}{\pi} \right)^{\frac{1}{2}} \left( \frac{k!}{(m+2k)!} \right)^{\frac{1}{2}} \left[ \alpha^2 (x'^2 + y'^2) \right]^{\frac{m}{2}} e^{\pm i m \phi} L_k^m \left[ \alpha^2 (x'^2 + y'^2) \right] \quad (15)$$





where  $\phi = \tan^{-1} \frac{y'}{x}$  and  $L_k^m$  are the Associated Laguerre polynomials:

$$L_k^m(\alpha^2 x^2 + \alpha^2 y^2) = \sum_{s=0}^m \frac{(m+k)!}{(k-s)!(m+s)!s!} [(-1)^s (\alpha^2 x^2 + \alpha^2 y^2)]^s \quad (16)$$

Substitution of equation (15) into equation (14) yields:

$$f(x, y, z_c) = \left(\frac{\alpha}{\pi}\right)^2 \sum_{m=0}^{\infty} \sum_{k=0}^{\infty} \frac{\epsilon_m (-1)^k k!}{(m+2k)!} (\alpha^2 x^2 + \alpha^2 y^2)^{m/2} L_k^m(\alpha^2 x^2 + \alpha^2 y^2) \cdot$$

$$\left[ B_{m+2k}^m(\alpha) \cos(m\phi) + D_{m+2k}^m(\alpha) \sin(m\phi) \right] e^{-(\alpha^2 x^2 + \alpha^2 y^2)} \quad (17)$$

where:

$$B_{m+2k}^m(\alpha) = \int_{-\pi}^{\pi} \int_{-\infty}^{\infty} g(y', \xi, z_c) \cos(m\xi) H_{m+2k}^{(\alpha y')} dy' d\xi \quad (18)$$

$$D_{m+2k}^m(\alpha) = \int_{-\pi}^{\pi} \int_{-\infty}^{\infty} g(y', \xi, z_c) \sin(m\xi) H_{m+2k}^{(\alpha y')} dy' d\xi \quad (19)$$

Equations (17), (18), and (19) are the basic equations used to obtain the density distribution of a completely asymmetric flow field.

### 3. The Numerical Procedure

The calculation of the unknown coefficients  $B_{m+2k}^m(\alpha)$  and  $D_{m+2k}^m(\alpha)$  in the series representation of  $f(x, y, z_c)$  as given by equation (17) is not analytically possible in general since the function  $g(y', \xi, z_c)$  representing the variation of fringe number is an experimentally measured quantity and thus not explicitly given as a function of the co-ordinates of a field point. If the analytical procedure is to be used to obtain the density from experimental observations of the fringe numbers, therefore, it is necessary to evaluate



the double integrals in equations (18) and (19) numerically. This is achieved by first noting that for every  $g(y', \xi, z_c)$  encountered experimentally, there is a circular domain outside which the fringe distribution is zero so that it is possible to replace the limits of integration of  $+\infty$  and  $-\infty$  in equations (18) and (19) by finite values. The function  $g(y', \xi, z_c)$  is then approximated by constant step values over elemental areas into which the domain is partitioned. This results in the B and D coefficients being represented by the double series:

$$B_{m+2k}^m(\alpha) = \sum_{i=0}^{I-1} \sum_{j=0}^{J-1} g(\xi_j + \Delta \xi_j, x_i + \Delta x_i) \int_{\xi_j}^{\xi_j + \Delta \xi_j} \cos(m\xi) d\xi \int_{x_i}^{x_i + \Delta x_i} H_{m+2k}(\alpha x) dx \quad (20)$$

and

$$D_{m+2k}^m(\alpha) = \sum_{i=0}^{I-1} \sum_{j=0}^{J-1} g(\xi_j + \Delta \xi_j, x_i + \Delta x_i) \int_{\xi_j}^{\xi_j + \Delta \xi_j} \sin(m\xi) d\xi \int_{x_i}^{x_i + \Delta x_i} H_{m+2k}(\alpha x) dx \quad (21)$$

Using the derivative formula for Hermite polynomials, the following equations result:

$$B_{m+2k}^m(\alpha) = \left[ \frac{1}{2\alpha m} (m+2k+1) \right] \sum_{i=0}^{I-1} \sum_{j=0}^{J-1} g(\xi_j + \Delta \xi_j, x_i + \Delta x_i) \cdot \left[ \sin(m\xi_{j+1}) - \sin(m\xi_j) \right] \cdot \left[ H_{m+2k+1}(\alpha x_{i+1}) - H_{m+2k+1}(\alpha x_i) \right] \quad (22)$$

$$D_{m+2k}^m(\alpha) = - \left[ \frac{1}{2\alpha m} (m+2k+1) \right] \sum_{i=0}^{I-1} \sum_{j=0}^{J-1} g(\xi_j + \Delta \xi_j, x_i + \Delta x_i) \cdot \left[ \cos(m\xi_{j+1}) - \cos(m\xi_j) \right] \cdot \left[ H_{m+2k+1}(\alpha x_{i+1}) - H_{m+2k+1}(\alpha x_i) \right] \quad (23)$$



Since it is not possible to sum over an infinite number of terms, equation (17) is replaced by the sum of a finite series:

$$f(x, y, z_c) = \left(\frac{\alpha}{\pi}\right)^2 \sum_{k=0}^K \sum_{m=0}^M \epsilon_m^{(-1)^k} \left[ \frac{k!}{(m+2k)!} \right] (\alpha^2 x^2 + \alpha^2 y^2) L_K^m(\alpha^2 x^2 + \alpha^2 y^2) \\ \cdot \left[ B_{m+2k}^m(\alpha) \cos(m\phi) + D_{m+2k}(\alpha) \sin(m\phi) \right] e^{-(\alpha^2 x^2 + \alpha^2 y^2)} \quad (24)$$

The accuracy of the representation depends on the values of K, M,  $\Delta\xi$  and  $\Delta x$  chosen and convergence of the series is influenced by the parameter  $\alpha$ .

## B. THE FLOW AROUND A RIGHT CIRCULAR CONE

### 1. Axisymmetric Case

The problem of the supersonic flow around a cone has been extensively studied by several investigators ever since it was first opened up by Busemann, Bourquard and Taylor and Maccoll. The basic approach to the problem is outlined below but a detailed description may be found in References 12, 13, 14 and 17.

Starting with the equations of motion of inviscid flow in three dimensions expressed in spherical co-ordinates:

$$\left. \begin{aligned} u \frac{\partial u}{\partial r} + \frac{v}{r} \frac{\partial u}{\partial \theta} + \frac{\omega}{r \sin \theta} \frac{\partial u}{\partial \phi} + \frac{1}{r} \frac{\partial p}{\partial r} - \frac{v^2 + \omega^2}{r} &= 0 \\ u \frac{\partial v}{\partial r} + \frac{v}{r} \frac{\partial v}{\partial \theta} + \frac{\omega}{r \sin \theta} \frac{\partial v}{\partial \phi} + \frac{1}{r} \frac{\partial p}{\partial \theta} + \frac{uv - \omega^2 \cot \theta}{r} &= 0 \\ u \frac{\partial \omega}{\partial r} + \frac{v}{r} \frac{\partial \omega}{\partial \theta} + \frac{\omega}{r \sin \theta} \frac{\partial \omega}{\partial \phi} + \frac{1}{r \sin \theta} \frac{\partial p}{\partial \phi} + \frac{u\omega + v\omega \cot \theta}{r} &= 0 \end{aligned} \right\} \quad (1)$$



and the equation of continuity:

$$\frac{d}{dr} (r r^2 u \sin \theta) + \frac{d}{d\theta} (r r v \sin \theta) + \frac{d}{d\phi} (r r w) = 0 \quad (2)$$

the cylindrical symmetry of the cone allows one to eliminate the velocity component  $w$  and all terms dependant on  $\phi$ . In addition, application of the condition that the flow be conical, that is, no variation of the flow parameters with  $r$ , reduces equations (1) to:

$$\left. \begin{aligned} \frac{du}{d\theta} - v &= 0 \\ \frac{dv}{d\theta} + u + \frac{1}{f v} \frac{df}{d\theta} &= 0 \end{aligned} \right\} \quad (3)$$

the first of these equations asserting that the flow must be irrotational. The equation of continuity similarly reduces to:

$$\frac{d}{d\theta} (f v \sin \theta) + 2 f u \sin \theta = 0 \quad (4)$$

Elimination of  $v$  between (3) and (4) yields:

$$\left\{ \frac{d^2 u}{d\theta^2} + u \right\} \frac{du}{d\theta} + \frac{1}{f} \frac{df}{d\theta} = 0 \quad (5)$$

Setting:

$$\frac{df}{d\theta} = \frac{df}{d\psi} \cdot \frac{d\psi}{d\theta} = a^2 \frac{d\psi}{d\theta} \quad (6)$$

the following ordinary differential equation is obtained:

$$\frac{d^2 u}{d\theta^2} + u = \frac{a^2 (u + v \cot \theta)}{(v^2 - a^2)} \quad (7)$$





From the Bernoulli equation:

$$\int \frac{d\rho}{\rho} + \frac{1}{2} (u^2 + v^2) = \frac{1}{2} c^2 \quad (8)$$

and with assumption of a perfect gas satisfying the equation:

$$\frac{p}{\rho^\gamma} = k \quad (9)$$

the velocity of sound  $a$  can be expressed in terms of the velocity components as:

$$a^2 = \frac{1}{2} (\gamma - 1) (c^2 - u^2 - v^2) \quad (10)$$

The density, pressure and temperature are then found to vary as:

$$\begin{aligned} (a) \quad \frac{\rho}{\rho_0} &= (c^2 - u^2 - v^2)^{\frac{\gamma}{\gamma-1}} \\ (b) \quad \frac{p}{p_0} &= \left( \frac{\rho}{\rho_0} \right)^{\frac{1}{\gamma}} = (c^2 - u^2 - v^2)^{\frac{1}{\gamma-1}} \\ (c) \quad \frac{T}{T_0} &= \left( \frac{a}{a_0} \right)^2 = (c^2 - u^2 - v^2) \end{aligned} \quad (11)$$

For the solution of the governing equation (7) to be physically meaningful, it is necessary to satisfy the boundary condition of no normal velocity at the cone surface and the jump conditions at the shock wave. The physical conditions on either side of a shock wave are given by the Rankine Hugoniot relations:

$$\left. \begin{aligned} \cos^2 \alpha &= \frac{(\gamma-1) + (\gamma+1) \left( \frac{x}{y} \right)}{2\gamma \left( \frac{U}{a_1} \right)^2} \\ \tan \beta &= \frac{(\gamma-1) + (\gamma+1) \left( \frac{x}{y} \right)}{(\gamma-1) \left( \frac{x}{y} \right) + (\gamma+1)} \\ \left( \frac{x}{y} \right)^{\frac{\gamma-1}{\gamma}} &= 1 + \frac{\gamma-1}{4\gamma \cos^2 \beta} \left\{ (\gamma-1) + (\gamma+1) \left( \frac{y}{x} \right) \right\} \end{aligned} \right\} \quad (12)$$



where, referring to Figure 11,

$\alpha$  = Angle between the normal to the shock wave and the streamlines in front of it.

$\beta$  = Angle between the normal to the shock wave and the streamlines immediately behind it.

$\phi$  = Angle between the streamline at any point and the radius vector from the vertex of the cone.

$U$  = Freestream velocity.

$a$  = Velocity of sound in the freestream.

$$\frac{x}{y} = p_w/p_1$$

$$\frac{x}{z} = p_w/p_o$$

$p_1$  = Pressure of the undisturbed gas in front of the shock wave.

$p_w$  = Pressure immediately behind the shock wave.

$p_o$  = Stagnation pressure behind the shock wave.

The boundary condition at the shock wave thus reduces to the requirement that the ratio  $(x/z)$  defined by the Rankine Hugoniot relations be equal to the pressure ratio  $(p/p_o)$  defined by equation (11a). This together with equations (12) defines the physical characteristics of the shock wave.

Many schemes have been employed in order to numerically integrate the governing differential equation and to satisfy the boundary conditions to yield the complete solution of the flow field. Results of some of these are tabulated in References 6 and 14. For the purposes of this report, the more recent results in Reference 6 have been used.



## 2. Flow Around Cones with Small Yaw

The governing differential equation for the flow around a yawed cone is developed on similar lines as that for axisymmetric flow with the difference that in this case, the velocity components, pressure and density are expressed as a series representation about the axial flow values. A detailed description of the procedure may be found in References 13, 15 and 17. An examination of the results reveals that although the flow is no longer irrotational, the flow field can still be regarded as conical. Furthermore, the shock wave in this case is still a cone of the same semi-apex angle as in the no-yaw case with the difference that the shock wave is itself yawed at an angle which is proportional to the angle of yaw of the cone with respect to the freestream.

In Reference 6, the method employed to obtain the flow properties is basically one of iteration. An estimate is made of the shape of the shock wave and this shape is improved in such a way that the normal velocity at the surface of the cone is made close to zero. The results are presented in the co-ordinate system shown in Figure 12. Values of  $u$ ,  $v$ ,  $w$ ,  $\frac{\rho}{\rho_{\infty}}$ , and  $p$  at various azimuthal angles  $\phi$  are given for various non-dimensional distances between the body and the shock wave. Such results are tabulated for cones of different half-cone angles, Mach number and angle of attack at which the flow can no longer be considered conical. For the case of a 10 degree half-angle cone,



this limiting angle of attack is 10 degrees at a Mach number of 3.0 and 11 degrees at a Mach number of 2.0.





#### IV. DESCRIPTION OF THE EXPERIMENT

##### A. NUMERICAL SIMULATION OF THE EXPERIMENT

The suitability of the computer program HOLOFER for handling cases with discontinuities in slope had been investigated by means of various test function inputs into the program in Reference 3. The accuracy of the inversion in these cases was reported to be within 3.8 percent. In order to verify the applicability of the program to the present investigation, known values of the density along one line of sight, obtained from Reference 6 at a particular cross-section in the flow, were fed in as input and Mode 1 operation of the computer program utilized. In this mode, the program calculates the fringe number array that would result from the specified density distribution and then uses this data as the input for inversion to obtain the density distribution. One of the primary objectives of this investigation was to determine the effect of opaque objects introduced into the flow field and the presence of the shock wave on the resulting inversion. It was found that the effect of the presence of the cone could be reduced by the introduction of a fictitious density distribution in the area occupied by it of a constant value equal to the density at the cone surface.



## B. EXPERIMENTAL PROCEDURE

### 1. Laboratory Techniques

It has been shown in Reference 10 that the transmitted intensity from a diffuse glass falls off below 30 percent of the incident intensity beyond viewing angles of  $\pm 8$  degrees. Thus this represents a limit on the field of view obtainable from a single hologram. For the flow around a right circular cone at incidence, there is planar symmetry and hence a 90 degree field of view is required for complete coverage of the total flow field. This coverage can be obtained by the simultaneous production of a number of holograms in various azimuthal positions as employed in Reference 3 or by a rotation of the viewing angle between each production of a single hologram. Taking advantage of the steadiness of the flow fields investigated, holograms covering various sectors of the flow field were obtained by rotating the cone to six positions in a 90 degree sector, one hologram being obtained in each case.

Complete angular coverage of the flow field was obtained by a rotation of the cone and spindle arrangement in the mount by an angle of 15 degrees between each hologram. Since it was desired to obtain the flow field at the same cross-section for the various angles of rotation, it was necessary to obtain the holographic interferograms in such a way that the line of sight was always perpendicular to the axis of the cone. For this purpose, a pair of grids were used, one on each wall of the test section, in which



the lines were designed to be parallel and perpendicular to the cone axis for a particular rotational position of the cone. The two grids were offset laterally with respect to each other in order to account for the rotation of the cone axis away from the central plane when the cone was rotated. On production of the holograms, the variable viewing property of light field holograms was utilized to line up the two grids thereby ensuring that the line of sight was normal to the axis of the cone. This would have involved a considerable amount of complexity and effort if a conventional Mach-Zehnder interferometer had been employed for the same purpose.

Since the coherence length of the pulsed laser was only about 2 cms. at the output used, it was necessary to maintain the optical path lengths in the reference and scene beams nearly equal. Since the scene beam path traversed 4 inches of plexiglas while the reference beam passed through two thick plano-convex lenses, it was necessary to compensate for this by making the reference beam path 3.5 inches longer than that of the scene beam. A reference to scene beam ratio of 4:1 was found to yield good holograms.

The holograms were obtained on Agfa-Gevaert 8E-75 holographic plates, 4" x 4" in size. Development was for 5 minutes in Kodak D-19 developer, thirty seconds in an acetic acid stop bath of standard dilution, five minutes in standard fixer, one minute water wash followed by immersion in a Kodak PhotoFlo wetting agent prior to drying. Reconstruction



of the scene was achieved by illuminating the hologram with the light from a helium-neon laser operating at a wavelength of 6328 Angstroms.

## 2. Photographic Techniques

To obtain reconstruction of the image from the hologram, various methods can be employed. In the usual method where the hologram is re-illuminated by a beam similar to the original reference beam as shown in Figure 13, each point on the photograph is produced by a series of non-parallel rays that appear to originate from various sources on the diffuse glass that was used to construct the hologram. An almost parallel set of rays can be selected by the positioning of a small aperture at the focal plane of the imaging lens as shown in Figure 14. A similar effect is achieved by illuminating the hologram by a conjugate beam of small diameter as depicted in Figure 15. Because of the small diameter of the reconstruction beam, the illuminated portion of the hologram represents a small aperture and thus the image produced has a large depth of field. This was of considerable advantage in the production of the interferograms from the holograms since it enabled the front and rear grids, the cone and the fringes to be simultaneously projected on a screen and thus made the task of obtaining the correct viewing angle and the interferogram quite easy to achieve. A photograph of the scene was obtained by focusing the camera at the desired plane in the test section, usually in such a manner so as to be in the plane of the fringes.





The lines of sight recorded on the photograph in this case represent the almost parallel pencil of rays from the diffuser that pass through the effective aperture in the hologram.

### 3. Data Reduction

To obtain photographic interferograms, the hologram was illuminated by the conjugate reference beam using a continuous wave laser operating at a wavelength of 6328 Angstroms. A camera back with viewingscreen was placed in the position of the real image as shown in Figure 13. By lining up the appropriate horizontal and vertical lines of the front and rear grids, the viewing angle corresponding to the particular line of sight desired was achieved. As the spacing of the lines on each grid was  $\frac{1}{2}$  inch and the two grids were physically  $7 \frac{7}{8}$  inches apart, a viewing angle of  $3^{\circ}38'$  was obtained by lining up a line on one of the grids with the adjacent one on the other. A f7.7 lens with full aperture and an exposure time of 4 seconds was used to obtain workable holograms on Poloroid Type 55 P/N film. The reduction of fringe shift was obtained by projecting the negative in a photoenlarger and by tracing the fringes, the cone surface, the shock wave and the grid line at the desired station at which the reduction was to be performed, on a sheet of paper. Some judgement was usually necessary in locating the centre of the fringes but in general the light fringes were found to be narrower than the dark fringes and a location of the fringes to within  $\pm 0.1$  of the fringe spacing in the freestream could be obtained. The



fringes in the region outside the shock were extended towards the cone surface and the fringe shift read at the points of intersection of the displaced fringes with a number of rays from the cone vertex. The assumption of locally conical flow in the region within two to three fringes on either side of the section was made in order to obtain the fringe displacements at the section from those at the points of intersection of the rays from the cone vertex with the fringes on either side of the section. The distance between the cone tip and the section at which reduction was performed was measured from the projected image and, since the actual distance between these points was known, it was possible to calculate the factor by which the projected image was magnified as compared with its true size. This magnification factor was then used to determine the actual radial distances from the cone axis at which the fringe shifts were obtained. The radius of the inversion circle was selected such that the maximum distance of the shock from the cone axis was at 95 percent of the radius of the inversion circle. From the data so obtained, the radial variation of fringe number was plotted and a smooth curve drawn through the points. The fringe number at 201 equidistant points was then read off from the curve and utilized as the input into the computer program HOLOFER in Mode 3. This mode utilizes raw data taken at the proper interval and directly read into the G array in the program by Subroutine READ. Further details about the use of this computer



program are outlined in Appendix C. For the axisymmetric case, it was necessary to feed in the fringe data along one line of sight only and to obtain the density variation along one radial line. For the asymmetric case, fringe data was fed in along six lines of sight in a 90 degree field of view and the inverted density field obtained along 9 radial lines spanning a 180 degree field of view on one side of the axis of planar symmetry of the flow. A typical reduction of an interferogram to obtain the radial variation of fringe number at a section is shown in Appendix A.



## V. EXPERIMENTAL RESULTS AND DISCUSSION

### A. DENSITY FIELD OBTAINED EXPERIMENTALLY

#### 1. Computer Simulation Results

The density distribution obtained from the AGARD 167 tables for the axisymmetric case was used as a test function in Computer program HOLOFER. The fringe distribution calculated from this density distribution was inverted to obtain the original density distribution. A plot of the original density distribution and that inverted by the program is shown in Figure 16. Since the Mach number for this inversion was 2.84, it was necessary to first interpolate the 13 values obtained from Reference 6 for a Mach number of 2.84, and then to obtain from these, the values at 201 equidistant points along a line of sight within the region of the inversion circle. This was done using Computer Program 1. As a side benefit obtained from a use of this program, the discontinuities in slope in the density distribution at the cone surface that would otherwise have resulted by assuming a constant value in the region occupied by the cone, were eliminated. Various values of K, M and interval size were experimented with to obtain the minimum deviation of the inverted density distribution from the input value in the region close to the shock wave. Increasing the value of K above 500 was found to have little effect on the accuracy, the maximum variation of the inverted density being 1.5





percent of the input density value at the point of inversion. The value of  $\alpha$  was found to affect the total number of terms in the series representation of the B and D coefficients required for convergence within the value of  $\epsilon$  specified. A value of  $K = 2000$ ,  $M = 5$ ,  $\alpha = 2.5$  and an interval size of 0.01 was found to yield the minimum effect of the shock discontinuity.

## 2. Experimental Results

### a. Axisymmetric Case

A photograph of the holographic interferogram obtained is shown in Figure 17(a). The fringe data obtained from a reduction of the two sides of the cone is shown in Figure 17(b). Since the flow was axisymmetric, an average of the two readings was taken and a curve plotted. The values at 201 equidistant points was read off, this being input into Subroutine READ of computer program HOLOFER as the G array. The density distribution obtained from the output of the inversion is shown in Figure 18. Also shown plotted is the density field obtained from the AGARD 167 tables interpolated for a Mach number of 2.84 by computer program 2, this being the Mach number of the tunnel obtained from pressure measurements. The pressure data obtained from the viscidorder is shown in Figure 19. The value of Mach number calculated from these pressure measurements compares favorably with the value obtained in earlier experiments from shadowgraphs of the flow in the tunnel. A comparison of the density distributions from the AGARD tables



and those obtained from the experiment show good agreement, the maximum variation in overall density being 8 percent of the theoretical density value.

b. Asymmetric Case

The views along which holograms were taken for the cone at 10 degrees angle of attack are shown in Figure 20 and photographs of the interferograms obtained are shown in Figures 21 to 26. Except for the 67.5 degree and 82.5 degree angles of view, the perturbation to the flow on the leeward side of the cone was insufficient to enable either the shock position or the fringe displacements on this portion of the flow field to be obtained. The fringe shifts in this region were, therefore, taken as being zero. A comparison of the shock wave position obtained experimentally from the interferograms with that from the AGARD 167 tables interpolated for a Mach number of 2.84 is shown in Figure 27. The fringe data were input into computer program HOLOFER starting with the 82.5 degree fringe distribution in order to be consistent with the plane of symmetry for which that program was written. The resulting density distribution output from the program was along the lines of sight indicated in Figure 28. A comparison of the experimentally obtained radial distributions with those from the AGARD 167 tables interpolated for a Mach number of 2.84 are shown in Figures 29 to 35.



## B. ERROR ANALYSIS

The errors in the final solution are mainly due to errors in the fringe data input into the computer program. One of the major sources of error was due to the difficulty in obtaining the slope of the fringe lines in the freestream to a very high degree of accuracy. From the results of the experiments conducted on a 10 degree half angle cone in Reference 18, it was apparent that the flow in regions close to the tip of the cone would be affected by the boundary layer on the cone whereas sections near the base of the cone would be affected by the wake and expansion of the flow. In order to obtain a flow which was locally nearly conical, it was thus necessary to reduce the interferograms at a section approximately 60 to 70 percent of the cone length downstream of the tip. At this section, however, the shock wave was about 1 inch from the axis of the cone and considering that the fringes in a region about  $\frac{1}{4}$  inch adjacent to the tunnel walls were affected by the boundary layer, this left a region of about  $\frac{3}{4}$  inch in which the fringes of the flow in the freestream were present. It was thus difficult to obtain the slope of the fringes very accurately and it is estimated that errors of approximately  $\pm 1$  mm. in the fringe data along any fringe could have resulted. However, since the fringe data along the section was obtained by interpolation between different fringes at varying radial distances from the cone axis, this would have resulted in a smoothing of the errors to about  $\pm 0.5$  mm. Since the maximum fringe shifts obtained



were in the region of 8 mm., an error of  $\pm 0.5$  mm. corresponds to an error of approximately  $\pm 8$  percent in the magnitudes of the fringe shifts obtained.

The errors between the experimental and theoretical density curves in Figure 18 reflect the above estimates of error quite well. The experimentally obtained density distribution is generally about 5% higher than the theoretical curve and this rises to a maximum of 8% close to the cone surface. Similar errors are apparent in general in Figures 29 to 35. However, in these curves the maximum error is somewhat higher probably due to the fact that reduction was performed at a section closer to the base of the cone than for the axisymmetric case. In so far as the general magnitude of the density is concerned, the experimentally obtained distribution follows the theoretical one fairly well. Except for the density distributions for  $\phi = 0^\circ$  and  $\phi = 22.5^\circ$ , the density starts to rise above the freestream value at a normalized radial distance from the cone axis of about 0.7, then assumes a nearly constant value before rising steeply again at a radial distance closer to the cone axis. This appears to be inconsistent with the data input into the program in which the radial distance of the shock from the cone axis is seen to decrease with increasing values of  $\phi$ .





## V. SUMMARY

### A. CONCLUSIONS

The finite fringe method for the production of holographic interferograms has been applied successfully to the determination of the three-dimensional density distribution of the flow around a 10 degree half angle cone. The method has been demonstrated to yield results within an accuracy of 8 percent for the axisymmetric case and within 13 percent for the asymmetric case. The magnitude of the errors are mainly a result of the constraints imposed by the existing wind tunnel size and the fact that the cone model used produced perturbations in the flow field of a fairly small magnitude so that small errors in measurement were reflected as relatively large percentage errors. The computer program HOLOFER has been evaluated for the effect of the shock and the cone and found to yield good results.

### B. ACKNOWLEDGEMENTS

The writer wishes to gratefully acknowledge Dr. D. J. Collins for his most valuable guidance and assistance throughout the course of this investigation; the technical staff of the Department of Aeronautics under R. Besel and T. Dunton, particularly N. Leckenby, G. Gulbranson, G. Middleton, G. Teaby for the fabrication and assembly of the models and equipment used in these experiments and



D. Lawrence for the preparation of the necessary drawings;  
and Mrs. C. Roper for her considerable effort in the final  
preparation and typing of this report.



A	PORT IDENTIFICATION
B	STEPPER POWER SUPPLY
C	TRANSDUCER POWER SUPPLY
D	24 V DC FOR STEPPING SWITCH
E	2V DC FOR PORT IDENTIFICATION
F	3V DC FOR TRANSDUCER EXCITER
G	SCANIVALVE
H	PRESSURE SIGNAL
I	VALVE PORT IDENTIFICATION
J	15 LEADS FROM MODEL PRESSURE PORTS
K	PLENUM TOTAL PRESSURE
L	10° HALF ANGLE CONE MODEL

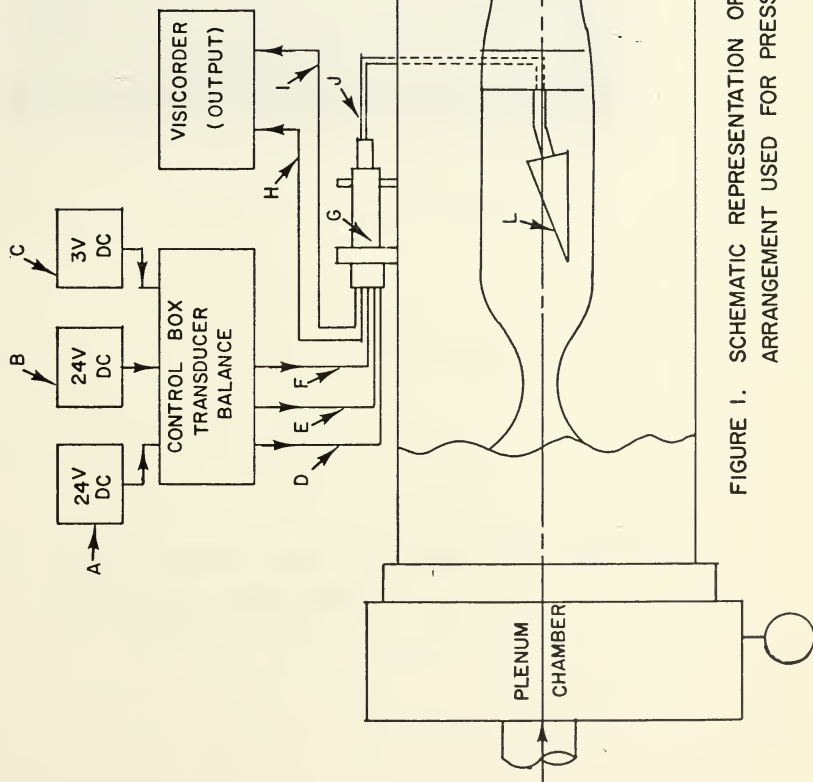


FIGURE 1. SCHEMATIC REPRESENTATION OF THE EQUIPMENT ARRANGEMENT USED FOR PRESSURE MEASUREMENT



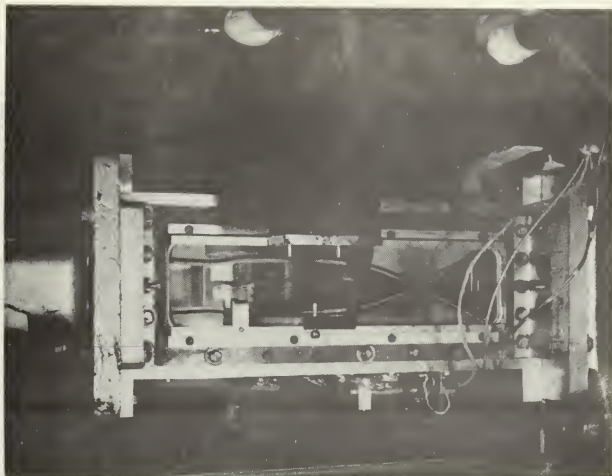


FIGURE 2. WIND TUNNEL TEST SECTION AND PRESSURE MEASURING EQUIPMENT





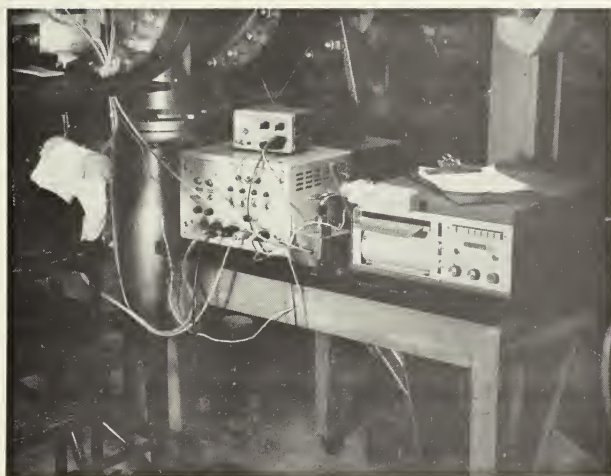


FIGURE 3. PRESSURE RECORDING EQUIPMENT, CONTROL BOX, AND POWER SUPPLIES







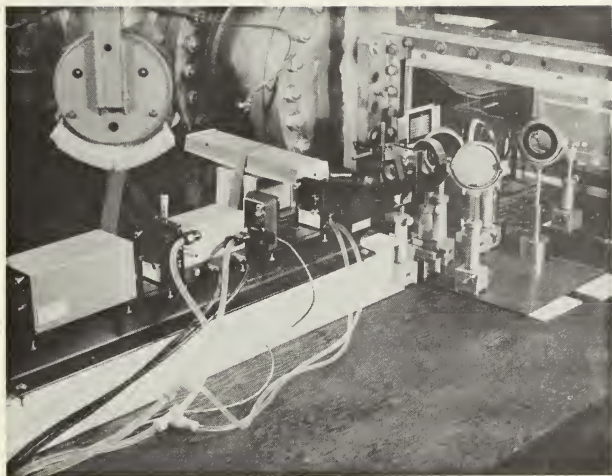


FIGURE 5a. HOLOGRAPHIC TABLE LASER CONTROL BOX  
AND TEMPERATURE CONTROL EQUIPMENT



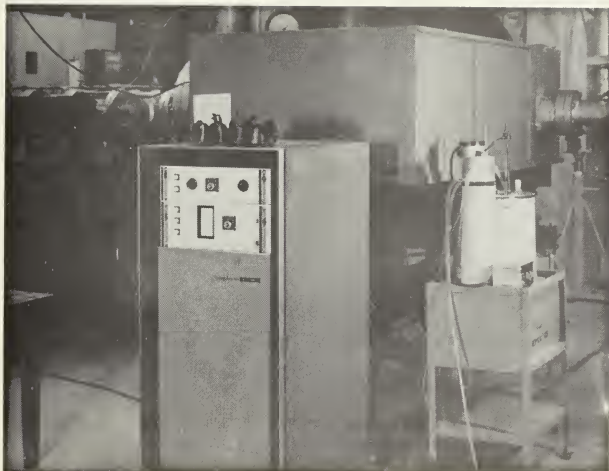


FIGURE 5b. DETAILS OF THE HOLOGRAPHIC ARRANGEMENT





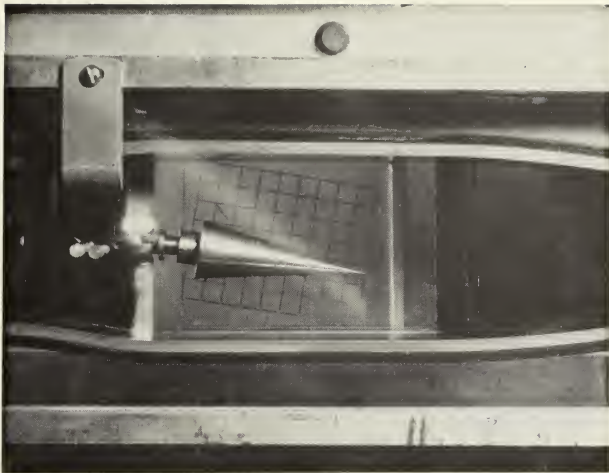


FIGURE 6. VIEW OF TEST SECTION SHOWING DETAILS OF  
MODEL, MOUNT, AND GRID



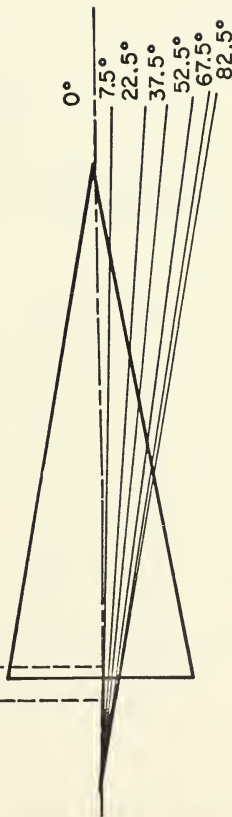
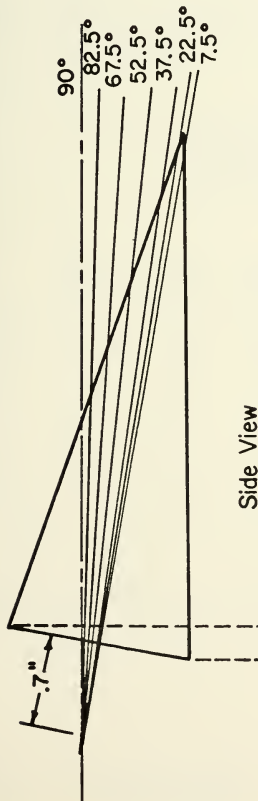
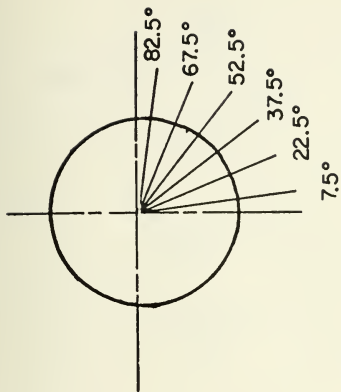


FIGURE 7a. POSITIONS OF THE CONE AXIS FOR VARIOUS ROTATIONAL POSITIONS OF THE CONE TIP



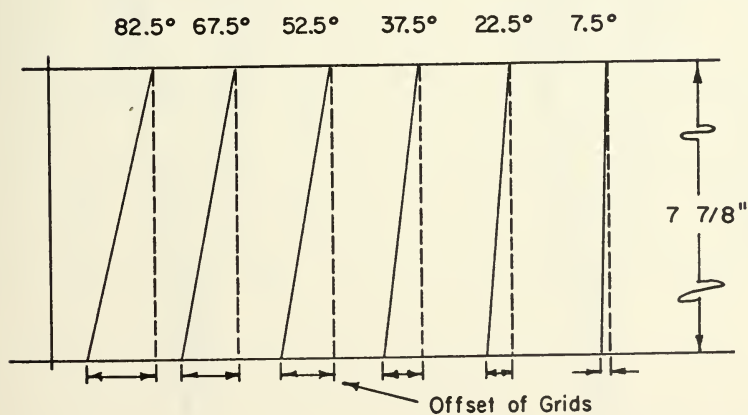
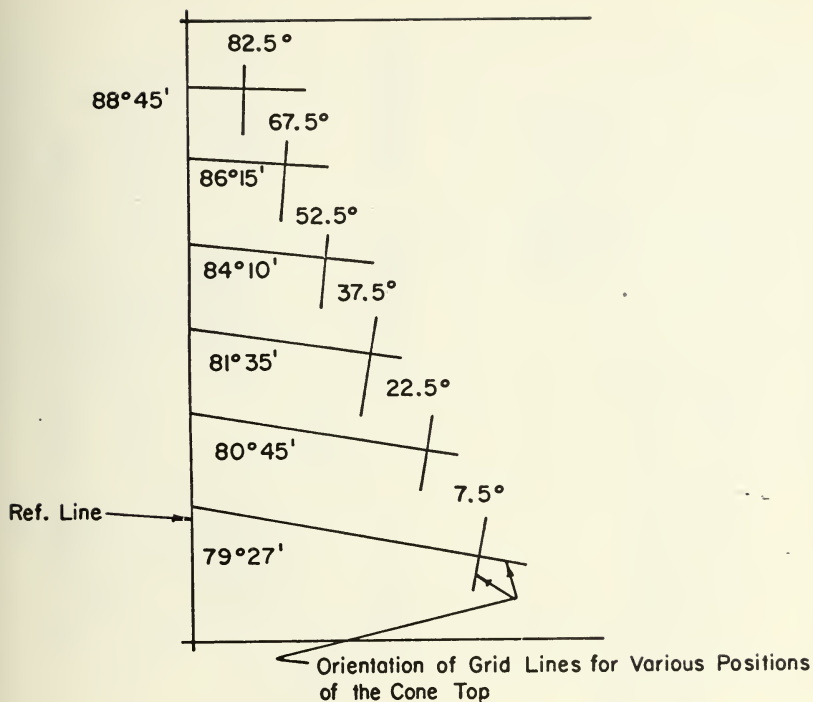


FIGURE 7b. ORIENTATION OF GRID LINES AND OFFSET OF THE GRIDS



ALL RADIALLY DRILLED HOLES .040 DIA

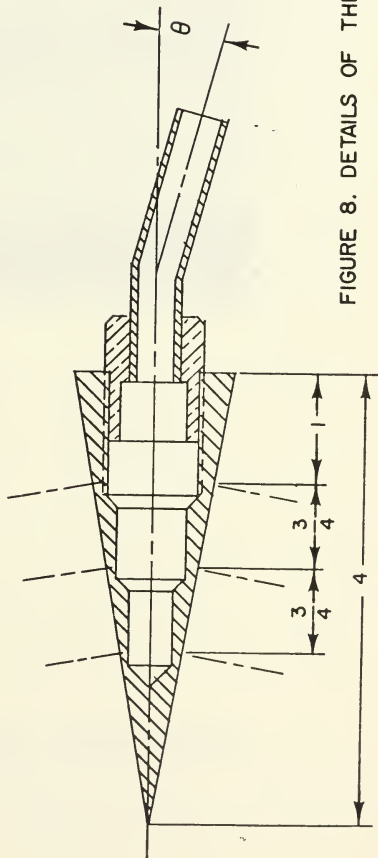
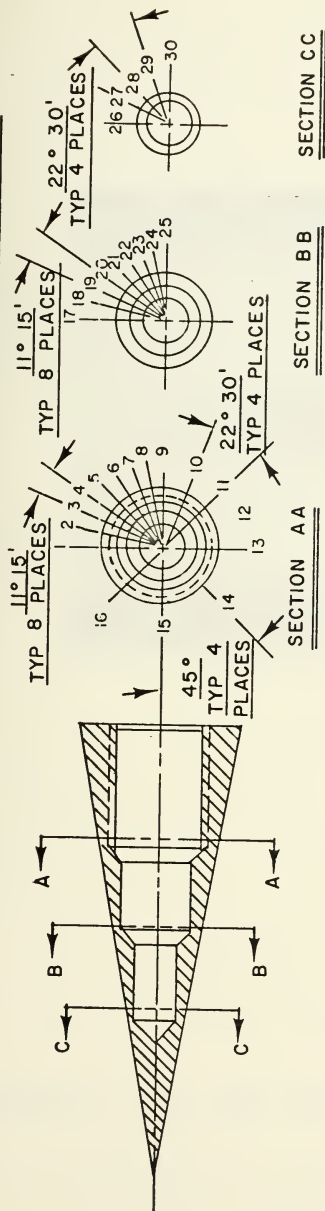


FIGURE 8. DETAILS OF THE CONE MODEL





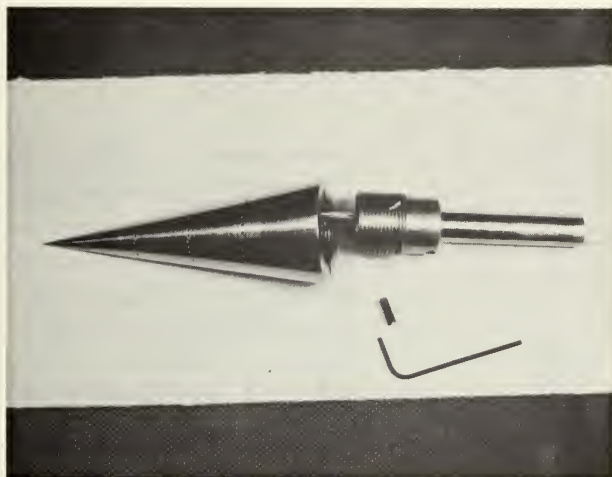


FIGURE 9. THE CONE AND SPINDLE ARRANGEMENT



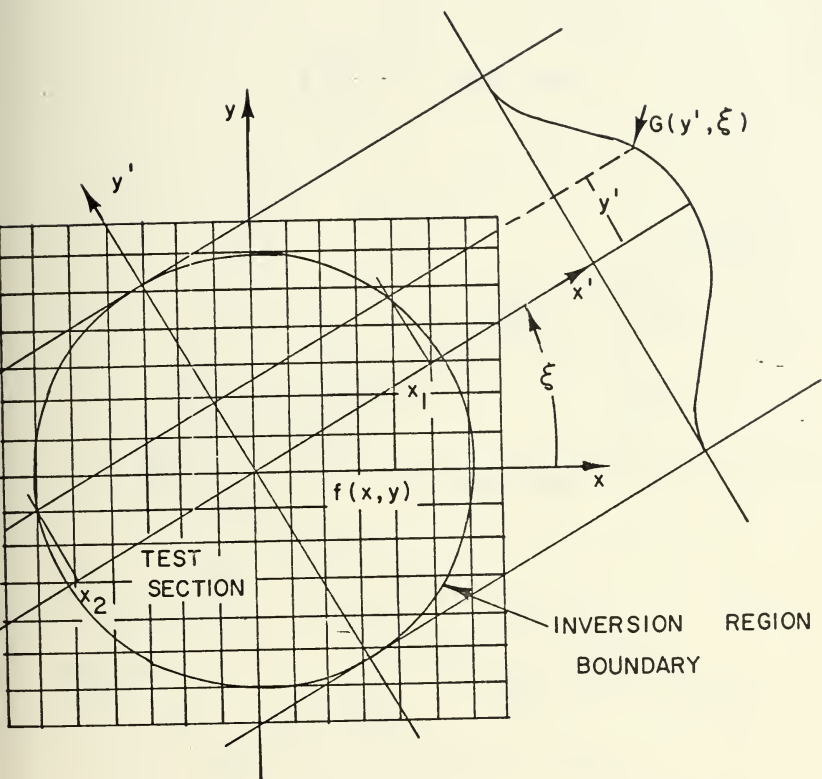


FIGURE 10. CO-ORDINATE SYSTEM USED FOR THE INVERSION OF FRINGE NUMBER TO DENSITY



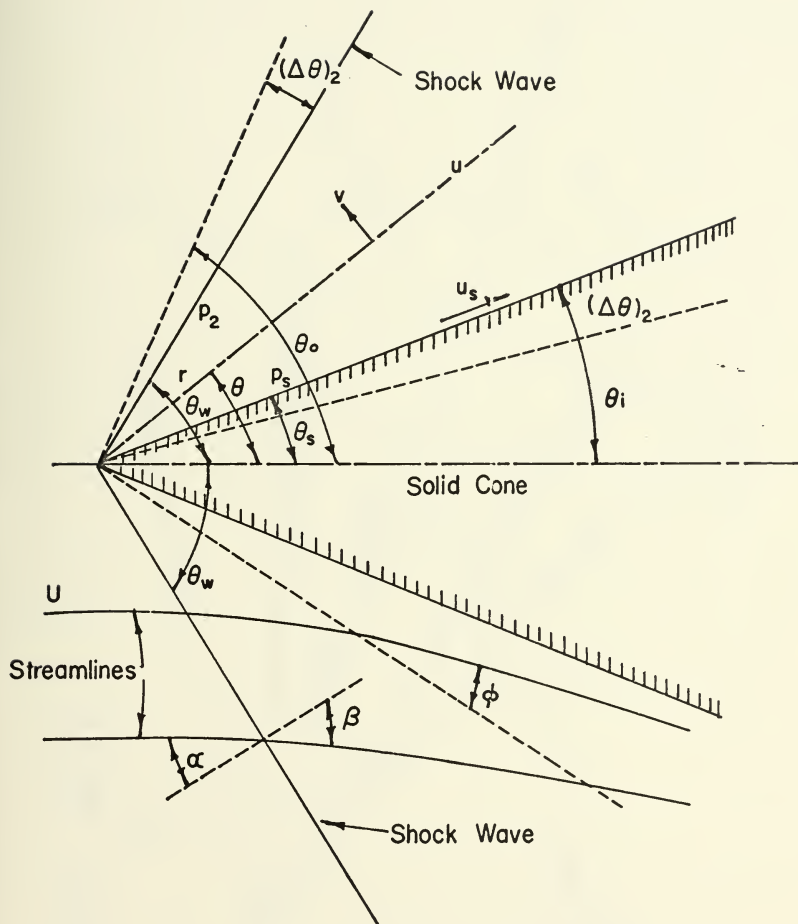


FIGURE II. CO-ORDINATE SYSTEM USED FOR THE GAS DYNAMIC EQUATION



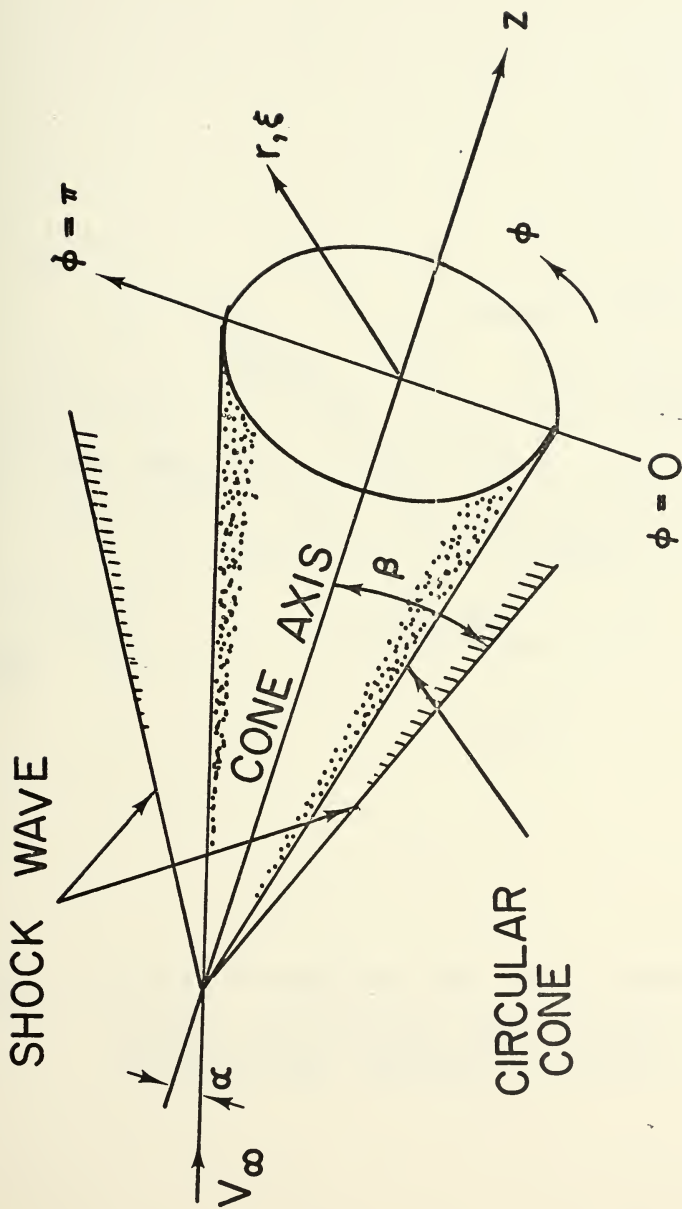


FIGURE 12. CO-ORDINATE SYSTEM USED IN REFERENCE 6





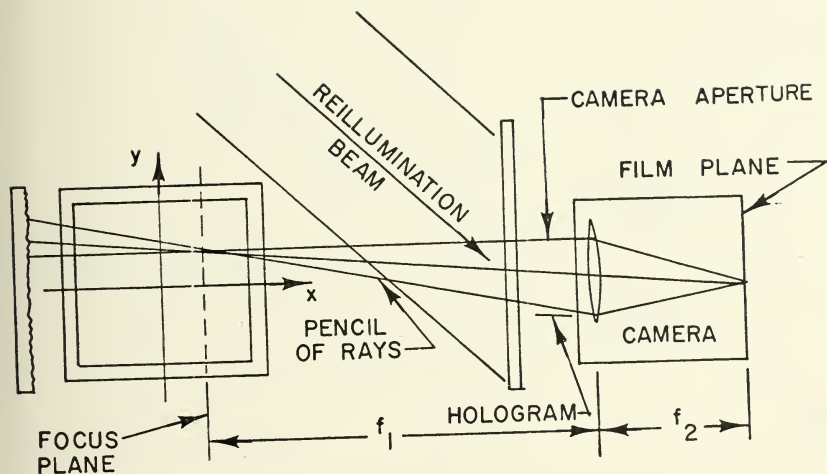


FIGURE 13. EFFECT OF APERTURE SIZE FOCUS PLANE POSITION ON THE PENCIL SIZE OF RAYS ABOUT A LINE OF SIGHT RECORDED BY CAMERA



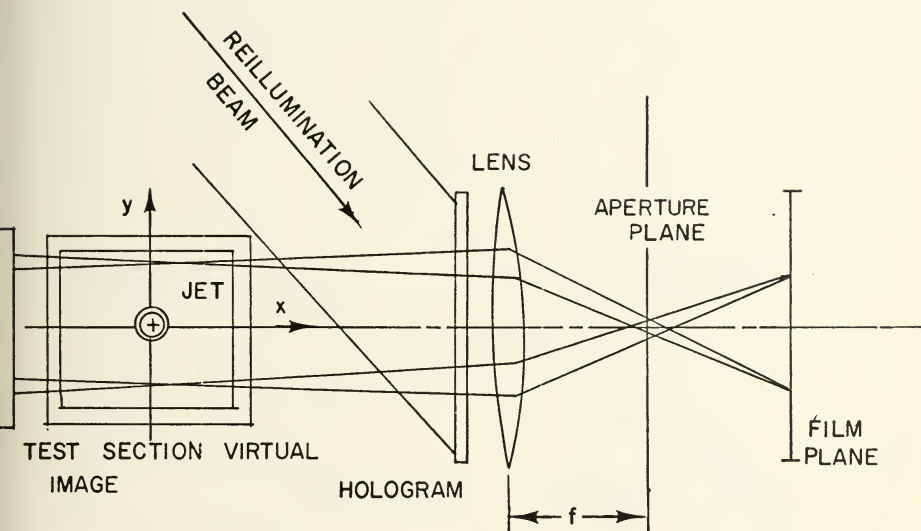


FIGURE 14. SPATIAL FILTERING TECHNIQUE FOR SELECTING PHOTOGRAPH OF CONSTANT ANGLE LINES OF LIGHT



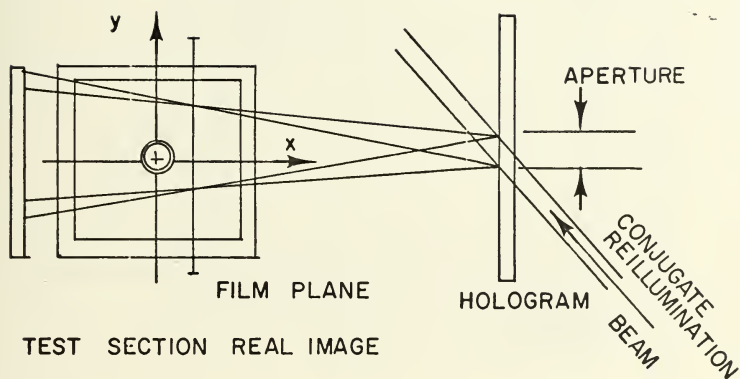


FIGURE 15. LENSLESS PHOTOGRAPHIC TECHNIQUE USING A CONJUGATE REFERENCE BEAM OF SMALL DIAMETER



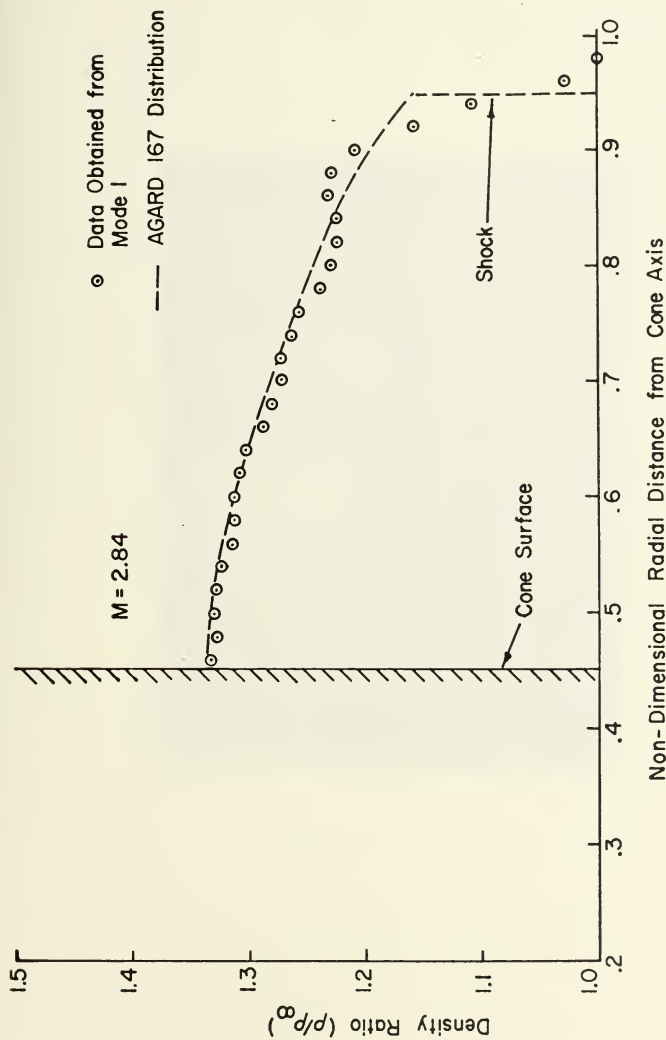


FIGURE 16.  
COMPARISON OF THE RADIAL DENSITY DISTRIBUTION OBTAINED FROM MODE I  
WITH THE AGARD 167 RADIAL DENSITY DISTRIBUTION - AXI-SYMMETRIC CASE





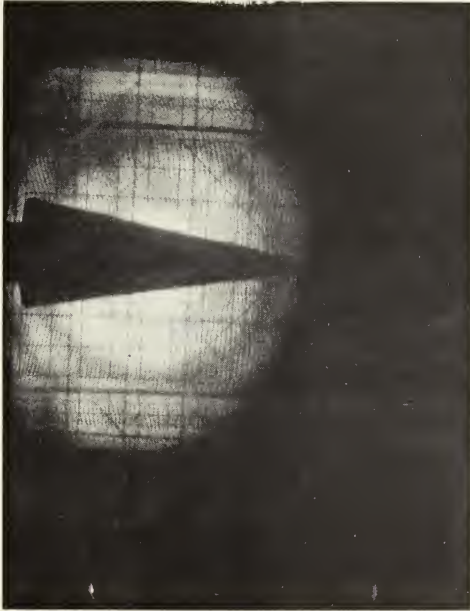


FIGURE 17a. HOLOGRAPHIC INTERFEROGRAM OBTAINED FOR THE AXI-SYMMETRIC CASE



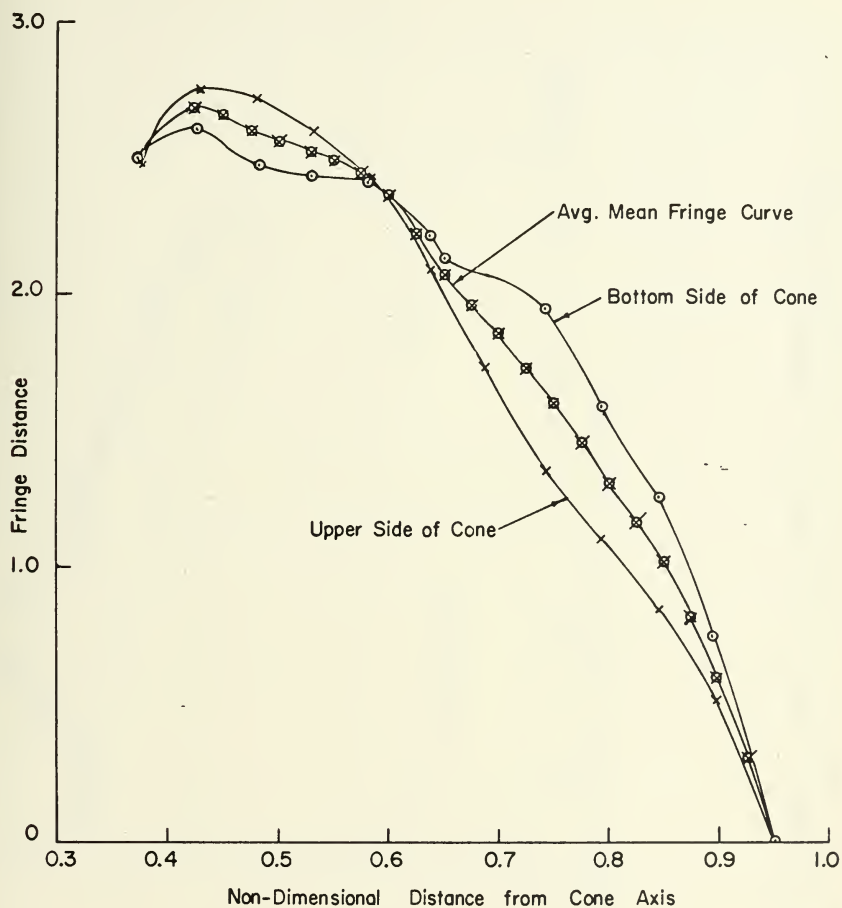


FIGURE 17b. RADIAL FRINGE DISTRIBUTION FROM A REDUCTION OF THE HOLOGRAPHIC INTERFEROGRAM FOR THE AXI-SYMMETRIC CASE



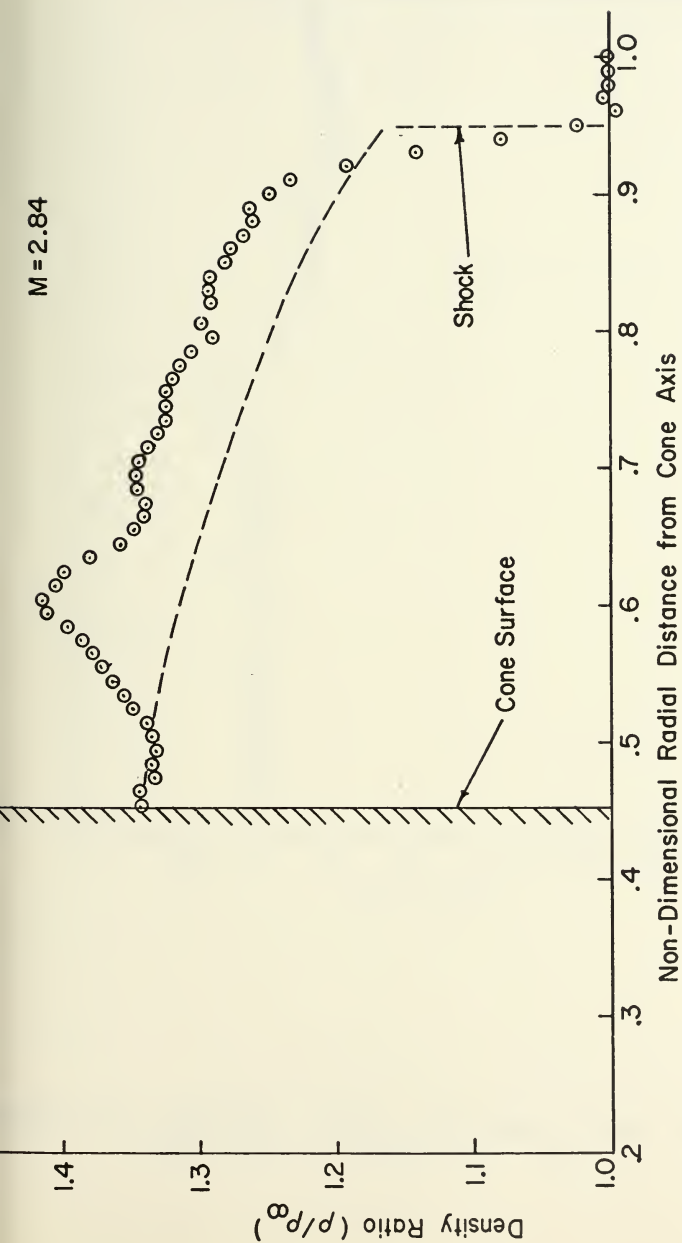


FIGURE 18.  
COMPARISON OF THE RADIAL DENSITY DISTRIBUTION OBTAINED FROM  
EXPERIMENT WITH THE AGARD 167 DISTRIBUTION - AXI-SYMMETRIC CASE



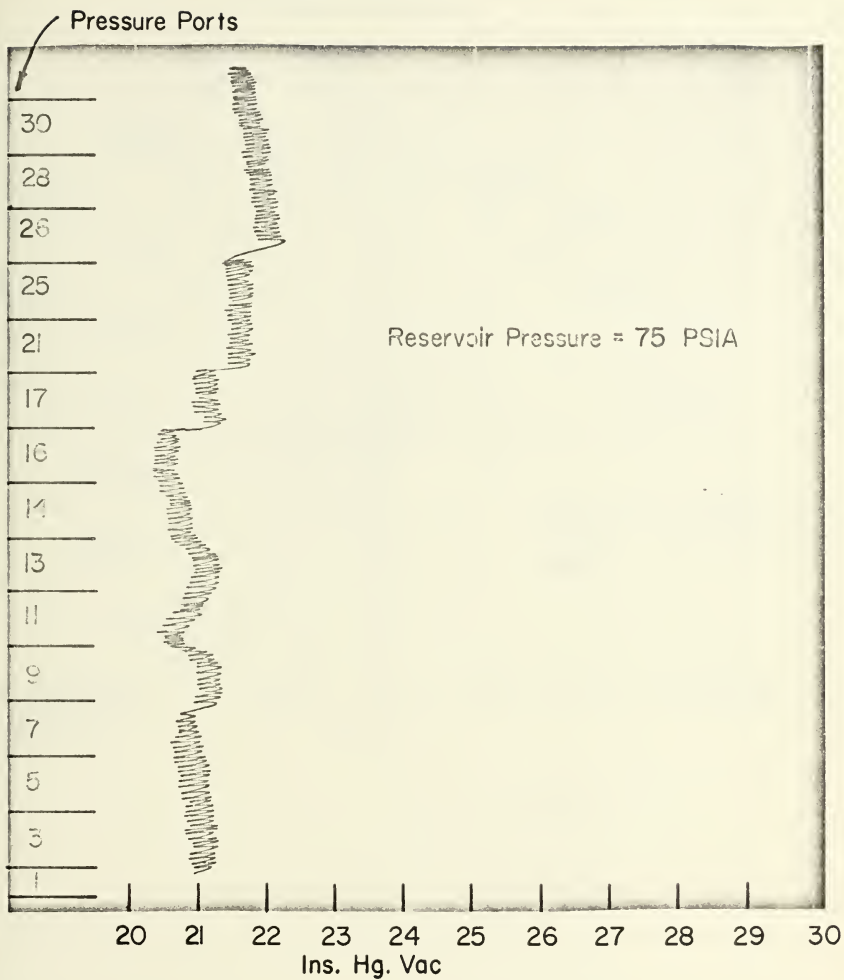


FIGURE 19. PRESSURE TRACE OBTAINED FROM THE VISCICORDER FOR THE AXI-SYMMETRIC CASE.





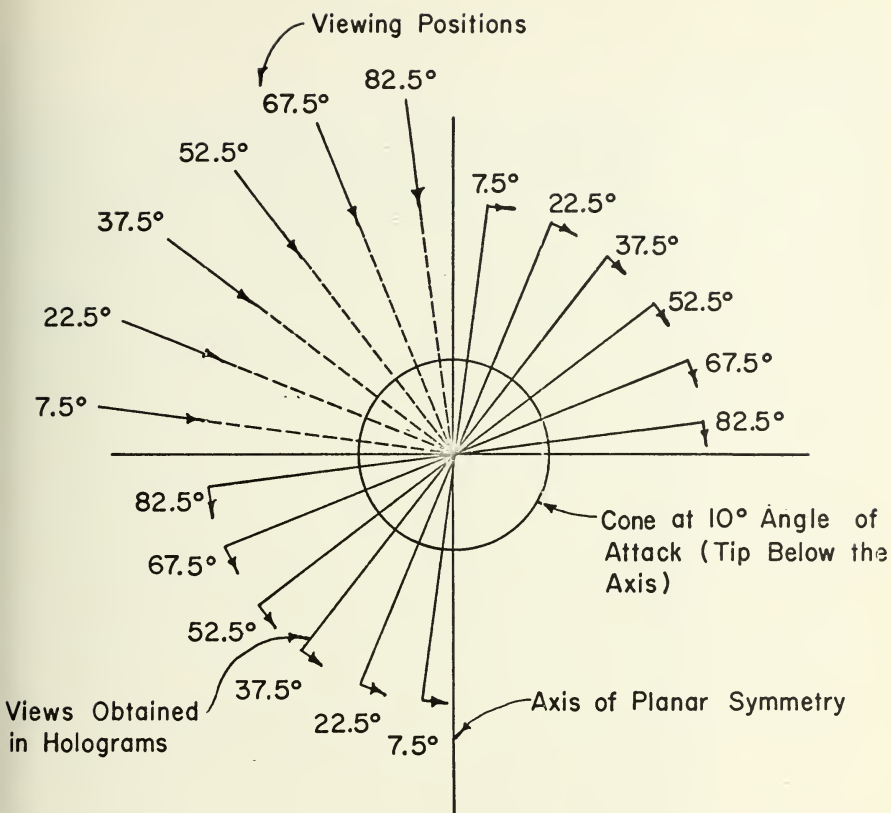


FIGURE 20. VIEWS ALONG WHICH HOLOGRAMS WERE OBTAINED FOR THE ASYMMETRIC CASE





FIGURE 21. HOLOGRAPHIC INTERFEROGRAM FOR  $7.5^\circ$   
ANGLE OF VIEW





FIGURE 22. HOLOGRAPHIC INTERFEROGRAM FOR  $22.5^\circ$   
ANGLE OF VIEW



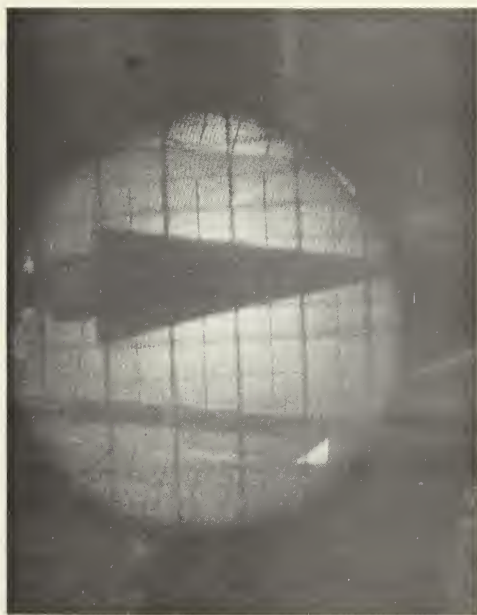


FIGURE 23. HOLOGRAPHIC INTERFEROGRAM FOR  $37.5^\circ$   
ANGLE OF VIEW



THE UNIVERSITY OF CHICAGO PRESS  
1967





FIGURE 24. HOLOGRAPHIC INTERFEROGRAM FOR  $52.5^\circ$   
ANGLE OF VIEW





FIGURE 25. HOLOGRAPHIC INTERFEROGRAM FOR  $67.5^\circ$   
ANGLE OF VIEW



THE UNIVERSITY OF CHICAGO PRESS  
5 E. JACKSON ST. CHICAGO, ILL. 60604-6161  
TEL: (312) 937-0700 FAX: (312) 937-0701  
WWW.CHICAGO.PRESS.EDU



FIGURE 26. HOLOGRAPHIC INTERFEROGRAM FOR  $82.5^\circ$   
ANGLE OF VIEW



THE UNIVERSITY OF CHICAGO PRESS  
1960

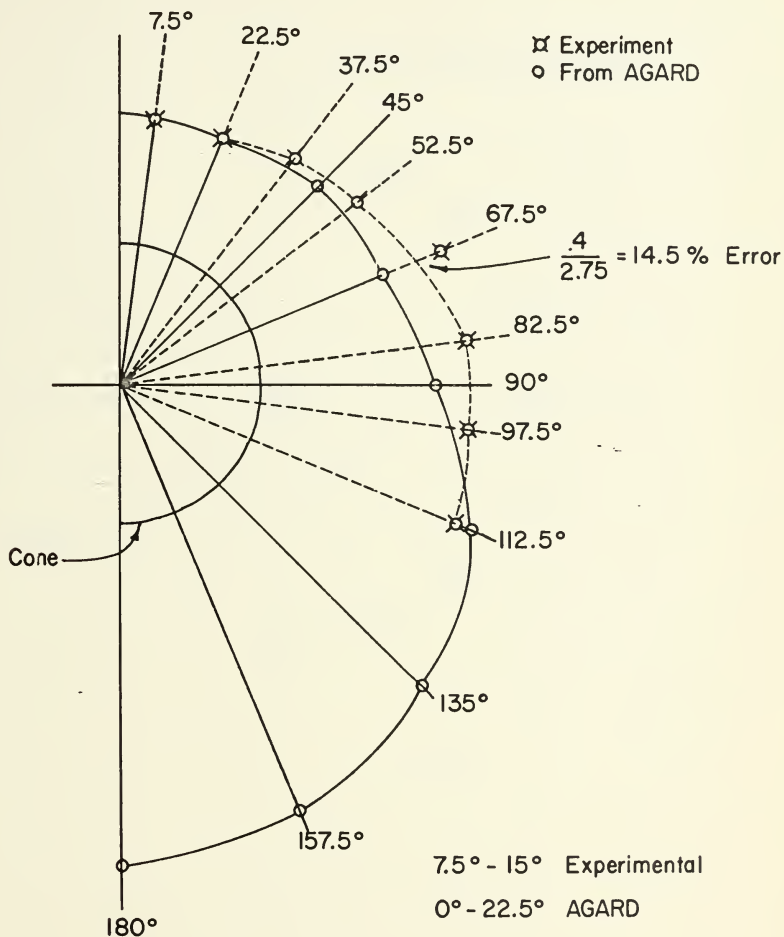


FIGURE 27. COMPARISON OF THE POSITION OF THE SHOCK WAVE OBTAINED EXPERIMENTALLY WITH THAT FROM AGARD 167 FOR  $M = 2.84$ , ASYMMETRIC CASE





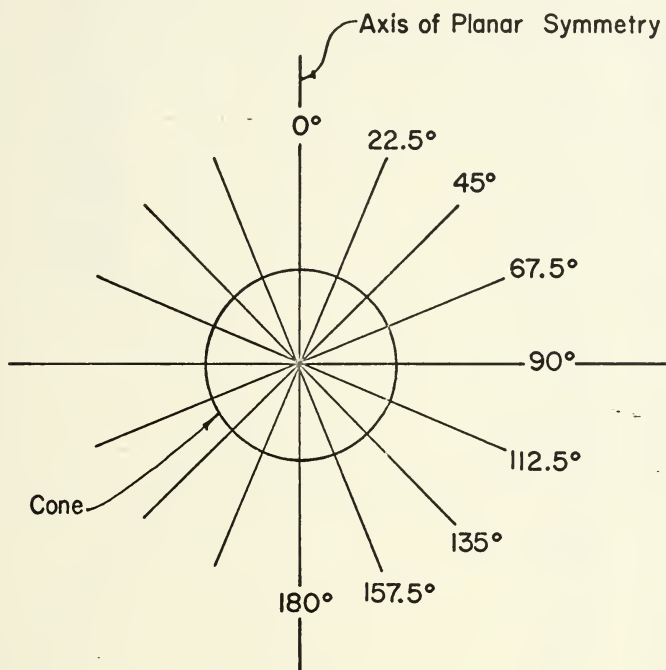


FIGURE 28. LINES OF SIGHT ALONG WHICH THE DENSITY FIELD WAS OBTAINED AFTER INVERSION, ASYMMETRIC CASE



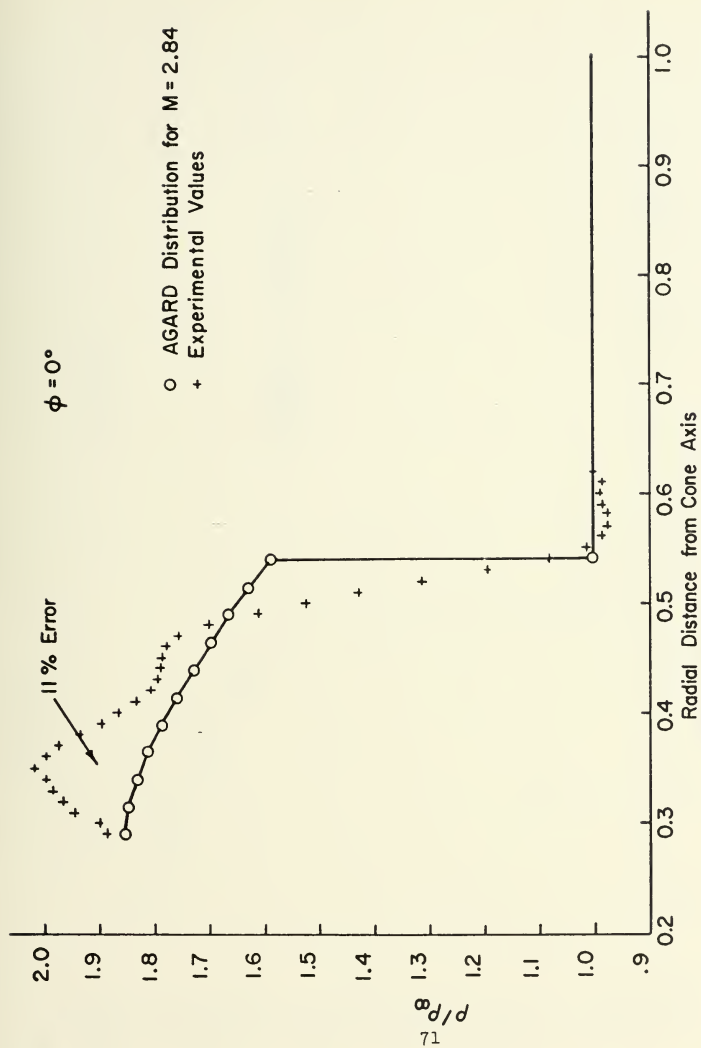


FIGURE 29. COMPARISON OF THE EXPERIMENTAL RADIAL DENSITY DISTRIBUTION  
WITH THE AGARD 167 DISTRIBUTION FOR THE ASYMMETRIC CASE  
AT  $M = 2.84$ ,  $\phi = 0^\circ$



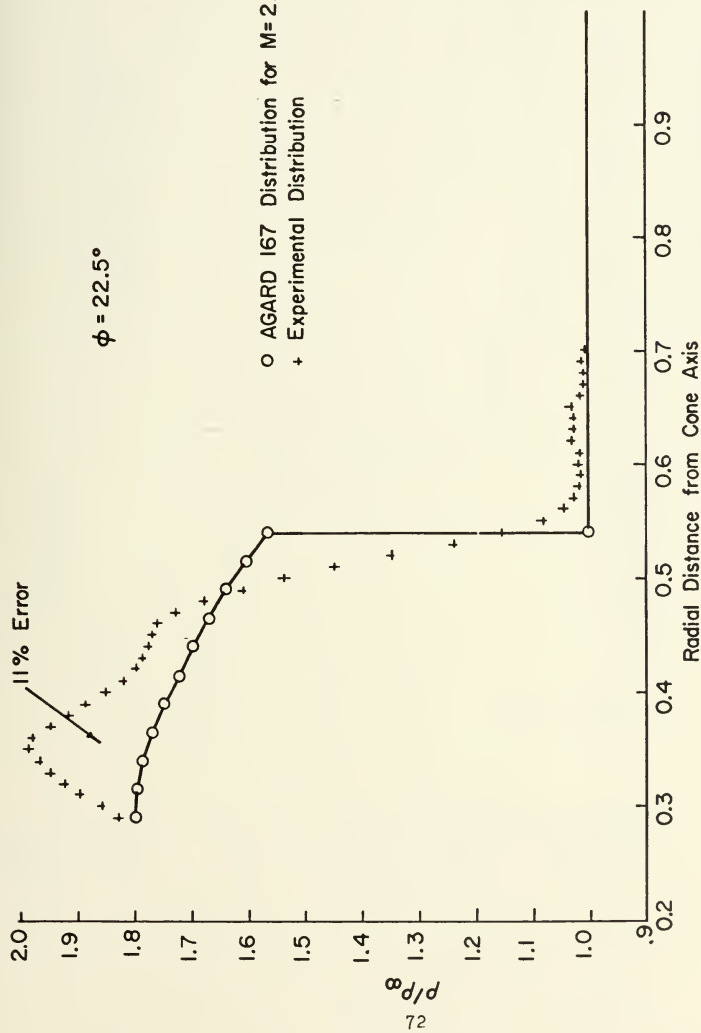


FIGURE 30. COMPARISON OF THE EXPERIMENTAL RADIAL DENSITY DISTRIBUTION WITH THE AGARD I67 DISTRIBUTION FOR THE ASYMMETRIC CASE AT  $M=2.84$ ,  $\phi = 22.5^\circ$



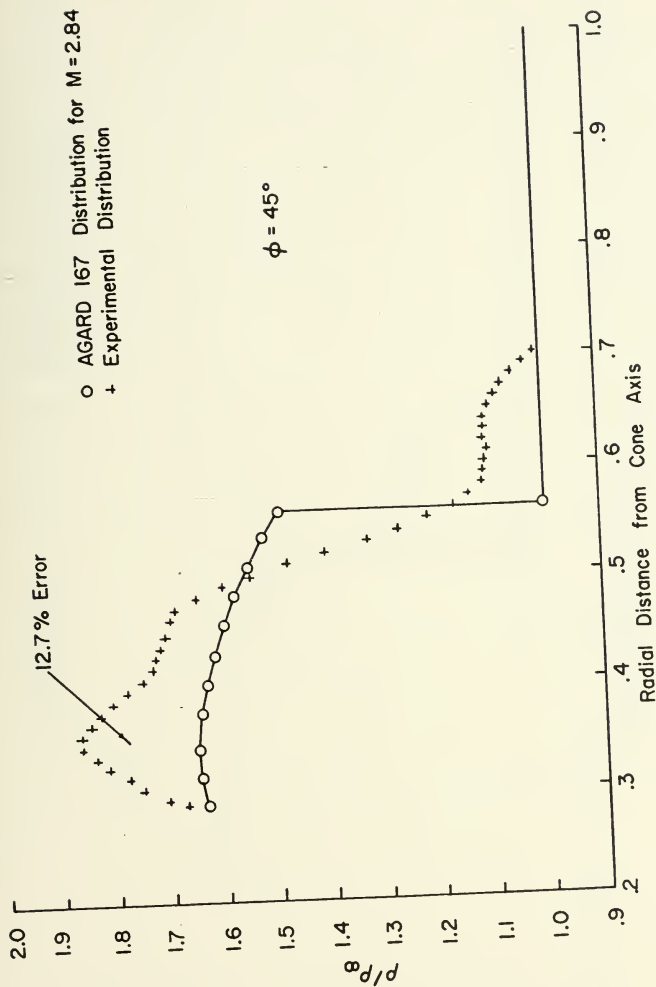


FIGURE 31. COMPARISON OF THE EXPERIMENTAL RADIAL DENSITY DISTRIBUTION  
 WITH THE AGARD 167 DISTRIBUTION FOR THE ASYMMETRIC CASE  
 AT  $M=2.84$ ,  $\phi = 45^\circ$





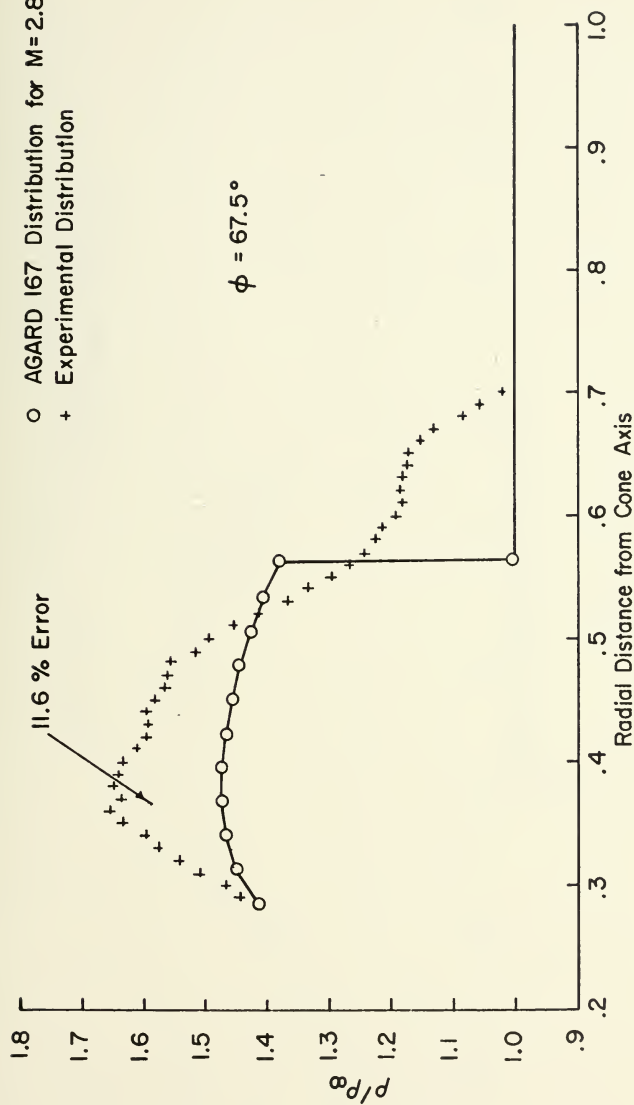


FIGURE 32. COMPARISON OF THE EXPERIMENTAL RADIAL DENSITY DISTRIBUTION  
 WITH THE AGARD 167 DISTRIBUTION FOR THE ASYMMETRIC CASE  
 AT  $M = 2.84$ ,  $\phi = 67.5^\circ$



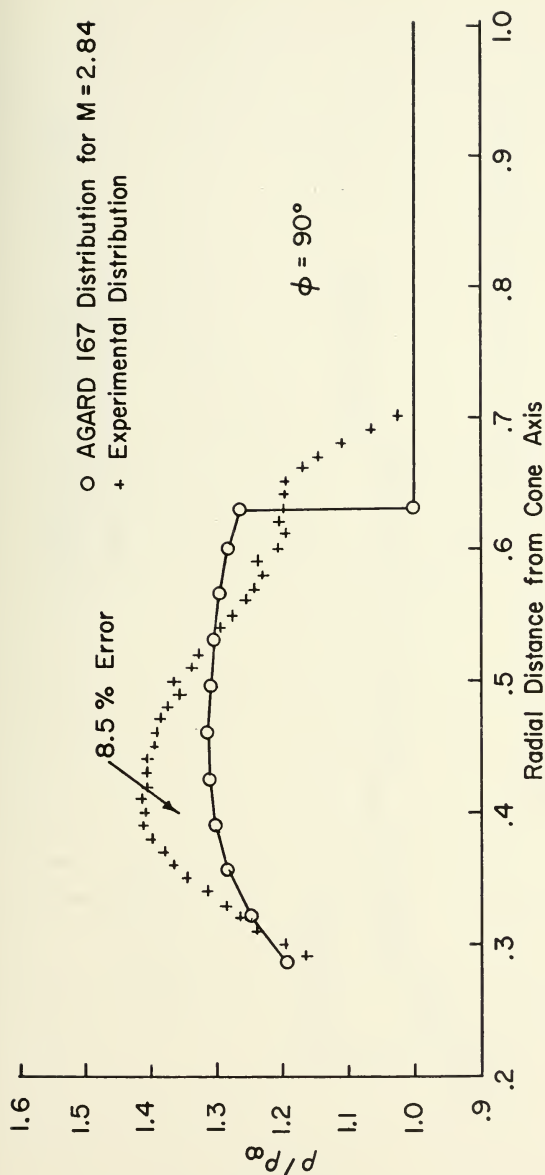


FIGURE 33. COMPARISON OF THE EXPERIMENTAL RADIAL DENSITY DISTRIBUTION WITH THE AGARD 167 DISTRIBUTION FOR THE ASYMMETRIC CASE AT  $M = 2.84$ ,  $\phi = 90^\circ$



○ AGARD I67 Distribution for  $M = 2.84$

+ Experimental Distribution

$\phi = 112.5^\circ$

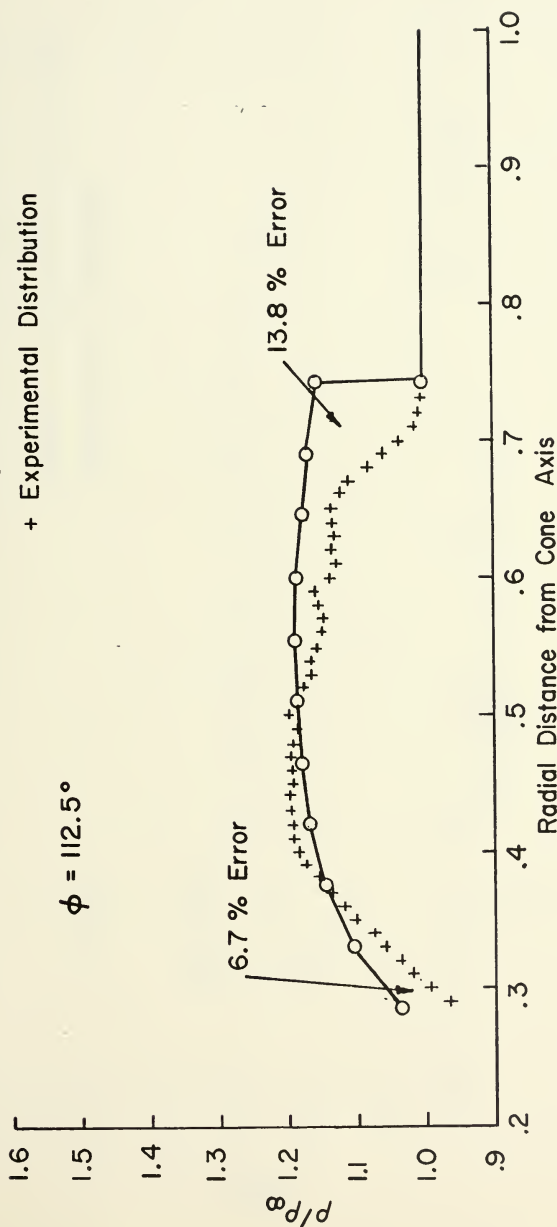


FIGURE 34. COMPARISON OF THE EXPERIMENTAL RADIAL DENSITY DISTRIBUTION WITH THE AGARD I67 DISTRIBUTION FOR THE ASYMMETRIC CASE AT  $M = 2.84$ ,  $\phi = 112.5^\circ$



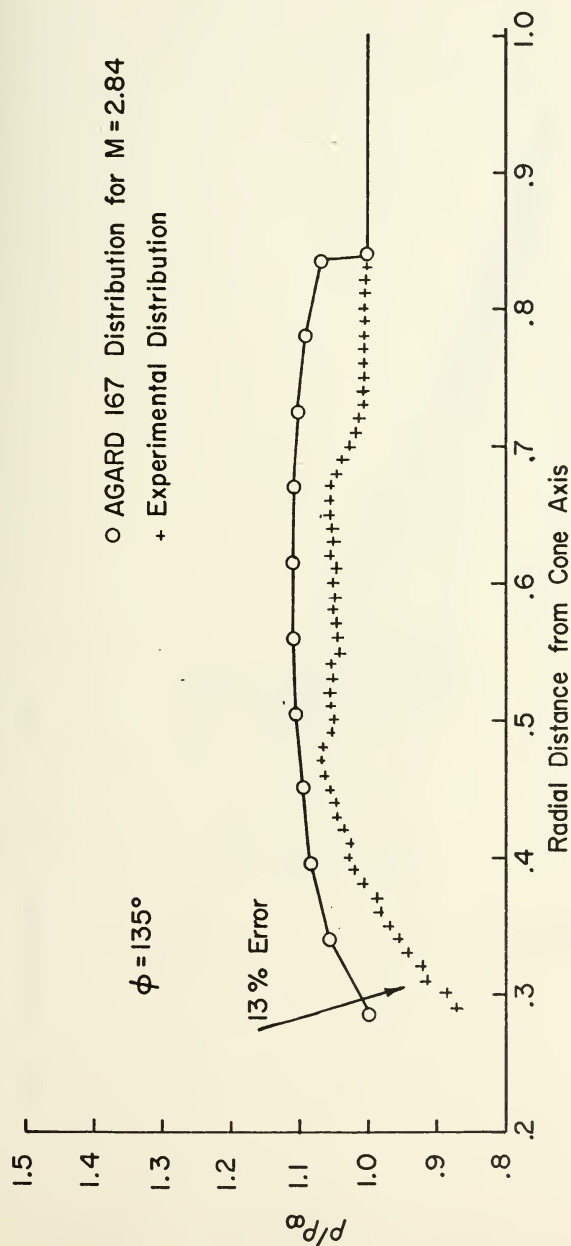
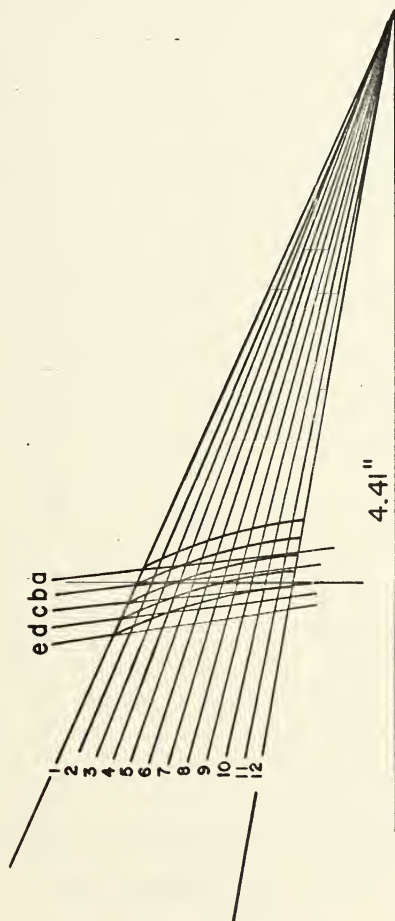


FIGURE 35. COMPARISON OF THE EXPERIMENTAL RADIAL DENSITY DISTRIBUTION WITH THE AGARD 167 DISTRIBUTION FOR THE ASYMMETRIC CASE AT  $M = 2.84$ ,  $\phi = 135^\circ$





$$\text{Avg. Fringe Dist.} = \frac{11.1}{4} = 2.775$$



$$\text{Magnif. Factor} = \frac{4.1''}{2.25''} = 1.8222''$$

FIGURE 36. TRACING OF THE PROJECTED IMAGE OF THE HOLOGRAPHIC INTERFEROGRAM FOR THE AXI-SYMMETRIC CASE



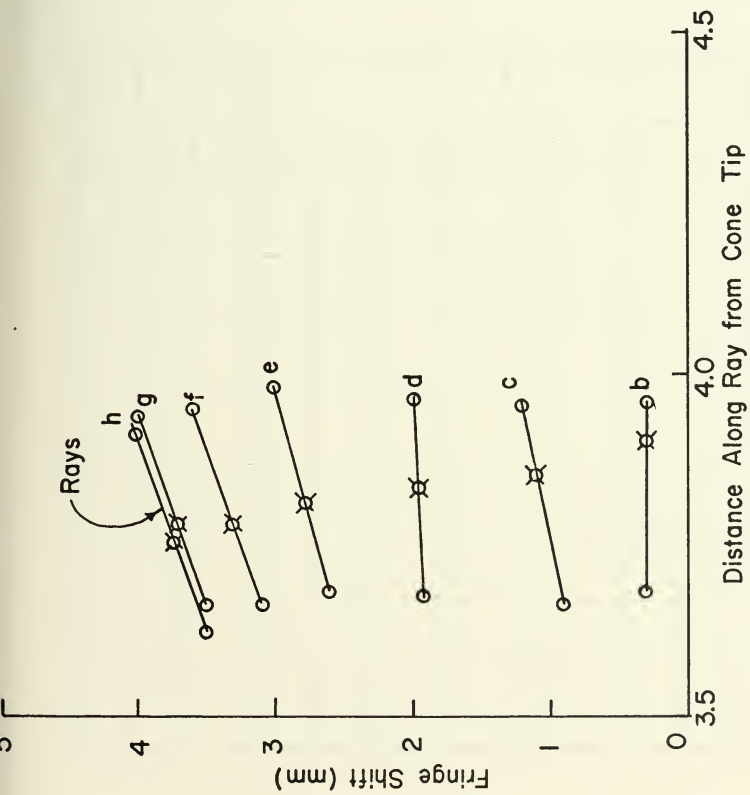


FIGURE 37. PLOT OF A TYPICAL FRINGE SHIFT VARIATION ALONG A RAY TO OBTAIN THE FRINGE SHIFT AT THE SECTION

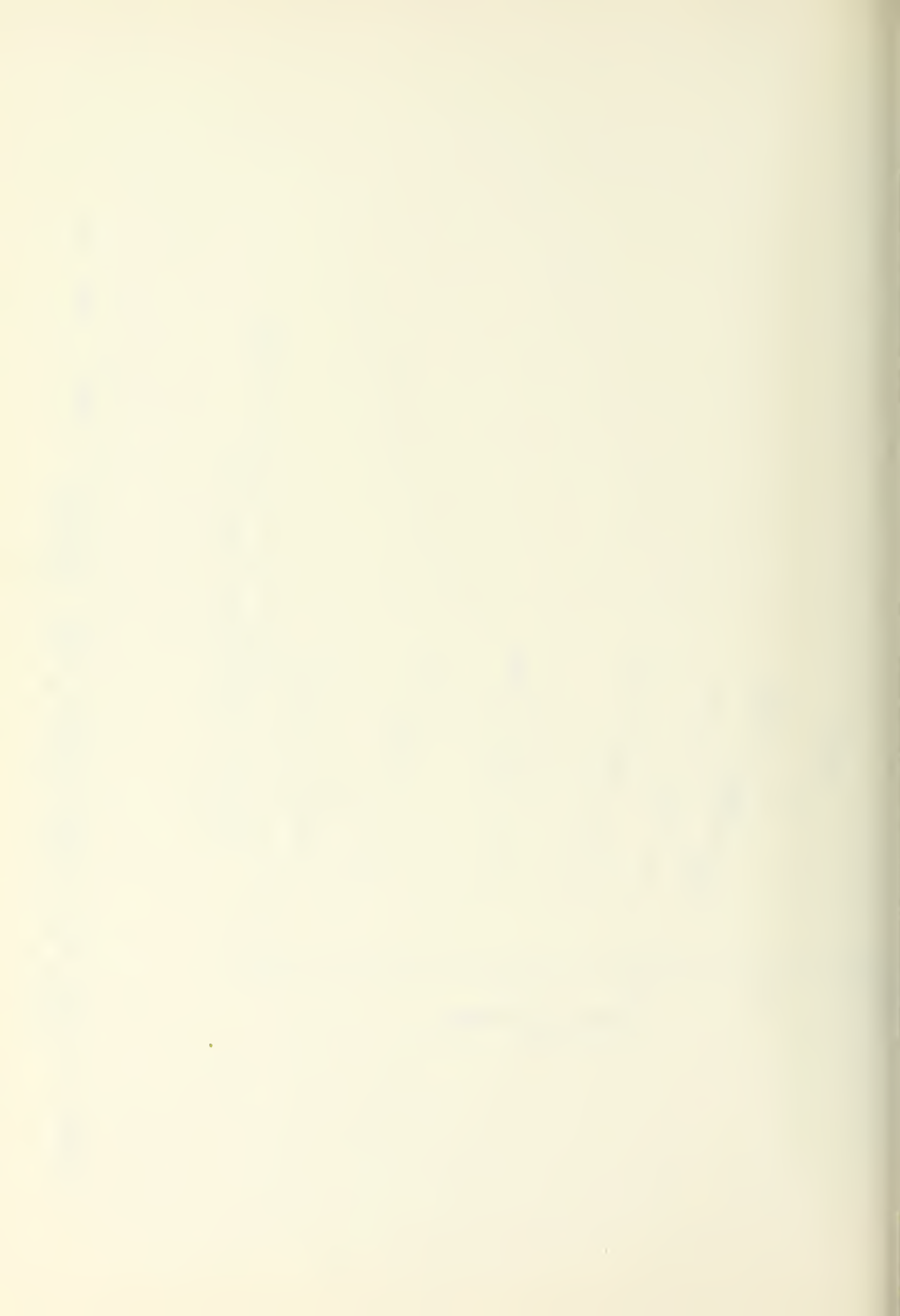


TABLE I

VARIATION OF FRINGE SHIFT WITH DISTANCE  
ALONG RAYS FROM THE CONE VERTEX

x = Fringe shift (mm.)

y = Distance from cone vertex along a ray (ins.)

Ray	Fringe 'a'		Fringe 'b'		Fringe 'c'		Fringe 'd'		Fringe 'e'		Section	
	x	y	x	y	x	y	x	y	x	y	x	y
1	0.0	4.50	0.0	4.63	0.0	4.75	0.0	4.89	0.0	5.0		4.48
2	2.0	4.37	2.1	4.49	1.9	4.63	1.7	4.77	1.0	4.92		4.44
3	3.3	4.26	5.5	4.40	3.6	4.50	3.2	4.64	2.1	4.78		4.40
4	4.1	4.17	4.4	4.29	4.4	4.41	4.1	4.53	3.5	4.68		4.36
5	4.9	4.08	4.9	4.21	5.4	4.32	5.0	4.43	4.7	4.58		4.32
6	5.5	4.02	5.6	4.13	6.1	4.24	5.5	4.35	5.6	4.48		4.28
7	6.0	3.95	6.1	4.08	6.6	4.18	6.0	4.29	6.4	4.14		4.26
8	6.4	3.91	6.8	4.03	7.2	4.13	6.7	4.22	6.9	4.34		4.23
9	6.6	3.87	7.2	3.97	7.7	4.08	6.6	4.18	7.4	4.28		4.21
10	6.6	3.84	7.3	3.92	7.8	4.03	6.6	4.14	7.7	4.23		4.18
11	6.5	3.80	7.1	3.91	7.2	4.0	6.5	4.10	7.7	4.19		4.15
12	6.3	3.79	6.4	3.90	7.1	3.99	6.3	4.08	7.3	4.17		4.14



TABLE II

RADIAL DISTANCE FROM THE CONE AXIS OF THE  
INTERSECTION OF RAYS WITH THE SECTION

Ray	Distance from cone axis	Normalized distance from cone axis
1	1.83	0.95
2	1.72	0.89
3	1.63	0.846
4	1.53	0.794
5	1.43	0.742
6	1.33	0.69
7	1.23	0.639
8	1.12	0.581
9	1.02	0.53
10	0.92	0.478
11	0.82	0.426
12	0.72	0.374



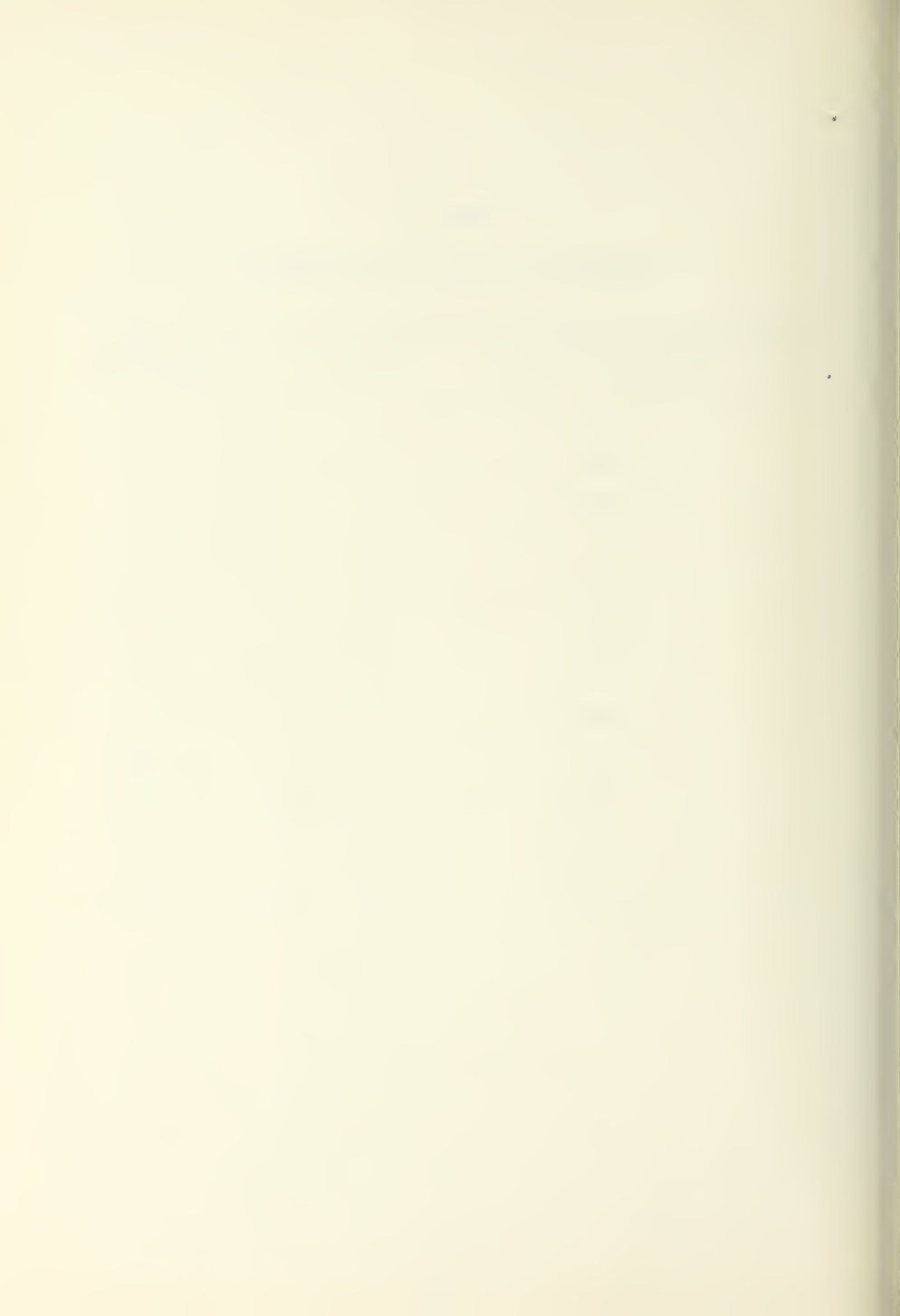


TABLE III

CALCULATION OF THE RADIAL VARIATION  
OF FRINGE NUMBER AT THE SECTION

Average fringe spacing in the freestream = 2.775 mm.

Ray	Normalized distance from cone axis	Fringe shift (mm.)	Fringe number
1	0.95	0.0	0.0
2	0.89	2.08	0.75
3	0.846	3.5	1.26
4	0.794	4.42	1.59
5	0.742	5.4	1.946
6	0.69	5.92	2.13
7	0.639	6.16	2.22
8	0.581	6.69	2.41
9	0.53	6.73	2.425
10	0.478	6.87	2.476
11	0.426	7.22	2.60
12	0.374	6.80	2.45



## APPENDIX A

### REDUCTION OF AN INTERFEROGRAM TO OBTAIN FRINGE SHIFT DATA

The reduction of only one side of the interferogram obtained for the axisymmetric case is indicated as an illustration of the procedure employed. After projection of the negative, the cone surface, the shock waves, the grid line at the section concerned and the fringes from the projected image were traced on a sheet of paper as shown in Figure 36. The distance between the cone surface and the shock at the section was divided into a convenient number of parts and rays drawn from the tip of the cone through these points. The fringe shift distances at the point of intersection of each displaced fringe and the rays were measured by means of a 7X PEAK scale magnifier as well as the average fringe spacing in the freestream. The radial distance from the cone axis to the intersection of each of the rays with the section was also measured as also the distance along each ray to the intersection with each fringe and with the section concerned. A tabulation of these results is shown in Tables 1, 2, and 3. For each ray, the fringe shift distance was then plotted against the distance along the ray as in Figure 37, and from these curves the fringe shift distance at the section was obtained. These fringe shift distances were divided by the average fringe spacing in the freestream to obtain the fringe numbers at the various



points concerned. From a measurement of the distance from the tip of the cone to the section on the projected image and comparison with the known distance, the magnification of the image with respect to the actual conditions existing in the wind tunnel was determined. The radius of the inversion circle was obtained by assuming the distance of the shock from the cone axis to be at 95% of the radius of the inversion circle. The distance from the cone axis of the various intersections of the rays from the cone vertex and the section were obtained as a fraction of the inversion circle radius. The fringe number at these points was then plotted against the non-dimensional distance from the cone axis as shown in Figure 17 and a smooth curve drawn through these points. The value of the fringe number in the region occupied by the cone was taken as a constant value equal to that at the cone surface. From the curve so obtained, values of the fringe number at 101 equidistant points were obtained on each side of the cone axis (including the value at the axis) so that a total of 201 data values resulted. This fringe data was read into Subroutine READ of computer program HOLOFER and inverted to obtain the required density field.

The use of 201 data points was essentially dictated by the necessity to be able to define the shock position accurately and to have the fringe distribution in the region between the shock and the cone described fairly well. Since



the fringe curve from which these points were obtained was plotted using only about 10 experimental fringe values, the use of 201 points does not imply a higher accuracy in the density distribution output from the computer program.





## APPENDIX B

### USE OF COMPUTER PROGRAM "HOLOFER"

This computer program is designed to invert the array of fringe numbers to obtain the associated density field using the inversion first proposed by C. D. Maldonado and described in Section III of this report. The computer program can be run in basically 3 modes as described below:

#### (a) Mode 1

This mode provides the basic testing capability of the program and uses various test functions listed in Subroutine FUNCT in order to generate a G array which is then inverted back to obtain the original input function. Functions other than those specified in FUNCT can also be read in on cards by specifying a test function number of 8.0 in the original list of 42 parameters read in into the main program HOLOVERT. In this case the main program first calls Subroutine FREAD to read in the data cards. The first card in this data deck consists of two values indicating the total number of cards to be read in and the 'Z' section at which inversion is being performed and is input according to format 89 of the subroutine. Thence follows one point per card according to format 88 representing the numerical test function being input. This mode was employed in the present case for inverting the 201 points that were obtained from the AGARD tables by interpolation using Computer Program 1.



Apart from an evaluation of the effect of discontinuities due to the shock and the cone, this method provided advance information on the magnitude of the fringe numbers to be expected in the experimental results.

(b) Mode 2

This mode obtains the G array at regular intervals from irregularly spaced values of the fringe number function by utilizing Subroutine SHEET. The fringe data may also be simulated by specifying NCODE=1 in which case one of the functions in FUNCT may be used to generate the G array. This mode has not been applied to the present investigation.

(c) Mode 3

In this mode, the fringe numbers are read in directly at regularly spaced points by Subroutine READ which is called by Subroutine GARRAY. The various parameters in the first two cards of Subroutine READ serve to identify the symmetry of the fringe field. The following parameters have been used in the cases dealt with in this report:

<u>Parameter</u>	<u>Axisymmetric Case</u>	<u>Asymmetric Case</u>
NOF	Any value specifying the run number.	Any value specifying the run number
IMAX	201	201
JMAX	1	24
ISYM	2	1
JSYM	101	1
IMS	101	201
JMS	1	1
Z	The 'Z' section at which inversion is performed.	The 'Z' section at which inversion is performed.



<u>Parameter</u>	<u>Axisymmetric Case</u>	<u>Asymmetric Case</u>
XO	0.	0.
YO	0.	0.
PHISYM	0.	0.

Further details regarding the computer program are contained in Reference 3. A listing of the program is, however, included in this appendix for reference.













```

95 FORMAT (/5X,*,*TST,FUN*,ADD,FUN*,GARRAY*,GRAPH*,LIN,PRT*,*,SET00400
1,MAP,BND*,/2X,6F10.0)
96 FORMAT (/5X,*,*A*,B*,C*,*D*,*E*,*,SET00420
1,FORMAT (/5X,*,/4X,6F10.3)
97 FORMAT (/5X,*,*S*,T*,*U*,*V*,*W*,*,SET00440
1,FORMAT (/3X,75A1)
98 IF (DGN.GE.4) WRITE (6,89) (AR(I),I=1,42)
NNN=2
IF (MODE.LI.0) NNN=1
IF (MODE.GT.5) NNN=3
IF (MODE.GT.5) MODE=MODE-10
NGP=0
IF (KLIMIT.LT.KEXTRA) KEXTRA=KLIMIT
IF (KLIMIT.LT.MEXTRA) MEXTRA=KLIMIT
IF (IPT.LI.0) NGP=IPT
IF (IPT.LI.0) IPT=IPT
ISYM=2-1-((FLOAT(JSYM)/2.-FLOAT(JSYM/2)))*2
IF (JSYM.EQ.0) ISYM=1
IF (JSYM.GT.JMAX) ISYM=2
IF (ISYM.EQ.1) JMAX=((JMAX+1)/2)*2
RJMX=JMAX
MSYM=JSYM
IF ((MSYM.EQ.0).OR.(MSYM.GT.JMAX)) MSYM=1
FCU=ISYM*JSYM*JMAX
IF ((JSYM.GT.JMAX).OR.(JSYM.EQ.0)) FCU=JMAX
QSYM=FCU/RJMX
IMS=(IMAX+ISYM-1)/ISYM
JMS=JMAX
IF (ISYM.EQ.1) JMS=(JMAX/2+1)/2
IF (JSYM.EQ.0) JMS=JMAX/2
MODE=ABS(AR(13))
XD=0.
YO=0.
ZD=0.
PHISYM=0.
HS=SIZE/2.
RHQS=1-286
BOX=RHQINF*BETA/RHOS/RLAMDA
RPTS=NPTS
XPR=0.
IF (NPTS.GT.1) XPR=XPRNG/(RPTS-1.)/2.
XPM=-XPR
PIE=3.141592653589793
MONE=1
WRITE (6,58) IMAX,JMAX,IMS,JMS,ISYM,JSYM,MSYM,QSYM,FCU
FORMAT (3X,*,IMAX,JMAX,IMS,JMS,ISYM,JSYM,MSYM,QSYM,FCU,/,
7I5,2F7.3/)

```

58

1



```

NTWO=2
IX=IMAX+JMAX
NF=1
IF ((MODE.EQ.1.) .AND. (NOF.EQ.8) .AND. (DGN.GE.1.)) WRITE (6,69)
IF ((MODE.EQ.1.) .AND. (NOF.EQ.8)) CALL FREAD (NO,RO,NF,ZD)
ZD=ZD
IF (DGN.GE.1.) WRITE (6,68)
CALL GARRAY (G,GA,NOF,DGN,MONE,XD,YO,PHISYM)
LM=1
IF ((LPT.EQ.0) .AND. (BND.EQ.0)) LM=0
IIMX=IMAX+1
IJMX=JMAX+1
IJMX=IMAX+JMAX
NBD=1
IF (JSYM.EQ.0) NBD=2
KBD=KLIMIT*NBD
DO 15 IJ=1,IJMX
  GALLJ=0
  IF (NAF.EQ.0) GO TO 16
  NF=IN2
  IF ((NAF.EQ.8) .AND. (DGN.GE.1.)) WRITE (6,69)
  IF ((NAF.EQ.8) .AND. (DGN.GE.1.)) CALL FREAD (NA,RA,NF,ZD)
  MST=MODE
  IF (DGN.GE.1.) WRITE (6,68)
  IF (NAF.NE.0) CALL GARRAY (GA,G,NAF,DGN,NTWO,XD,YO,PHISYM)
  MODE=MST
  DO 6 IJ=1,IJMX
    GALLJ=G(IJ)+GA(IJ)
    RLINS=NLINS
    IF (NAF.EQ.8) WRITE (6,88) NA,(RA(L),L=1,NA)
    IF (NOF.EQ.8) WRITE (6,87) NO,(RO(I),I=1,NO)
    IF (LM.EQ.0) GO TO 14
    RB(I)=-1.
    DO 1 I=2,7
      RB(I)=RB(I-1)+.5
    TRIE=2.*PIE
    MPIE=-PIE
    DXP=0.
    DXP=0.
    IF (NLINS.GT.1) DYP=YPRNG/(RLINS-1.)
    IF (NPTS.GT.1) DXP=XPRNG/(RPTS-1.)
    IF ((DGN.GE.1.) .AND. (NNN.EQ.2)) WRITE (6,64)
    IF (NNN.EQ.2) CALL BDGEN (G,H,SCF,DGN,NBD,BDA,KBD)
    DO 5 J=1,NLINS
      IF (DGN.GE.1.) WRITE (6,67) J
    RJM=J-1
    PHI=PHI+DELPHI*RJM

```

CAL01160  
 CAL01170  
 CAL01180  
 CAL01190  
 CAL01200  
 CAL01210  
 CAL01220  
 CAL01230  
 CAL01240  
 CAL01250  
 CAL01260  
 CAL01270  
 CAL01280  
 CAL01290  
 CAL01300  
 CAL01310  
 CAL01320  
 CAL01330  
 CAL01340  
 CAL01350  
 CAL01360  
 CAL01370  
 CAL01380  
 CAL01390  
 CAL01400  
 CAL01410  
 CAL01420  
 CAL01430  
 CAL01440  
 CAL01450  
 CAL01460  
 CAL01470  
 CAL01480  
 CAL01490  
 CAL01500  
 CAL01510  
 CAL01520  
 CAL01530  
 CAL01540  
 CAL01550  
 CAL01560  
 CAL01570  
 CAL01580  
 CAL01590  
 CAL01600  
 CAL01610  
 CAL01620  
 CAL01630



```

YP(J)=YPZERO+DYP*RJM
PSI=(PHI+90.)*PIE/180.
TAU=PSI-PHISYM
IF (LPT.EQ.0) GO TO 9
IF (LPT.EQ.1) WRITE (6,78) (ST,I=1,124)
IF (LPT.EQ.1) WRITE (6,74) (ST,I=1,95)
IF (LPT.EQ.1) AND.(LPT.GT.1) READ (5,79) ZZ
WRITE (6,86)
WRITE (6,85) Z,PHI,YP(J)
WRITE (6,76)
IF (MODE.EQ.1) WRITE (6,83) (RB(I),I=1,7)
IF (MODE.GT.1) WRITE (6,80) (RB(I),I=1,7)
WRITE (6,81) (DH,I=1,54),(PL,I=1,13)
YC=0
DO 3 I=1,NPTS
RJM=1-I,NPTS
THEO(I,I,J)=0.
CA(I,J)=0.
FA(I,J)=0.
ERR(I)=0.
CALC(I,J)=0.
RHO(I)=0.
XP(I)=XPZERO+DXP*RJM
XP1I=ABS(XP(I))
IF (XP1I.LT.1.E-10) XP(I)=0.
RS=SQRT(XP(I)**2+YP(J)**2)/HS
IF (RS.GT.1) GO TO 13
IHT=ATANM(YP(J),XP(I))
IF (XP1I.EQ.0.) IHT=0.
SIG=TAU-PIE/2.+IHT
IF (SIG.GT.PIE) SIG=SIG-PIE
IF (SIG.LT.MPIE) SIG=SIG+PIE
SIGI=SIG
XS=RS*CS(SIG)
IF (DGN.GE.1) WRITE (6,44) SIG
FORMAT (1,SIG=,E10.3)
IF (DGN.GE.5) WRITE (6,57) PHI,DELPHI,PSI,TAU,IHT,SIG,SIGI,XS,YS
FORMAT (1,ANGLES=,10E10.3)
RI=1
F=0.
IF (DGN.GE.2.) WRITE (6,66) I
CALL FUNCT (XS,YS,FA(I,J),NAF,DGN,NTWO)
IF (MODE.EQ.1) CALL FUNCT (XS,YS,F,NDF,DGN,MONE)
THEO(I,J)=F
IF (NNN.GE.2) REWIND 3
IF (NNN.GE.2) CALL FIELD (RS,SIGI,SOLN,NBD,BDA,DGN,KBD)
IF (NNN.EQ.1) CALL FIELD2 (RS,SIGI,SOLN,G,H,SCF,DGN)

```

9

44

57





CAL02120  
CAL02130  
CAL02140  
CAL02150  
CAL02160  
CAL02170  
CAL02180  
CAL02190  
CAL02200  
CAL02210

CAL02260  
CAL02270  
CAL02280  
CAL02290  
CAL02300  
CAL02310  
CAL02320  
CAL02330  
CAL02340  
CAL02350  
CAL02360  
CAL02370  
CAL02380  
CAL02390  
CAL02400  
CAL02410  
CAL02420  
CAL02430  
CAL02440  
CAL02450  
CAL02460  
CAL02470  
CAL02480  
CAL02490  
CAL02500  
CAL02510  
CAL02520  
CAL02530  
CAL02540  
CAL02550  
CAL02560  
CAL02570  
CAL02580  
CAL02590

```

CA(I)=SOLN/BOX/HS
CALC(I,J)=CA(I)-FA(I,J)
RHO(I)=RHOINF*(CALC(I,J)+1.)
ERR(I)=CA(I)
IF (MODE.EQ.1) ERR(I)=(CALC(I,J)-THEO(I,J))
IF (MODE.EQ.1) THEO(I,J)=FA(I,J)
IF (LPT.EQ.0) GO TO 3
LC=0
TL(I)=BL
TTL=0
IF ((XP(I).GT.XPM).AND.(XP(I).LT.XPR)) TTL=1.
IF (IC.EQ.5) IC=0
IF (IC.EQ.0) TL(I)=PL
DO 2 L=2,62
  TL(L)=BL
  IF ((I.EQ.1).OR.(TTL.EQ.1).OR.(I.EQ.NPTS)) TL(L)=PL
  IF (LC.EQ.10) LC=0
  IF ((IC.EQ.0).AND.(LC.EQ.0)) TL(L)=PL
  LC=LC+1
  TL(2)=PL
  TL(22)=PL
  TL(62)=PL
  IC=IC+1
  RLW=(CA(I)+1.)*20.+2.5
  LW=RLW
  IF (LW.GT.62) LW=62
  IF (LW.LT.2) LW=2
  TL(LW)=SC
  RLY=(FA(I,J)+1.)*20.+2.5
  LY=RLY
  IF (LY.GT.62) LY=62
  IF (LY.LT.2) LY=2
  IF (NAF.NE.0) TL(LY)=ST
  RLX=(THEO(I,J)+1.)*20.+2.5
  LX=RLX
  IF (LX.GT.62) LX=62
  IF (LX.LT.2) LX=2
  IF (MODE.EQ.1) TL(LX)=OH
  RLZ=(CALC(I,J)+1.)*20.+2.5
  LZ=RLZ
  IF (LZ.GT.62) LZ=62
  IF (LZ.LT.2) LZ=2
  TL(LZ)=EX
  WRITE (6,82) MOUT,KOUT,INDEX,THEO(I,J),ERR(I),CALC(I,J),RHO(I),
1 XPL(I),TL(I),L=1,62)
  IF ((NPTS.LE.20).AND.(I.NE.NPTS)) WRITE (6,79)
  CONTINUE
  IF (LPT.NE.0) WRITE (6,81) (DH,I=1,54),(PL,I=1,13)

```

13

2

3



CAL02600  
CAL02610  
CAL02620  
CAL02630  
CAL02640  
CAL02650  
CAL02660  
CAL02670  
CAL02680  
CAL02690  
CAL02700  
CAL02710  
CAL02720  
CAL02730  
CAL02740  
CAL02750  
CAL02760  
CAL02770  
CAL02780  
CAL02790  
CAL02800  
CAL02810  
CAL02820  
CAL02830  
CAL02840  
CAL02850  
CAL02860  
CAL02870  
CAL02880  
CAL02890  
CAL02900  
CAL02910  
CAL02920  
CAL02930  
CAL02940  
CAL02950  
CAL02960  
CAL02970  
CAL02980  
CAL02990  
CAL03000  
CAL03010  
CAL03020  
CAL03030  
CAL03040  
CAL03050  
CAL03060  
CAL03070

```

TMAX=0.
TMIN=0.
IE=0
BE=0.
EB=0.
DO 4 I=1,NPTS
  TH=THEO(I,J)      TMAX=TH
  IF (TH.GT.TMAX)    TMIN=TH
  IF (TH.LT.TMIN)    TMIN=TH
  ER=ABS(CALC(I,J)-TH)
  IF (ER.LE.BE) GO TO 4
  BE=ER
  IE=I
  CONTINUE
4  TMM=I
  TMM=TMAX-TMIN
  EB=RHOIN*(CALC(IE,J)-THEO(IE,J))
  IF (TMM.NE.0.) BE=(CALC(IE,J)-THEO(IE,J))*100./TMM
  IF ((MODE.EQ.1).AND.(LPT.NE.0)) WRITE (6,75) EB,XP(IE),BE
  IF (DELPHI.NE.0.) YP(J)=PHI
  CONTINUE
5  IF (BND.EQ.0.) GO TO 14
  IF (LPT.EQ.1) WRITE (6,78) (ST,I=1,124)
  IF (LPT.EQ.1) WRITE (6,74) (ST,I=1,95)
  IF (LPT.EQ.1).AND.(LPT.GT.1) READ (5,79) ZZ
  IF (CM5.EQ.1).AND.(LPT.GT.1) READ (5,79) ZZ
  CALL MAP (NPTS,NLINS,CALC,NOF,Z,BND)
  IF (DGN.NE.0.) WRITE (6,83)
  CALL MAP (NPTS,NLINS,CALC,NOF,Z,BND)
  IF (NAF.NE.0.) GO TO 10
  NAO=10*NOF+NAF
  IF (DGN.EQ.1).AND.(NGP.EQ.-3)) WRITE (6,62)
  IF (NGP.EQ.-3) CALL GPUNCH (Z,XO,YO,PHISYM,NAO,IMAX,JMAX,G)
  DO 7 I=1,IJMX
    G(I)=G(I)-GX(I,J)
  IF (IPT.EQ.1) GO TO 11
  IF (IPT.EQ.1).OR.(IPT.EQ.3) WRITE (6,78) (ST,I=1,124)
  IF (IPT.EQ.2).OR.(IPT.EQ.4) WRITE (6,74) (ST,I=1,95)
  IF ((CM5.EQ.1).AND.((IPT.EQ.2).OR.(IPT.EQ.4))) READ (5,79) ZZ
  CALL GPRINT (G,MONE)
  IF (NGP.EQ.-1) CALL GPUNCH (Z,XO,YO,PHISYM,NOF,IMAX,JMAX,G)
  IF (IPT.EQ.3) WRITE (6,78) (ST,I=1,124)
  IF (IPT.EQ.4) WRITE (6,74) (ST,I=1,95)
  IF (CM5.EQ.1).AND.((IPT.EQ.4)) READ (5,79) ZZ
  IF (IPT.EQ.3) CALL GPRINT (GA,NTWO)
  IF (IPT.EQ.0) GO TO 12
  IF (KPT.EQ.1).OR.(KPT.EQ.3) WRITE (6,78) (ST,I=1,124)
  IF (KPT.EQ.2).OR.(KPT.EQ.4) WRITE (6,74) (ST,I=1,95)
  IF (CM5.EQ.1).AND.((KPT.EQ.2).OR.(KPT.EQ.4))) READ (5,79) ZZ
  IF (DGN.EQ.1) WRITE (6,61)
  CALL GPRINT (G,GA,JMS)

```



```

12  WRITE (6,78) (EX,I=1,124)
    AGAIN=ST
    IF (CMS.NE.1.) READ(5,60) AGAIN
    IF (AGAIN.EQ.BL) GO TO 20
    WRITE (6,79)
    FORMAT (6F12.7)
    89  THE INPUT DATA FOR ADD-ON FUNCTION NO.8 ('I3,
    88  1, POINTS) WAS: '(//11F10.3//)
    87  1, POINTS) WAS: '(//11F10.3//)
    86  1, POINTS) WAS: '(//11F10.3//)
    85  FORMAT (1H//, ' THE INVERTED CROSS SECTION FOR: ')
    14HY, ' =, F8.3, ' CM., ' /10X, ' PHI=, ' F8.3, ' DEGREES, ' /10X,
    270X, ' * = ADD-ON FUNCTION, '
    84  FORMAT (1, ' ADJUST PAGE, HIT SPACE AND RETURN. ')
    83  FORMAT (1, ' LIMIT MAX ORIGINAL ABS. COMPUTED (MG/CC), ' /1
    1 K TERM FUNCTION ERROR FUNCTION DENSITY, ' 6H X, ' F4.1,
    26F10.1)
    82  1, (2X, 12, 1X, 13, 1X, 14, 1X, F9.4, 2X, F7.3, 1X, F9.4, 1X, F7.3,
    1F7.3, 1X, 62A1)
    81  FORMAT (3X, 54A1, 2X, A1, 12(4X, A1))
    80  1, LIMIT MAX, ' 3X, ' ADD-ON, ' 6X, ' THE, ' 4X, ' DENSITY (MG/CC), ' /
    1, M K TERM, ' 2X, ' FUNCTION, ' 5X, ' SUM, ' 3X, ' FUNCTION DENSITY, ' ,
    26H X, ' F4.1, 6F10.1)
    79  FORMAT (1X, F10.3)
    78  FORMAT (1X, 124A1)
    77  FORMAT (1X, //)
    76  1, INVERTED SUM, ' 70X, ' X = COMPUTED FUNCTION, '
    75  1, ' , ' 4X, F10.2, ' LARGEST ERROR: ' , F8.6, ' GMS/CC; AT ' 3HX, ' =, F6.3
    74  FORMAT (1X, 47A1, ' SET PAGE, HIT SPACE, RETURN ' , 48A1)
    69  FORMAT (1, ' CALL FREAD, '
    68  FORMAT (1, ' CALL GARRAY, '
    67  FORMAT (1, ' LINE, ' 13, ' DO LOOP, ' )
    66  FORMAT (1, ' POINT, ' 13, ' CALL FUNCT, ' )
    65  FORMAT (1, ' CALL FIELD, '
    64  FORMAT (1, ' CALL BDGEN, '
    63  FORMAT (1, ' CALL MAP, '
    62  FORMAT (1, ' CALL GPUNCH, '
    61  FORMAT (1, ' CALL GLOT, '
    60  FORMAT (80A1)
    STOP
    END
C000001
C

```



```

SUBROUTINE BDGEN (G,H,SCF,DGN,NBD,BDA,KBD)
C
C BDGEN EVALUATES THE B AND D COEFFICIENTS FOR ALL M AND K, AND WRITES
C THE ARRAY LINEARLY ON DISK.
C
COMMON IMAX,JMAX,IIMX,JJMX,IJMX,ALPHA,SIZE,EPS,MODE,BOX,SD,IX,Z
COMMON /TAB/ INDEX,KEXTRA,ME,XTRA,KLIMIT,MLIMIT,KOUT,MOUT
COMMON /SYM/ ISYM,JSYM,MSYM,FCU,IHS,JMS,QSYM
DIMENSION G(IJMX),H(IIMX,5),SCF(JJMX,6),BDA(KBD)
C INITIALIZE THE VALUES:
INDEX=0
KLG=NBD*KLIMIT
REWIND 3
JJMX=6
IIMX2=(IIMX+1)/2
PIE=3.141592653589793
RIMAX=IMAX
KLMP=KLIMIT+1
DX=2./RIMAX
RJMAX=JMAX
DXI=2.*PIE/FCU
C INITIALIZE THE MODIFIED HERMITE POLYNOMIAL ARRAY; VECTORS:
C (1)=H1, (2)=H2, (3)=ALPHA*X(I), (4)=HM+2 STORED, (5)=HM+1 STORED
DO 1 I=1,IIMX2
RII=I
IIM=IIMX-I+1
H(I,1,3)=ALPHA*(RII*DX-DX-1.)
H(IIM,3)=-H(I,1,3)
H(I,1,2)=H(I,1,3)
H(I,2)=H(I,1,3)*H(I,1)-1./3.
H(IIM,1)=-H(I,1)
H(IIM,2)=H(I,1,2)
H(I,5)=H(I,1,2)
H(IIM,5)=H(IIM,2)
H(I,4)=H(I,1)
H(IIM,4)=H(IIM,1)
SIGN=1.
C INITIALIZE THE SIN/COS ARRAY:
DO 2 J=1,JJMX
RJM=J-1
SCF(J,1)=0.
SCF(J,2)=1.
SCF(J,3)=SIN(RJM*DXI-PIE/2.)
SCF(J,4)=COS(RJM*DXI-PIE/2.)
SCF(J,5)=0.
SCF(J,6)=0.
MS=0
C COMMENCE THE M LOOP:

```

```

SUB00030
SUB00040
SUB00050
SUB00060
SUB00070
SUB00080
SUB00090
SUB00100
SUB00110
SUB00120
SUB00130
SUB00140
SUB00150
SUB00160
SUB00170
SUB00180
SUB00190
SUB00200
SUB00210
SUB00220
SUB00230
SUB00240
SUB00250
SUB00260
SUB00270
SUB00280
SUB00290
SUB00300
SUB00310
SUB00320
SUB00330
SUB00340
SUB00350
SUB00360
SUB00370
SUB00380
SUB00390
SUB00400
SUB00410
SUB00420
SUB00430
SUB00440
SUB00450
SUB00460
SUB00470
SUB00480
SUB00490
SUB00500

```





```

DO 7 MP=1,MLIMIT
M=MP-1
RM=RM
SIGN=-SIGN
IF (DGN.LE.-4) WRITE (6,88) SCF(1,1),SCF(2,1),SCF(1,2),SCF(2,2)
TEST FOR SYMMETRY SKIPS:
IF (MS.EQ.MSYM) MS=0
TOTAL=0.
MS=MS+1
IF (MS.NE.1) GO TO 6
C COMMENCE THE K LOOP:
DO 5 KP=1,KLIMIT
K=KP-1
PK=K*P
RK=K
INDEX=INDEX+1
C CALL THE B & D COEFFICIENTS AND WRITE THEM ON DISK:
CALL BD (M,K,G,H,SCF,B,D,JMX6)
IF (DGN.EQ.3) WRITE(6,89) M,K,B,D
IF (DGN.LE.-2) WRITE (6,89) M,K,B,D
IF (DGN.LE.-4) WRITE (6,88) H(1,1),H(1,2),H(1,4),H(1,5)
KK=K*NBD+1
K2=K*P*NBD
BDA(K2)=D
BDA(KK)=B
C GENERATE THE NEXT ORDER OF THE SET OF HERMITE POLYNOMIALS FOR NEW K:
ORDER=M+2*KP+1
HA=SQRT(PK*(PK+RM))/ORDER
HB=2.*SQRT((PK+1)*(RM+PK+1.))/(ORDER+1.)/(ORDER+2.)
DO 5 II=1,IIMX2
IIM=IIMX-1+1
H(II,1)=2.*H(II,3)*H(II,2)-HA*H(II,1)
H(II,1)=SIGN*H(II,1)
H(II,2)=HB*H(II,3)*H(II,1)-ORDER*H(II,2)
C ADVANCE THE SIN/COS ARRAY FOR THE NEXT M:
DO 3 J=1,JYX
IF (DGN.LE.-5) WRITE (6,87) (SCF(J,NT),NT=1,6)
FORMAT(1,5) SIN/COS MX1:8E10.3)
STEM=SCF(J,1)
SCF(J,1)=SCF(J,1)*SCF(J,4)+SCF(J,2)*SCF(J,3)
SCF(J,2)=SCF(J,2)*SCF(J,4)-STEM*SCF(J,3)
DO 4 J=1,JMAX
SCF(J,5)=SCF(J+1,1)-SCF(J,1)
SCF(J,6)=SCF(J+1,2)-SCF(J,2)
WRITE (3) (BDA(I),I=1,KBD)
IF (DGN.LE.-3) WRITE (6,88) (BDA(I),I=1,10)
IF (LSYM.GT.JMAX) RETURN
RM=RM+1

```

SUB00510  
SUB00520  
SUB00530  
SUB00540  
SUB00550  
SUB00560  
SUB00570  
SUB00580  
SUB00590  
SUB00600  
SUB00610  
SUB00620  
SUB00630  
SUB00640  
SUB00650  
SUB00660  
SUB00670  
SUB00680  
  
SUB00690  
SUB00700  
SUB00710  
SUB00720  
SUB00730  
SUB00740  
SUB00750  
SUB00760  
SUB00770  
SUB00780  
SUB00790  
SUB00800  
SUB00810  
SUB00820  
SUB00830  
SUB00840  
SUB00850  
SUB00860  
SUB00870  
SUB00880  
SUB00890  
SUB00900  
SUB00910  
SUB00920  
SUB00930  
SUB00940  
SUB00950  
SUB00960  
SUB00970



```

C REGENERATE THE HERMITE ARRAY FOR NEW M, K=0:
DO 7 II=1, IIMX2
  IIM=IIMX-II+1
  H(II,2)=H(II,4)*SQRT(RM)/(RM+1.)
  H(II,1)=H(II,5)*(RM+2.)
  H(II,1)=-SIGN#H(II,1)
  H(II,1)=2.*SQRT(RM+1.)*(H(II,3)*H(II,1)-(RM+1.)*H(II,2))
  H(II,2)=H(II,2)/(RM+2.)/(RM+3.)
  H(II,4)=H(II,1)
  H(II,5)=H(II,2)
79 FORMAT (' M=', I4, ' K=', I4, ' B=', E10.4, ' D=', E10.4)
88 RETURN
END
C000002
C

SUBROUTINE FIELD (RS, SIG, SOLN, NBD, BDA, DGN, KBD)
C
C FIELD EVALUATES THE VALUE OF THE FIELD FUNCTION AT A PARTICULAR
C POINT DESIGNATED IN CYLINDRICAL COORDINATES, BY USING THE INVERSION
C EQUATION OF MALDONADO, ET.AL. FIELD USES THE ARRAY OF B & D
C COEFFICIENTS GENERATED IN SUBROUTINE BDGEN.
C
COMMON IMAX, JMAX, IIMX, JIMX, IJMX, ALPHA, SIZE, EPS, MODE, BOX, SD, IX, Z
COMMON /TAB/ INDEX, KEXTRA, MEXTRA, KLIMIT, MLIMIT, KOUT, MOUT
COMMON /SYM/ ISYM, JSYM, MSYM, FCU, IMS, JMS, QSYM
DIMENSION BDA(KBD), STK(52), STM(52)
C INITIALIZE THE VALUES:
INDEX=0
MTIMER=0
KOUT=0
MOUT=0
MMAX=0
KMAX=0
TOTAL=0.
IJMX6=IJMX*6
REWIND 3
AR=ALPHA*RS
ARG=AR*#2
EXPON=EXP(-ARG)
PIE=3.141592653589793
APP=ALPHA/PIE/PIE
M=0
RM=M
RIMAX=IMAX
DX=2./RIMAX
C
SUB000980
SUB000990
SUB001000
SUB001010
SUB001020
SUB001030
SUB001040
SUB001050
SUB001060
SUB001070
SUB001080
SUB001090
SUB001100
SUB001110
SUB001120
SUB001130
C
SUB001140
SUB001150
SUB001160
SUB001170
SUB001180
SUB001190
SUB001200
SUB001210
SUB001220
SUB001230
SUB001240
SUB001250
SUB001260
SUB001270
SUB001280
SUB001290
SUB001300
SUB001310
SUB001320
SUB001330
SUB001340
SUB001350
SUB001360
SUB001370
SUB001380
SUB001390
SUB001400
SUB001410
SUB001420
SUB001430

```



SUB01440  
SUB01450  
SUB01460  
SUB01470  
SUB01480  
SUB01490  
SUB01500  
SUB01510  
SUB01520  
SUB01530  
SUB01540  
SUB01550  
SUB01560  
SUB01570  
SUB01580  
SUB01590  
SUB01600  
SUB01610  
SUB01620  
SUB01630  
SUB01640  
SUB01650  
SUB01660  
SUB01670  
SUB01680  
SUB01690  
SUB01700  
SUB01710  
SUB01720  
SUB01730  
SUB01740  
SUB01750  
SUB01760  
SUB01770  
SUB01780  
SUB01790  
SUB01800  
SUB01810  
SUB01820  
SUB01830  
SUB01840  
SUB01850  
SUB01860  
SUB01870  
SUB01880  
SUB01890  
SUB01900  
SUB01910

```

RJMAX=JMAX
SIGN=1.
STK(1)=0.
STM(1)=0.
SMS=0.
CMS=1.
SM=SIGN(SIG)
CM=COS(SIG)
MEP=ME*EXTRA+1
DO 16 MB=1,MEP
  STM(MB)=0.
  FM=1.
  MS=0.
  C      COMMENCE THE M LOOP:
  2      SIGN=-SIGN
      K=0
      RK=K
      RM=M
      ARM=1.
      IF (M.NE.0) ARM=ARM**M
      KTIMER=0
      KEP=KE*EXTRA+1
      DO 15 KB=1,KEP
        STK(KB)=0.
        SIGNK=-1.
        C      COMPUTE THE K=0 & K=1 ORDERS OF LAGUERRE POLYNOMIAL FOR GIVEN M:
        15      PM=0.
            P=SQRT(1./FM)
            PP=CRM+1.-ARG)*SQRT(1./FM/(RM+1.))
            C      TEST FOR SYMMETRY SKIPS:
            IF (MS.EQ.MSYM) MS=0
            MS=MS+1
            IF (MS.NE.1) GO TO 7
            C      READ A LINE OF B & D COEFFICIENTS FOR GIVEN M:
            READ (3) (BDA(I),I=1,KBD)
            IF (IDGN.LE.-6) WRITE (6,88) (BDA(I),I=1,10)
            C      COMMENCE THE K LOOP:
            3      INDEX=INDEX+1
            SIGNK=-SIGNK
            C      COMPUTE THE M,K SUMMATION TERM:
            KK=K#NBD+1
            B=BDA(KK)
            D=0.
            IF (NBD.EQ.2) D=BDA(KK+1)
            BRACKET=B
            IF (RM.EQ.0.) GO TO 4
            BRACKET=B*CMS+D*SMS
            ADD=SIGNK*BRACKET*P*ARM
            4

```



```

SUB01920
SUB01930
SUB01940
SUB01950
SUB01960
SUB01970
SUB01980
SUB01990
SUB02000
SUB02010
SUB02020
SUB02030
SUB02040
SUB02050
SUB02060
SUB02070
SUB02080
SUB02090
SUB02100
SUB02110
SUB02120
SUB02130
SUB02140
SUB02150
SUB02160
SUB02170
SUB02180
SUB02190
SUB02200
SUB02210
SUB02220
SUB02230
SUB02240
SUB02250
SUB02260
SUB02270
SUB02280
SUB02290
SUB02300
SUB02310
SUB02320
SUB02330
SUB02340
SUB02350
SUB02360
SUB02370
SUB02380
SUB02390

TOTAL=TOTAL+ADD
IF (DCN.GT.-5) GO TO 5
STOT=TOTAL*EXPON*APP/BOX/SIZE
WRITE (6,89) M,K,STOT,ADD,BRAKET,P,ARM,B,CMS,D,SMS
ESTABLISH CHECK,K AS THE RELATIVE SIZE OF THE M,K TERM OF THE SERIES:
5 CHECK=ABS(ADD)
IF (TOTAL.GT.EPS) CHECK=ABS(ADD/TOTAL)
C ADVANCE THE K INDEX:
K=K+1
RK=K
DO 10 KA=1,KEXTRA
KB=KEXTRA-KA+1
STK(KB+1)=STK(KB)
10 STK(2)=TOTAL
ORDER=M+2*K+1
C GENERATE THE NEXT ORDER OF LAGUERRE POLYNOMIAL FOR NEW K:
PM=P
PP=PP*(ORDER-ARG)-PM*SQRT(RK*(RM+RK))
PP=PP/SORT((RK+1.)*(RM+RK+1.))
C SET K TIMER TO PROVIDE EXTRA K TERMS AFTER CHECK < EPS:
KTIMER=KTIMER+1
IF (K.GE.KLIMIT) GO TO 6
IF (CHECK.GE.EPS) KTIMER=0
IF (KTIMER.LE.KEXTRA) GO TO 3
GO TO 7
6 KOUT=KOUT+1
IF (KEXTRA.EQ.0) GO TO 7
TOTAL=0.
DO 11 KA=1,KEXTRA
11 TOTAL=TOTAL+STK(KA+1)
RX=KEXTRA
TOTAL=TOTAL/RX
C END OF K LOOP; ADVANCE M:
M=M+1
RM=M
RNM=SMS
STP=SMS*CMS*CMS*SMI
SMS=SMS*CMS*SMI
CMS=CMS*CMS*SMI
IF (K.GT.KMAX) KMAX=K
FM=FM*RM
DO 12 MA=1,MEXTRA
12 STM(MB+1)=STM(MB)
MB=MEXTRA-MA+1
STM(2)=TOTAL
C SET M TIMER FOR EXTRA M TERMS:
IF (MS.EQ.1) MTIMER=MTIMER+1
IF (JSYM.GT.JMAX) GO TO 9

```









SUB02850  
SUB02860  
SUB02870  
SUB02880  
SUB02890  
SUB02900  
SUB02910  
SUB02920  
SUB02930  
SUB02940  
SUB02950  
SUB02960  
SUB02970  
SUB02980  
SUB02990  
SUB03000  
SUB03010  
SUB03020  
SUB03030  
SUB03040  
SUB03050  
SUB03060  
SUB03070  
SUB03080  
SUB03090  
SUB03100  
SUB03110  
SUB03120  
SUB03130  
SUB03140  
  
SUB03160  
SUB03170  
SUB03180  
SUB03190  
SUB03200  
SUB03210  
SUB03220  
SUB03230  
SUB03240

SUB03250  
SUB03260  
SUB03270  
SUB03280  
SUB03290  
SUB03300

```

1      DH=H(I)-H(I)
      B=B+G(IJ)*S*DH
      B=B*QSYM/2.
      RETURN
2      DO 3 J=1,JMAX
      JS=J+JMX4
      S=SCF(JS)/RM
      DO 3 I=1,IMAX
      I1=I+1
      I1=IMAX*(J-1)+I
      DH=H(I1)-H(I)
      B=B+G(IJ)*S*DH
      B=B*QSYM
      RETURN
3      IF (M.NE.0) GO TO 6
4      S=DX1
      DO 5 J=1,JMAX
      DO 5 I=1,IMAX
      I1=I+1
      I1=IMAX*(J-1)+I
      DH=H(I1)-H(I)
      B=B+G(IJ)*S*DH
      B=B/2.
      RETURN
5      DO 7 J=1,JMAX
      JS=J+JMX4
      J2=JS+JMX
      S=SCF(JS)/RM
      C=SCF(J2)/RM
      DO 7 I=1,IMAX
      I1=I+1
      I1=IMAX*(J-1)+I
      DH=H(I1)-H(I)
      B=B+G(IJ)*S*DH
      B=B*QSYM
      RETURN
66     FORMAT (' BD:',4I5,10F6.2)
7      D=D-G(IJ)*C*DH
      RETURN
      END
      C000004
      C

```

SUBROUTINE FIELD2 (RS,SIG,SOLN,G,H,SCF,DGN)

C FIELD2 COMPUTES THE SAME INVERSION AS SUBROUTINE FIELD, EXCEPT THAT  
C THE COEFFICIENTS B AND D ARE COMPUTED INDIVIDUALLY AS USED BY  
C CALLING BD. DISK STORAGE IS NOT REQUIRED, BUT COMPUTING TIME IS  
C MUCH GREATER. FIELD2 IS UTILIZED BY SPECIFYING A NEGATIVE MODE ON



```

C THE INPUT PARAMETER.
C FIELD EVALUATES THE VALUE OF THE FIELD FUNCTION AT A PARTICULAR
C POINT DESIGNATED IN CYLINDRICAL COORDINATES, BY USING THE INVERSION
C EQUATION OF MALDONADO, ET AL. FIELD CALLS SUBROUTINES BD & GARRAY.
SUB03310
SUB03320
SUB03330
SUB03340
SUB03350
SUB03360
SUB03370
SUB03380
SUB03390
SUB03400
SUB03410
SUB03420
SUB03430
SUB03440
SUB03450
SUB03460
SUB03470
SUB03480
SUB03490
SUB03500
SUB03510
SUB03520
SUB03530
SUB03540
SUB03550
SUB03560
SUB03570
SUB03580
SUB03590
SUB03600
SUB03610
SUB03620
SUB03630
SUB03640
SUB03650
SUB03660
SUB03670
SUB03680
SUB03690
SUB03700
SUB03710
SUB03720
SUB03730
SUB03740
SUB03750
SUB03760
SUB03770
SUB03780

C COMMON IMAX, JMAX, IIMX, JJMX, IJMX, ALPHA, SIZE, EPS, MODE, BOX, SD, IX, Z
COMMON /TAB/ INDEX, KEXTRA, MEXTRA, KLIMIT, ALIMIT, KOUT, MOUT
COMMON /SYM/ ISYM, JSYM, MSYM, FCU, IMS, JMS, QSYM
C DIMENSION G(IJMX), H(IIMX,5), SCF(JJMX,6)
C INITIALIZE THE VALUES:
INDEX=0
IIMX=0
JJMX=0
KOUT=0
MOUT=0
MMAX=0
KMAX=0
TOTAL=0.
JJMX6=JJMX*6
IIMX2=(IIMX+1)/2
AR=ALPHA*RS
ARG=AR**2
EXPON=EXP(-ARG)
PIE=3.141592653589793
APP=ALPHA/PIE/PIE
M=0
RM=M
RIMAX=IMAX
DX=2./RIMAX
RJMAX=JMAX
DXI=2.*PIE/FCU
C INITIALIZE THE MODIFIED HERMITE POLYNOMIAL ARRAY; VECTORS:
C (1)=H1, (2)=H2, (3)=ALPHA*X(I), (4)=HM+2 STORED, (5)=HM+1 STORED
DO I=1, IIMX2
  RI=I
  IIM=IIMX-I+1
  IIM=IIMX-I+1
  H(I,1,3)=ALPHA*(RI*DX-DX-1.)
  H(I,1,3)=-H(I,1,3)
  H(I,1,2)=2.*H(I,1,3)
  H(I,1,2)=(H(I,1,3))*H(I,1,1)
  H(IIM,1)=H(I,1,1)
  H(IIM,2)=H(I,1,2)
  H(I,1,5)=H(I,1,2)
  H(IIM,5)=H(IIM,2)
  H(I,1,4)=H(I,1,1)
  H(IIM,4)=H(IIM,1)
  SIGN=1.
  PM=1.
C INITIALIZE THE SIN/COS ARRAY:

```



```

SUB03790
SUB03800
SUB03810
SUB03820
SUB03830
SUB03840
SUB03850
SUB03860
SUB03870
SUB03880
SUB03890
SUB03900
SUB03910
SUB03920
SUB03930
SUB03940
SUB03950
SUB03960
SUB03970
SUB03980
SUB03990
SUB04000
SUB04010
SUB04020
SUB04030
SUB04040
SUB04050
SUB04060
SUB04070
SUB04080
SUB04090
SUB04100
SUB04110
SUB04120
SUB04130
SUB04140
SUB04150
SUB04160
SUB04170
SUB04180
SUB04190
SUB04200
SUB04210
SUB04220
SUB04230
SUB04240
SUB04250
SUB04260

DO 11 J=1,JMX
  RJM=J-1
  SCF(J,1)=0.
  SCF(J,2)=1.
  SCF(J,3)=SIN(RJM*DXI-PIE)
  SCF(J,4)=COS(RJM*DXI-PIE)
  SCF(J,5)=0.
  SCF(J,6)=0.
  MS=0
11  COMMENCE THE M LOOP:
2    SIGN=-SIGN
    K=0
    RK=K
    ARM=1.
    IF (M.NE.0) ARM=AR***
    KTIMER=0
    SIGNK=-1.
    PM=0.
    C COMPUTE THE K=0 & K=1 ORDERS OF LAGUERRE POLYNOMIAL FOR GIVEN M:
      P=SQRT(1./FM)
      PP=(RM+1.-ARG)*SQRT(1./FM/(RM+1.))
    C ADVANCE THE SIN/COS ARRAY FOR NEW M:
      DO 12 J=1,JMX
        SCF(J,1)=SCF(J,1)*SCF(J,4)+SCF(J,2)*SCF(J,3}
        SCF(J,2)=SCF(J,2)*SCF(J,4)-SCF(J,1)*SCF(J,3}
        DO 13 J=1,JMAX
          SCF(J,2)=SCF(J+1,1)-SCF(J,1)
          SCF(J,3)=SCF(J+1,2)-SCF(J,2)
12  C TEST FOR SYMMETRY SKIPS:
        IF (MS.EQ.MSYM) MS=0
        TOTAL=0.
        MS=MS+1
        IF (MS.NE.1) GO TO 7
        RMS=RM*SIG
        CMS=COS(RMS)
        SMS=SIN(RMS)
    C COMMENCE THE K LOOP:
      INDEX=INDEX+1
      SIGNK=-SIGNK
    C CALL THE B & D COEFFICIENTS AND COMPUTE THE M,K SUMMATION TERM:
      CALL BD (M,K,G,H,SCF,B,D,JMX*6)
      IF (DGN.LE.-2.) WRITE (6,89) M,K,B,D
      BRACKET=B
      IF (RM.EQ.0.) GO TO 4
      BRACKET=BRACKET+D*SMS
      ADD=SIGNK*BRACKET*P*ARM
      TOTAL=TOTAL+ADD
    C ESTABLISH CHECK AS THE RELATIVE SIZE OF THE M,K TERM OF THE SERIES:

```





```

SUB04270
SUB04280
SUB04290
SUB04300
SUB04310
SUB04320
SUB04330
SUB04340
SUB04350
SUB04360
SUB04370
SUB04380
SUB04390
SUB04400
SUB04410
SUB04420
SUB04430
SUB04440
SUB04450
SUB04460
SUB04470
SUB04480
SUB04490
SUB04500
SUB04510
SUB04520
SUB04530
SUB04540
SUB04550
SUB04560
SUB04570
SUB04580
SUB04590
SUB04600
SUB04610
SUB04620
SUB04630
SUB04640
SUB04650
SUB04660
SUB04670
SUB04680
SUB04690
SUB04700
SUB04710
SUB04720
SUB04730
SUB04740

CHECK=ABS(ADD)
IF (TOTAL.GT.EPS) CHECK=ABS(ADD/TOTAL)
C ADVANCE THE K INDEX:
K=K+1
RK=K
ORDER=M+2*K+1
C GENERATE THE NEXT ORDER OF LAGUERRE POLYNOMIAL FOR NEW K:
PM=PP
PP=PP*(ORDER-ARG)-PM*SQRT(RK*(RM+RK))
PP=PP/SQRT((RK+1.)*(RM+RK+1.))
C GENERATE THE NEXT ORDER OF THE SET OF HERMITE POLYNOMIALS FOR NEW K:
HA=SQRT(RK*(RK+RM))/ORDER
HB=2.*SQRT((RK+1.)*(RM+RK+1.))/(ORDER+1.)/(ORDER+2.)
DO 5 I=1,IIMX2
IIM=IIMX-I+1
HII,1)=2.*H(II,3)*H(II,2)-HA*H(II,1))
HII,1)=SIGN*H(II,1)
HII,2)=HB*(H(II,3)*H(II,1)-ORDER*H(II,2))
C SET K TIMER TO PROVIDE EXTRA K TERMS AFTER CHECK < EPS:
KTIMER=KTIMER+1
IF (K.GE.KLIMIT) GO TO 6
IF (CHECK.GE.EPS) KTIMER=0
IF (KTIMER.LE.KEXTRA) GO TO 3
GO TO 7
C END OF K LOOP; ADVANCE M AND COMPUTE NEW TOTAL:
KOUT=KOUT+1
M=M+1
IF (K.GT.KMAX) KMAX=K
RM=FM*RM
C REGENERATE THE HERMITE ARRAY FOR NEW M, K=0:
DO 8 I=1,IIMX2
IIM=IIMX-I+1
HII,2)=HII,4)*SQRT(RM)/(RM+1.)
HII,1)=HII,5)*SQRT(RM)/(RM+2.)
HII,1)=SIGN*H(II,1)
HII,2)=2.*SQRT(RM+1.)*H(II,3)*H(II,1)-(RM+1.)*H(II,2))
HII,2)=HII,2)/(RM+2.)/(RM+3.)
HII,4)=HII,1)
HII,5)=HII,2)
C SET M TIMER FOR EXTRA M TERMS:
IF (MS.EQ.1) MTIMER=MTIMER+1
IF (JSYM.GT.JMAX) GO TO 9
IF (K.GT.KEXTRA) MTIMER=0
IF (M.GE.KLIMIT) GO TO 9
IF (MTIMER.LE.MEXTRA) GO TO 2
C END OF M LOOP; COMPUTE OUTPUT SOLN.

```



```

9      MOUT=M-1
      IF (KOUT.EQ.0) KOUT=KMAX-1
      SOLN=TOTAL*EXPON*APP/2.
      FORMAT ('M=,I4,', K=,I4,', B=,E10.4,', D=,E10.4)
      RETURN
      END
89
C000005
C
SUBROUTINE GARRAY (G,GA,NOF,DGN,NUMB,XO,YO,PHISYM)
C
C GARRAY FILLS THE DATA ARRAY OVER AN ORTHOGONAL AREA WITH
C THE REGULAR DATA OBTAINED BY THE METHOD CORRESPONDING TO THE
C PARTICULAR MODE:
C
C   MODE 1 - DATA OBTAINED BY SAMPLING A KNOWN FUNCTION SUPPLIED
C             IN SUBROUTINE FUNCT AND SAMPLED IN SUBROUTINE GOLF.
C
C   MODE 2 - DATA OBTAINED BY GENERATING A REGULAR ARRAY FROM
C             IRREGULAR EXPERIMENTAL INPUT DATA READ IN. CALLS
C             SUBROUTINE SHEET. (EXPERIMENTAL DATA MAY
C             BE SIMULATED, SEE 'SHEET')
C
C   MODE 3 - UTILIZES RAW DATA TAKEN AT THE PROPER INTERVAL,
C             OR PREVIOUSLY GENERATED, AND READ DIRECTLY INTO THE
C             GARRAY. CALLS SUBROUTINE READ.
C
C COMMON IMAX,JMAX,IMX,JMX,IJMX,JSYM,ALPHA,SIZE,EPS,MODE,BOX,SD,IX,Z
C COMMON /SYM/ JSYM,JSYM,MSYM,FCU,IMS,JMS,QSYM
C COMMON /IO/ CMS,IN1,IN2,IN4
C DIMENSION G(IMAX,JMAX),GA(IMAX,JMAX)
C PIE=3.141592653589793
C HS=SIZE/2.
C IF (MODE.GT.3) MODE=1
C RIMX=IMAX
C JIMX=JMAX
C DELR=SIZE/RIMX
C DELXI=2.*PIE/FCU
C IF (MODE.GT.1) GO TO 2
C DO 1 J=1,JMS
C RJ=J
C XI=(RJ-.5)*DELXI-PIE
C J2=J+2*(JMS-J)
C J3=J+JMAX/2
C J4=J2+JMAX/2
SUB004750
SUB004760
SUB004770
SUB004780
SUB004790
SUB004800
SUB004810
SUB004820
SUB000010
SUB000020
SUB000030
SUB000040
SUB000050
SUB000060
SUB000070
SUB000080
SUB000090
SUB000100
SUB000110
SUB000120
SUB000130
SUB000140
SUB000150
SUB000160
SUB000170
SUB000180
SUB000190
SUB000200
SUB000210
SUB000220
SUB000230
SUB000240
SUB000250
SUB000260
SUB000270
SUB000280
SUB000290
SUB000300
SUB000310
SUB000320
SUB000330
SUB000340
SUB000350
SUB000360
SUB000370
SUB000380

```



```

SUB000390
SUB000400
SUB000410
SUB000420
SUB000430
SUB000440
SUB000450
SUB000460
SUB000470
SUB000480
SUB000490
SUB000500
SUB000510
SUB000520
SUB000530
SUB000540
SUB000550
SUB000560
SUB000570
SUB000580
SUB000590
SUB000600
SUB000610
SUB000620

DO 1 I=1,IMS
RI=I
II=I*MAX+1-I
R=(RI-.5)*DELR-HS
CALL GOLF (R,XI,GIJ,NOF,DGN,NUMB)
C 1 I,J=GIJ
IF (ISYM.EQ.2) G(I,I,J)=GIJ
IF (ISYM.EQ.2) GO TO 1
G(I,I,J3)=GIJ
IF (JSYM.EQ.0) GO TO 1
G(I,J2)=GIJ
G(I,I,J4)=GIJ
CONTINUE
GO TO 4
1
2 IF (MODE.GT.2) GO TO 3
CALL SHEET (G,GA,XO,YO,PHISYM,NOF)
GO TO 4
3 CALL READ (Z,XO,YO,PHISYM,NOF,IMAX,JMAX,G)
4 IF (DGN.GE.2) WRITE (6,39)
39 RETURN
FORMAT (' GARRAY RETURNS')
END
C000006
C

```

```

SUB000630
SUB000640
SUB000650
SUB000660
SUB000670
SUB000680
SUB000690
SUB000700
SUB000710
SUB000720
SUB000730
SUB000740
SUB000750
SUB000760
SUB000770
SUB000780
SUB000790
SUB000800
SUB000810
SUB000820
SUB000830
SUB000840

SUBROUTINE GOLF (R,XI,GIJ,NOF,DGN,NUMB)
C
C GOLF COMPUTES THE FUNCTION G(R,XI) FOR A PARTICULAR LINE OF SIGHT
C FROM A KNOWN FUNCTION CONTAINED IN SUBROUTINE FUNCT.
C
COMMON IMAX,JMAX,IIMX,JJMX,IJMX,ALPHA,SIZE,EPS,MODE,BOX,SD,IX,Z
ZERO=0.
LMAX=I*MAX*3
RLMAX=LMAX
DELXP=SIZE/RLMAX
SXI=SIN(XI)
CXI=COS(XI)
DELXS=DELXP*CXI
DELYS=DELXP*SXI
XP=DELXP*.5*SIZE/2.
XS=XP*CXI-R*SXI
YS=XP*SXI+R*CXI
GIJ=0.
DO 1 L=1,LMAX
RL=L
CALL FUNCT(XS,YS,F,NOF,DGN,NUMB)
GIJ=GIJ+F
C

```



```

1      XS=XS*DELYS
      YS=YS*DELYS
      IF (GIJ.NE.0.) GIJ=GIJ*DELYP*BOX
      IF (SD.EQ.0.) OR (NUMB.EQ.1) GO TO 2
      IF (DON.GE.3) WRITE (6,28) IX
      CALL GAUSS (IX,SD,ZERO,RV)
      GIJ=GIJ+RV
2      IF (DON.GE.3) WRITE (6,29) R,XI,GIJ
      RETURN
29     FORMAT (' R=',F8.3,' XI=',F8.3,' GIJ=',F8.3)
28     FORMAT (' GAUSS, IX=',I8)
      END
C000007
C

      SUBROUTINE FUNCT (XS,YS,F,NOF,DGN,NUMB)
C
CP67USERID 109580XJ
C
C      FUNCT EVALUATES AS INPUT FUNCTION AT POSITION (X,Y) IN THE TEST
C      SECTION COORDINATE SYSTEM. NOF IDENTIFIES THE EQUATION USED.
C
COMMON IMAX,IMAX,IIMX,IJMX,ALPHA,SIZE,EPS,MODE,BOX,SD,IX,Z
COMMON /EQPAR/A,B,C,D,E,P,Q,S,T,U,V,W,RO,RA,NO,NA,N1,N2
DIMENSION RO(101),RA(101)
AA=A
BB=B
CC=C
DD=D
EE=E
PP=P
IF (NUMB.LE.1) GO TO 50
AA=S
BB=T
CC=U
DD=V
EE=W
PP=Q
PIE=3.141592653589793
HS=SIZE/2.
R=SQRT(XS**2+YS**2)/HS
F=0.
IF (R.GT.1.) GO TO 11
IF (NOF.LE.0) GO TO 11
C
C 1. AXISYMMETRIC GAUSSIAN:
SUB00850
SUB00860
SUB00870
SUB00880
SUB00890
SUB00900
SUB00910
SUB00920
SUB00930
SUB00940
SUB00950
SUB00960
SUB00970
SUB00980
SUB00990
SUB01000
SUB01020
SUB01030
SUB01040
SUB01050
SUB01060
SUB01070
SUB01080
SUB01090
SUB01100
SUB01110
SUB01120
SUB01130
SUB01140
SUB01150
SUB01160
SUB01170
SUB01180
SUB01190
SUB01200
SUB01210
SUB01220
SUB01230
SUB01240
SUB01250
SUB01260
SUB01270
SUB01280

```





```

1 IF (NOF.GT.1) GO TO 2
C F=AA*EXP(-1.*(R*HS/BB)**2)
C GO TO 11
SUB011290

2. ADJUSTABLE RECTANGULAR STEP FUNCTION:
C IF (NOF.GT.2) GO TO 3
C F=PP
C IF ((ABS(XS-DD)).LE.BB).AND.(ABS(YS-EE).LE.CC)) F=AA
C GO TO 11
SUB011300
SUB011310
SUB011320
SUB011330
SUB011340
SUB011350
SUB011360
SUB011370
SUB011380
SUB011390
SUB011400
SUB011410
SUB011420
SUB011430
SUB011440
SUB011450
SUB011460
SUB011470
SUB011480
SUB011490
SUB011500
SUB011510
SUB011520
SUB011530
SUB011540
SUB011550
SUB011560
SUB011570
SUB011580
SUB011590
SUB011600
SUB011610
SUB011620
SUB011630
SUB011640
SUB011650
SUB011660
SUB011670
SUB011680
SUB011690
SUB011700
SUB011710
SUB011720
SUB011730
SUB011740
SUB011750
SUB011760
SUB011770
SUB011780
SUB011790

3. DISPLACABLE ELLIPTICAL GAUSSIAN:
C IF (NOF.GT.3) GO TO 4
C F=AA*EXP(-1.*(((XS-DD)/BB)**2+((YS-EE)/CC)**2))
C GO TO 11
SUB011800
SUB011810
SUB011820
SUB011830
SUB011840
SUB011850
SUB011860
SUB011870
SUB011880
SUB011890
SUB011900
SUB011910
SUB011920
SUB011930
SUB011940
SUB011950
SUB011960
SUB011970
SUB011980
SUB011990
SUB012000

4. CONSTANT:
C IF (NOF.GT.4) GO TO 5
C F=AA
C GO TO 11
SUB012010
SUB012020
SUB012030
SUB012040
SUB012050
SUB012060
SUB012070
SUB012080
SUB012090
SUB012100
SUB012110
SUB012120
SUB012130
SUB012140
SUB012150
SUB012160
SUB012170
SUB012180
SUB012190
SUB012200

5. ADJUSTABLE AND DISPLACABLE ELLIPTIC RAMP FUNCTION:
C IF (NOF.GT.5) GO TO 6
C RBC=SQRT(((XS-DD)/BB)**2+((YS-EE)/CC)**2)
C F=0
C IF (RBC.LT.1.) F=AA*((1.-RBC)**PP)
C GO TO 11
SUB012210
SUB012220
SUB012230
SUB012240
SUB012250
SUB012260
SUB012270
SUB012280
SUB012290
SUB012300
SUB012310
SUB012320
SUB012330
SUB012340
SUB012350
SUB012360
SUB012370
SUB012380
SUB012390
SUB012400
SUB012410
SUB012420
SUB012430
SUB012440
SUB012450
SUB012460
SUB012470
SUB012480
SUB012490
SUB012500
SUB012510
SUB012520
SUB012530
SUB012540
SUB012550
SUB012560
SUB012570
SUB012580
SUB012590
SUB012600
SUB012610
SUB012620
SUB012630
SUB012640
SUB012650
SUB012660
SUB012670
SUB012680
SUB012690
SUB012700
SUB012710
SUB012720
SUB012730
SUB012740
SUB012750
SUB012760
SUB012770
SUB012780
SUB012790
SUB012800

6. DISPLACABLE ELLIPTIC STEP FUNCTION:
C IF (NOF.GT.6) GO TO 7
C RBC=SQRT(((XS-DD)/BB)**2+((YS-EE)/CC)**2)
C F=0
C IF (RBC.LT.1.) F=AA
C GO TO 11
SUB012810
SUB012820
SUB012830
SUB012840
SUB012850
SUB012860
SUB012870
SUB012880
SUB012890
SUB012900
SUB012910
SUB012920
SUB012930
SUB012940
SUB012950
SUB012960
SUB012970
SUB012980
SUB012990
SUB013000
SUB013010
SUB013020
SUB013030
SUB013040
SUB013050
SUB013060
SUB013070
SUB013080
SUB013090
SUB013100
SUB013110
SUB013120
SUB013130
SUB013140
SUB013150
SUB013160
SUB013170
SUB013180
SUB013190
SUB013200
SUB013210
SUB013220
SUB013230
SUB013240
SUB013250
SUB013260
SUB013270
SUB013280
SUB013290
SUB013300
SUB013310
SUB013320
SUB013330
SUB013340
SUB013350
SUB013360
SUB013370
SUB013380
SUB013390
SUB013400
SUB013410
SUB013420
SUB013430
SUB013440
SUB013450
SUB013460
SUB013470
SUB013480
SUB013490
SUB013500
SUB013510
SUB013520
SUB013530
SUB013540
SUB013550
SUB013560
SUB013570
SUB013580
SUB013590
SUB013600
SUB013610
SUB013620
SUB013630
SUB013640
SUB013650
SUB013660
SUB013670
SUB013680
SUB013690
SUB013700
SUB013710
SUB013720
SUB013730
SUB013740
SUB013750
SUB013760
SUB013770
SUB013780
SUB013790
SUB013800

7. CIRCULAR COSINE-SQUARED FUNCTION OF BB MAXIMA:
C IF (NOF.GT.7) GO TO 8
C F=AA*COS((2.*BB-1.)*PI*R/2.)*2
C GO TO 11
SUB013810
SUB013820
SUB013830
SUB013840
SUB013850
SUB013860
SUB013870
SUB013880
SUB013890
SUB013900
SUB013910
SUB013920
SUB013930
SUB013940
SUB013950
SUB013960
SUB013970
SUB013980
SUB013990
SUB014000
SUB014010
SUB014020
SUB014030
SUB014040
SUB014050
SUB014060
SUB014070
SUB014080
SUB014090
SUB014100
SUB014110
SUB014120
SUB014130
SUB014140
SUB014150
SUB014160
SUB014170
SUB014180
SUB014190
SUB014200
SUB014210
SUB014220
SUB014230
SUB014240
SUB014250
SUB014260
SUB014270
SUB014280
SUB014290
SUB014300
SUB014310
SUB014320
SUB014330
SUB014340
SUB014350
SUB014360
SUB014370
SUB014380
SUB014390
SUB014400
SUB014410
SUB014420
SUB014430
SUB014440
SUB014450
SUB014460
SUB014470
SUB014480
SUB014490
SUB014500
SUB014510
SUB014520
SUB014530
SUB014540
SUB014550
SUB014560
SUB014570
SUB014580
SUB014590
SUB014600
SUB014610
SUB014620
SUB014630
SUB014640
SUB014650
SUB014660
SUB014670
SUB014680
SUB014690
SUB014700
SUB014710
SUB014720
SUB014730
SUB014740
SUB014750
SUB014760
SUB014770
SUB014780
SUB014790
SUB014800

8. NUMERICAL FUNCTION: REQUIRES AN INPUT ARRAY READ IN BY
C SUBROUTINE FREAD; N FOLLOWED BY N POINT VALUES. (101 MAX)
C A CONSTANT VALUE AA IS ADDED TO THE FUNCTION.
C IF (NOF.GT.8) GO TO 9
C IF (NUMB.LE.1) N=NO
C IF (NUMB.GT.1) N=NA
C NM=N-1
C NNM=N-2
C RN=N

```



SUB01770  
SUB01780  
SUB01790  
SUB01800  
SUB01810  
SUB01820  
SUB01830  
SUB01840  
SUB01850  
SUB01860  
SUB01870  
SUB01880  
SUB01890  
SUB01900  
SUB01910  
SUB01920  
SUB01930  
SUB01940  
SUB01950  
SUB01960  
SUB01970  
SUB01980  
SUB01990  
SUB02000  
SUB02010  
SUB02020  
SUB02030

```
RI=R*(RN-1.)+1.
IR=INT(RI)
RIR=FLOAT(IR)
DI=RI-RIR
IF (NUMB.LE.1) F=RO(IR)
IF (NUMB.GT.1) F=RA(IR)
IF ((IR.NE.N).AND.(NUMB.LE.1)) F=F+DI*(RO(IR+1)-RO(IR))
IF ((IR.NE.N).AND.(NUMB.GT.1)) F=F+DI*(RA(IR+1)-RA(IR))
F=F*AA+BB
GO TO 11
```

```
9. SPECIAL FUNCTION: MAY BE WRITTEN FOR THE OCCASION AND
   INSERTED IN SUBROUTINE SPFUN
   IF (NOF.GT.9) GO TO 10
   CALL SPFUN (XS,YS,F)
   GO TO 11
```

```
   EQUATIONS NO. 10 AND BEYOND ARE SET TO ZERO.
   F=0.
```

```
11. IF (DGN.GE.4) WRITE (6,99) XS,YS,F
   FORMAT (' XS=',F8.3,' YS=',F8.3,' F=',F8.3)
   RETURN
END
C000008
```

```
   SUBROUTINE SPFUN (XS,YS,F)
```

```
   SPFUN IS A SPECIAL ROUTINE FOR EQ'N NO. 9. ANY FUNCTION MAY BE
   ENTERED.
```

```
COMMON /EQPARA/ A,B,C,D,E,P,Q,S,T,U,V,W,RQ,RA,NO,NA,N1,N2
DIMENSION RO(101),RA(101)
F=0.
IF ((ABS(XS).LE.B).AND.(ABS(YS).LE.C)) F=A
RETURN
END
```

```
C000009
C
```

SUB02040  
SUB02050  
SUB02060  
SUB02070  
SUB02080  
SUB02090  
SUB02100  
SUB02110  
SUB02120  
SUB02130  
SUB02140  
SUB02150  
SUB02160



SUBROUTINE SHEET (G,D,XO,YO,PHISYM,NOF)

SHEET READS IRREGULARLY SPACED VALUES OF THE LINE INTEGRAL, AS  
OBTAINED FROM HOLOGRAPHIC INTERFEROGRAMS. THE INTEGRAL LINES MAY BE  
DEFINED EITHER BY GRID INTERCEPT POSITIONS, OR BY ANGLE AND RADIUS  
ABOUT THE CENTER OF THE LABORATORY COORDINATE SYSTEM CENTER. LINES  
MUST BE ENTERED IN CONSECUTIVE ORDER FROM LOWEST (NEG.) TO HIGHEST  
(POS.) RADIUS. DATA MAY BE SIMULATED BY SPECIFYING NCODE=1,  
FOLLOWED BY APERTURE POSITIONS FOR A FUNCTION NUMBER IN SUBFUNCT.

COMMON IMAX,JMAX,IIMX,JJMX,IJMX,ALPHA,SIZE,EPS,MODE,BOX,SD,IX,Z  
COMMON /SYM/ISYM,JSYM,MSYM,FCU,IMS,JMS,QSYM  
COMMON /IO/ CMS,IN1,IN2,IN4  
DIMENSION G(IMAX,JMAX),D(IMAX,JMAX),XI(303),RR(303)  
DIMENSION XG(303),XD(303),YG(303),YD(303),XI(303),YI(303)  
NAR=303  
PIE=3.141592653589793  
MPIE=-PIE  
TPIE=2.\*PIE  
MPIE=MPIE/2.  
PIET=PIE/2.  
ZERO THE ARRAYS:  
DO 1 I=1,IMAX  
DO 1 J=1,JMAX  
G(I,J)=0.  
D(I,J)=0.  
DO 2 I=1,NAR  
XG(I)=0.  
XD(I)=0.  
YG(I)=0.  
YD(I)=0.  
XI(I)=0.  
XJ(I)=0.  
RR(I)=0.  
2 C READ THE BASIC DATA:  
IF (CMS.EQ.1.) REWIND 1  
READ (IN1,59) NOF,NCODE  
READ (IN1,58) Z,XO,YO,PHISYM,XXM,XMX,XMN,YMX,YMN  
READ (IN1,59) JM  
RIMX=IMAX  
DR=SIZE/RIMX  
R=(-DR-SIZE)/2.  
RZO=SQRT(XO\*\*2+YO\*\*2)  
GAM=ATANM(YO,XO)  
TP=3-1SYM  
BT=JSYM  
DAN=PIE\*TP/BT  
HS=SIZE/2.  
SUB02170  
SUB02180  
SUB02190  
SUB02200  
SUB02210  
SUB02220  
SUB02230  
SUB02240  
SUB02250  
SUB02260  
SUB02270  
SUB02280  
SUB02290  
SUB02300  
SUB02310  
SUB02320  
SUB02330  
SUB02340  
SUB02350  
SUB02360  
SUB02370  
SUB02380  
SUB02390  
SUB02400  
SUB02410  
SUB02420  
SUB02430  
SUB02440  
SUB02450  
SUB02460  
SUB02470  
SUB02480  
SUB02490  
SUB02500  
SUB02510  
SUB02520  
SUB02530  
SUB02540  
SUB02550  
SUB02560  
SUB02570  
SUB02580  
SUB02590  
SUB02600  
SUB02610  
SUB02620  
SUB02630  
SUB02640



```

SUBO2650
SUBO2660
SUBO2670
SUBO2680
SUBO2690
SUBO2700
SUBO2710
SUBO2720
SUBO2730
SUBO2740
SUBO2750
SUBO2760
SUBO2770
SUBO2780
SUBO2790
SUBO2800
SUBO2810
SUBO2820
SUBO2830
SUBO2840
SUBO2850
SUBO2860
SUBO2870
SUBO2880
SUBO2890
SUBO2900
SUBO2910
SUBO2920
SUBO2930
SUBO2940
SUBO2950
SUBO2960
SUBO2970
SUBO2980
SUBO2990
SUBO3000
SUBO3010
SUBO3020
SUBO3030
SUBO3040
SUBO3050
SUBO3060
SUBO3070
SUBO3080
SUBO3090
SUBO3100
SUBO3110
SUBO3120

```

```

C 3
C 4
C 5
C 6
C 7
C 8
C 9
C 10
C 11
C 12
C 13
C 14
C 15
C 16
C 17
C 18
C 19
C 20
C 21
C 22
C 23
C 24
C 25
C 26
C 27
C 28
C 29
C 30
C 31
C 32
C 33
C 34
C 35
C 36
C 37
C 38
C 39
C 40
C 41
C 42
C 43
C 44
C 45
C 46
C 47
C 48
C 49
C 50
C 51
C 52
C 53
C 54
C 55
C 56
C 57
C 58
C 59
C 60
C 61
C 62
C 63
C 64
C 65
C 66
C 67
C 68
C 69
C 70
C 71
C 72
C 73
C 74
C 75
C 76
C 77
C 78
C 79
C 80
C 81
C 82
C 83
C 84
C 85
C 86
C 87
C 88
C 89
C 90
C 91
C 92
C 93
C 94
C 95
C 96
C 97
C 98
C 99
C 100
C 101
C 102
C 103
C 104
C 105
C 106
C 107
C 108
C 109
C 110
C 111
C 112
C 113
C 114
C 115
C 116
C 117
C 118
C 119
C 120
C 121
C 122
C 123
C 124
C 125
C 126
C 127
C 128
C 129
C 130
C 131
C 132
C 133
C 134
C 135
C 136
C 137
C 138
C 139
C 140
C 141
C 142
C 143
C 144
C 145
C 146
C 147
C 148
C 149
C 150
C 151
C 152
C 153
C 154
C 155
C 156
C 157
C 158
C 159
C 160
C 161
C 162
C 163
C 164
C 165
C 166
C 167
C 168
C 169
C 170
C 171
C 172
C 173
C 174
C 175
C 176
C 177
C 178
C 179
C 180
C 181
C 182
C 183
C 184
C 185
C 186
C 187
C 188
C 189
C 190
C 191
C 192
C 193
C 194
C 195
C 196
C 197
C 198
C 199
C 200
C 201
C 202
C 203
C 204
C 205
C 206
C 207
C 208
C 209
C 210
C 211
C 212
C 213
C 214
C 215
C 216
C 217
C 218
C 219
C 220
C 221
C 222
C 223
C 224
C 225
C 226
C 227
C 228
C 229
C 230
C 231
C 232
C 233
C 234
C 235
C 236
C 237
C 238
C 239
C 240
C 241
C 242
C 243
C 244
C 245
C 246
C 247
C 248
C 249
C 250
C 251
C 252
C 253
C 254
C 255
C 256
C 257
C 258
C 259
C 260
C 261
C 262
C 263
C 264
C 265
C 266
C 267
C 268
C 269
C 270
C 271
C 272
C 273
C 274
C 275
C 276
C 277
C 278
C 279
C 280
C 281
C 282
C 283
C 284
C 285
C 286
C 287
C 288
C 289
C 290
C 291
C 292
C 293
C 294
C 295
C 296
C 297
C 298
C 299
C 300
C 301
C 302
C 303
C 304
C 305
C 306
C 307
C 308
C 309
C 310
C 311
C 312
C 313
C 314
C 315
C 316
C 317
C 318
C 319
C 320
C 321
C 322
C 323
C 324
C 325
C 326
C 327
C 328
C 329
C 330
C 331
C 332
C 333
C 334
C 335
C 336
C 337
C 338
C 339
C 340
C 341
C 342
C 343
C 344
C 345
C 346
C 347
C 348
C 349
C 350
C 351
C 352
C 353
C 354
C 355
C 356
C 357
C 358
C 359
C 360
C 361
C 362
C 363
C 364
C 365
C 366
C 367
C 368
C 369
C 370
C 371
C 372
C 373
C 374
C 375
C 376
C 377
C 378
C 379
C 380
C 381
C 382
C 383
C 384
C 385
C 386
C 387
C 388
C 389
C 390
C 391
C 392
C 393
C 394
C 395
C 396
C 397
C 398
C 399
C 400
C 401
C 402
C 403
C 404
C 405
C 406
C 407
C 408
C 409
C 410
C 411
C 412
C 413
C 414
C 415
C 416
C 417
C 418
C 419
C 420
C 421
C 422
C 423
C 424
C 425
C 426
C 427
C 428
C 429
C 430
C 431
C 432
C 433
C 434
C 435
C 436
C 437
C 438
C 439
C 440
C 441
C 442
C 443
C 444
C 445
C 446
C 447
C 448
C 449
C 450
C 451
C 452
C 453
C 454
C 455
C 456
C 457
C 458
C 459
C 460
C 461
C 462
C 463
C 464
C 465
C 466
C 467
C 468
C 469
C 470
C 471
C 472
C 473
C 474
C 475
C 476
C 477
C 478
C 479
C 480
C 481
C 482
C 483
C 484
C 485
C 486
C 487
C 488
C 489
C 490
C 491
C 492
C 493
C 494
C 495
C 496
C 497
C 498
C 499
C 500
C 501
C 502
C 503
C 504
C 505
C 506
C 507
C 508
C 509
C 510
C 511
C 512
C 513
C 514
C 515
C 516
C 517
C 518
C 519
C 520
C 521
C 522
C 523
C 524
C 525
C 526
C 527
C 528
C 529
C 530
C 531
C 532
C 533
C 534
C 535
C 536
C 537
C 538
C 539
C 540
C 541
C 542
C 543
C 544
C 545
C 546
C 547
C 548
C 549
C 550
C 551
C 552
C 553
C 554
C 555
C 556
C 557
C 558
C 559
C 560
C 561
C 562
C 563
C 564
C 565
C 566
C 567
C 568
C 569
C 570
C 571
C 572
C 573
C 574
C 575
C 576
C 577
C 578
C 579
C 580
C 581
C 582
C 583
C 584
C 585
C 586
C 587
C 588
C 589
C 590
C 591
C 592
C 593
C 594
C 595
C 596
C 597
C 598
C 599
C 600
C 601
C 602
C 603
C 604
C 605
C 606
C 607
C 608
C 609
C 610
C 611
C 612
C 613
C 614
C 615
C 616
C 617
C 618
C 619
C 620
C 621
C 622
C 623
C 624
C 625
C 626
C 627
C 628
C 629
C 630
C 631
C 632
C 633
C 634
C 635
C 636
C 637
C 638
C 639
C 640
C 641
C 642
C 643
C 644
C 
```





SUB03130  
SUB03140  
SUB03150  
SUB03160  
SUB03170  
SUB03180  
SUB03190  
SUB03200  
SUB03210  
SUB03220  
SUB03230  
SUB03240  
SUB03250  
SUB03260  
SUB03270  
SUB03280  
SUB03290  
SUB03300  
SUB03310  
SUB03320  
SUB03330  
SUB03340  
SUB03350  
SUB03360  
SUB03370  
SUB03380  
SUB03390  
SUB03400  
SUB03410  
SUB03420  
SUB03430  
SUB03440  
SUB03450  
SUB03460  
SUB03470  
SUB03480  
SUB03490  
SUB03500  
SUB03510  
SUB03520  
SUB03530  
SUB03540  
SUB03550  
SUB03560  
SUB03570  
SUB03580  
SUB03590  
SUB03600

```

RRH=10000.
XH=RRH*COS(XIH)
YH=RRH*SIN(XIH)
IF (LPR.EQ.1) GO TO 7
YTX=-RR(INT)*SIN(XI(INT))-YO
YTN=-RR(INT)*SIN(XI(INT))-YO
XTX=RR(INT)*COS(XI(INT))-XO
XTN=RR(INT)*COS(XI(INT))-XO
UA=TAN(XI(INT))
UB=YTX-UA*XTX
UD=YTN-UC*XTN
UH=(UD-UB)/(UA-UC)
YH=XH+UA*UB
RRH=SQR((XH-XD)**2+(YH-YO)**2)
XIH=ATAN((YH-YO)/(XH-XD))
CONTINUE
DO 9 I=1,IM
IF (XY(I).NE.3.) GO TO 8
BAS=SQR((RRH**2-RR(I)**2)
XI(I)=XIH-ATANM(RR(I),BAS)
GO TO 9
XI(I)=ATANM((YH-YD(I))/(XH-XD(I)))
RR(I)=RRH*SIN(XI(I)-XIH)
CONTINUE
ANGLES AND RADII ARE NOW FILLED FOR ALL POINTS IN THIS LINE.
VACATE THE SET OF VECTORS TO BE USED AS TEMPORARY STORAGE:
DO 10 I=1,IM
XD(I)=0.
YD(I)=0.
XG(I)=0.
YG(I)=0.
XY(I)=D(I,J)
XR(I)=0.
D(I,J)=0.
XI(I)=0.
CONVERT THE LINE TO REGULAR RADII USING INTERPOLATION:
RR(I)=R+DR
CALL SPLINE(YG,XY,IM,RR(I),D(I,J))
DO 11 I=2,IMAX
RI=I
RR(I)=R+DR*RI
CALL SPLINE(YG,XY,IM,RR(I),D(I,J))
GENERATE THE VECTOR OF ANGLES FOR THIS COLUMN AND STORE IN G ARRAY:
DO 12 I=1,IMAX
BAS=SQR((RRH**2-RR(I)**2)
G(I,J)=XIH-ATANM(RR(I),BAS)

```







```

C      FIND THA MAX ANGLE IN THE ROW:
      XY(JM2)=JM2
      SB=XG(JM2)
      DO 20 J=1,JM2
      IF (XG(J).LE.SB) GO TO 20
      SB=XG(J)
      XY(JM2)=J
      CONTINUE
20 C      DETERMINE THE ORDER OF INCREASING ANGLE IN THE ROW
      SB=XG(JM2)
      JJ=2
      JSA=XY(JJ-1)
      SA=XG(JJ-1)
      JTS=0
      DO 22 J=1,JM2
      IF (XG(J).LE.SA) GO TO 22
      IF (XG(J).GT.SB) GO TO 22
      SB=XG(J)
      XY(JJ)=J
      JTS=1
      CONTINUE
22 C      IF (JTS.EQ.0) JM2=JJ
      JJ=JJ+1
      IF (JJ.LE.JM2) GO TO 21
      DO 23 J=1,JM2
      JX=XY(J)
      YD(J)=XG(JX)
      INTERPOLATE:
      DX1=2.*PIE/FCU
      XI(J)=DX1/2.-PIE-PHISYM
      CALL SPLINE (XG,YD,JM2,XI(J),G(I,J))
      DO 24 J=2,JMS
      XI(J)=XI(J-1)+DX1
      CALL SPLINN (XG,YD,JM2,XI(J),G(I,J))
      DO 25 J=1,JMS
      XIJ=XI(J)
      XU=XMX
      IF ((XIJ.GE.O.).AND.(XIJ.LT.PIE)) XU=XMN
      YU=YMN
      IF ((XIJ.GE.MPIT).AND.(XIJ.LT.PIT)) YU=YMX
      XL=XMN
      IF ((XIJ.GE.O.).AND.(XIJ.LT.PIE)) XL=XMX
      YL=YMX
      IF ((XIJ.GE.MPIT).AND.(XIJ.LT.PIT)) YL=YMN
      SXIJ=SIGN(XIJ)
      CXIJ=COS(XIJ)
      RMN=(XO-XL)*SXIJ-(YO-YU)*CXIJ
      RMX=(XO-XU)*SXIJ-(YO-YU)*CXIJ

```

SUB04090  
SUB04100  
SUB04110  
SUB04120  
SUB04130  
SUB04140  
SUB04150  
SUB04160  
SUB04170  
SUB04180  
SUB04190  
SUB04200  
SUB04210  
SUB04220  
SUB04230  
SUB04240  
SUB04250  
SUB04260  
SUB04270  
SUB04280  
SUB04290  
SUB04300  
SUB04310  
SUB04320  
SUB04330  
SUB04340  
SUB04350  
SUB04360  
SUB04370  
SUB04380  
SUB04390  
SUB04400  
SUB04410  
SUB04420  
SUB04430  
SUB04440  
SUB04450  
SUB04460  
SUB04470  
SUB04480  
SUB04490  
SUB04500  
SUB04510  
SUB04520  
SUB04530  
SUB04540  
SUB04550  
SUB04560



```

DO 25 I=1,IMAX
IF (RR(I).LT.RMN) G(I,J)=0.
IF (RR(I).GT.RMX) G(I,J)=0.
CONTINUE
25 EXPAND SYMMETRY SECTOR INTO AN ORTHOGONAL INTERVAL.
IF (ISYM.EQ.2) GO TO 27
DO 26 J=1,JMS
J2=JMAX/2+1-J
J3=JMAX/2+J
J4=JMAX+1-J
DO 26 I=1,IMAX
I1=IMAX+1-I
G(I,J2)=G(I,J)
G(I1,J3)=G(I,J)
G(I1,J4)=G(I,J)
26 RETURN
C FOR EVEN SYMMETRY, AVERAGE THE GARRAY COLUMNS.
27 IMS=(2*IMAX+1)/2
DO 28 J=1,IMS
I1=IMAX+1-I
GSI=(G(I,J)+G(I1,J))/2.
28 G(I,J)=GSI
RETURN
59 FORMAT (5I5)
58 FORMAT (10F7.3)
END
C000010
C

FUNCTION ATANM(Y,X)
C COMPUTES THE ARCTAN OF Y/X BETWEEN -PI AND +PI.
C
PIE=3.141592653589793
PI2=PIE/2.
ATANM=SIGN(PI2,Y)
IF (X.NE.0.) ATANM=ATAN(Y/X)
IF (X.GE.0.) RETURN
IF (X.LE.0.) ATANM=PIE+ATANM
IF (Y.LT.0.) ATANM=-PIE+ATANM
RETURN
END
C000011
C
SUBO4570
SUBO4580
SUBO4590
SUBO4600
SUBO4610
SUBO4620
SUBO4630
SUBO4640
SUBO4650
SUBO4660
SUBO4670
SUBO4680
SUBO4690
SUBO4700
SUBO4710
SUBO4720
SUBO4730
SUBO4740
SUBO4750
SUBO4760

SUBO4780
SUBO4790
SUBO4800
SUBO4810
SUBO4820
SUBO4830
SUBO4840
SUBO4850
SUBO4860

SUBO4870
SUBO4880
SUBO4890
SUBO4900
SUBO4910
SUBO4920
SUBO4930
SUBO4940
SUBO4950
SUBO4960
SUBO4970
SUBO4980
SUBO4990
SUBO5000
SUBO5010

```





```

SUBROUTINE SIM (XD,YD,XG,YG,D,R,XI,XY,XO,YO,PS,XM,XN,YM,YN,I,IM,
10G,NF)
C SIM SIMULATES THE FRINGE NUMBER DATA ONE WOULD OBTAIN FROM THE
C HOLOGRAPHIC INTERFEROGRAM PROCESS FOR A KNOWN FUNCTION AS
C CONTAINED IN SUBROUTINE FUNCT. THE GRID BOX DIMENSIONS MUST
C EXCEED THE INVERSION CIRCLE SIZE, AND APERTURE POINTS SPECIFIED
C MUST FALL BETWEEN XI=-40 DEGREES; AND XI=+130 DEGREES.
C
COMMON IMAX,JMAX,IIMX,JJMX,IJMX,ALF,SIZ,EPS,MOD,BOX,SD,IX,Z
COMMON /IO/ CMS,INI,IN2,IN4
READ (IN1,29) XH,YH
ZER=0.
RIM=IM
RI=I
DX=(XM-XN)/(RIM-1.)
DY=(YM-YN)/(RIM-1.)
XI=XM-(RIM-1.)*DX
YI=YM-(RIM-1.)*DY
X11=ATANM (YH-YI,XH-XI)-PS
RRH=SQRT((XH-XO)**2+(YH-YO)**2)
X10=ATANM(YH-YO,XH-XO)-PS
R1=RRH*SIN(X11-X10)
IF ((1.GT.1.) .AND. (1.LT.IM)) GO TO 1
IF (ABS(R1).LT.SIZ/2.) R1=SIGN(SIZ/2.,R1)
XY=3.
GO TO 2
1 CALL GOLF (R,XI,D,NR,ZER,ZER)
XD=XN
YD=YN
IF (XH-NE.XI) YD=YI-(X1-XN)*(YH-YI)/(XH-X1)
IF (YS.GE.YN) GO TO 2
YD=YN
IF (YH-NE.YI) XD=XI-(Y1-YN)*(XH-X1)/(YH-Y1)
RETURN
FORMAT (10F7.3)
END
C000012
C
SUBROUTINE FREAD (NO,RO,NF,ZZ)
C FREAD READS THE NUMERIC ARRAY WHICH IS USED FOR EQUATION 8 OF
C SUBROUTINE FUNCT. FIRST CARD IS NUMBER OF POINTS (N.GE.1),
C FOLLOWED BY ONE POINT PER CARD.
C
DIMENSION RO(101)
SUB050020
SUB050030
SUB050040
SUB050050
SUB050060
SUB050070
SUB050080
SUB050090
SUB050100
SUB050110
SUB050120
SUB050130
SUB050140
SUB050150
SUB050160
SUB050170
SUB050180
SUB050190
SUB050200
SUB050210
SUB050220
SUB050230
SUB050240
SUB050250
SUB050260
SUB050270
SUB050280
SUB050290
SUB050300
SUB050310
SUB050320
SUB050330
SUB050340
SUB050350
SUB050360
SUB050370
SUB050380
SUB000010
SUB000020
SUB000030
SUB000040
SUB000050
SUB000060
SUB000070
SUB000080
SUB000090

```



READ (NF,89) NO,ZZ  
 WRITE(6,90) NO,ZZ  
 DO 10 I=1,NO  
 READ(NF,88) RO(I)  
 WRITE(6,88) RO(I)  
 CONTINUE  
 10 FORMAT(15,F9.3)  
 89  
 88  
 90  
 RETURN  
 END  
 C000013  
 C

SUBROUTINE GPRINT (G,NUMB)  
 C  
 C PRINT PRINTS THE DATA ARRAY 'G', WHICH WAS INPUT TO  
 C THE PROGRAM IN SUBROUTINE GARRY.  
 C  
 COMMON IMAX,JMAX,IIMX,JJMX,IJMX,ALPHA,SIZE,EPS,MODE,BOX,SD,IX,Z  
 DIMENSION G(IJMX)  
 DIMENSION X(15)  
 DATA HYP,VERT,1H-,1H/  
 IF (NUMB.EQ.1) WRITE (6,99) MODE,Z  
 IF (NUMB.EQ.2) WRITE (6,92) Z  
 JI2=JMAX/2  
 RJMAX=JMAX  
 RJMAX=IMAX  
 DX=SIZE/RJMAX  
 DXI=360./RJMAX  
 C INTRVL SETS THE NUMBER OF TERMS PRINTED PER LINE. IF IT IS ALTERED,  
 C ONE MUST ALSO REDIMENSION X AND ALTER FORMATS 98, 97, AND 95.  
 INTRVL=15  
 IB=1  
 IT=IB+INTRVL-1  
 IF (IT.GT.IMAX) IT=IMAX  
 1  
 IBT=IT-IB+1  
 WRITE (6,98) (II,II=IB,IT)  
 DO 2 I=1,IBT  
 RI=IB-1+I  
 X(I)=-SIZE/2.+(RI-.5)\*DX  
 2  
 LM=#IBT+1  
 WRITE (6,97) (X(I),I=1,IBT)  
 WRITE (6,96) (HYP,L=1,LM),VERT  
 JMH=JM2+1  
 DO 3 J=JMH,JMAX  
 RJ=J



```

3      XI=-180.+DXI*(RJ-.5)
      IGB={J-1}*IMAX+IB
      IGT=IGB-IB+IT
      WRITE (6,95) J,XI,(G(L),L=IGB,IGT)
      WRITE (6,94) (HYP,L=1,LM),VERT
      IB=IB+INTRVL
      ITOLD=IT
      IT=IT+INTRVL
      IF (ITOLD.LT. IMAX) GO TO 1
      WRITE (6,93)
      FORMAT (1H1//, THE ARRAY OF INPUT DATA (G), OBTAINED BY GARRAY,
1      MODE=1,11, FOR Z=F7.3, CM:;)
      FORMAT (//11X, I=,15I7)
      FORMAT (11X, X=,15F7.3)
      FORMAT (11X, J=,15I7)
      FORMAT (2X,13=F9.2,1,15F7.3)
      FORMAT (14X,1,15I7)
      FORMAT (//5X)
      FORMAT (1H1//, THE ADD-ON FUNCTION GARRAY FOR Z=F7.3, CM:;)
      RETURN
      END
C000014
C

```

```

SUBROUTINE GPUNCH (Z,XO,YO,PHS,NOF,IMX,JMX,G)
GPUNCH PUNCHES OUT THE FIRST NON-SYMMETRIC PORTION OF GARRAY
C (OR WRITES IT ON FILE 7 IN CMS VERSION)
C
      COMMON /SYM/ ISM,JSM,MSM,FCU,IMS,JMS,QSM
      DIMENSION G(IMX,JMX)
      WRITE (7,39) NOF,IMX,JMX,ISM,JSM,IMS,JMS
      WRITE (7,38) ((G(I,J),I=1,IMS),J=1,JMS)
      FORMAT(10I5)
      FORMAT(10F7.3)
      RETURN
      END
C000015
C

```

```

SUBROUTINE READ (Z,XO,YO,PHISYM,NOF,IMAX,JMAX,G)
C READS THE NON-SYMMETRIC PORTION OF THE GARRAY AND EXPANDS IT TO AN
C ORTHOGONAL SET. NOTE, INSURE SUFFICIENT DIMENSIONS IN MAIN PROGRAM.
C
      COMMON /SYM/ ISYM,JSYM,MSYM,FCU,IMS,JMS,QSYM

```

SUB000510  
SUB000520  
SUB000530  
SUB000540  
SUB000550  
SUB000560  
SUB000570  
SUB000580  
SUB000590  
SUB000600  
SUB000610  
SUB000620  
SUB000630  
SUB000640  
SUB000650  
SUB000660  
SUB000670  
SUB000680  
SUB000690  
SUB000700  
SUB000710  
SUB000720  
SUB000730

SUB000740  
SUB000750  
SUB000760  
SUB000770  
SUB000780  
SUB000790  
SUB000800  
SUB000810  
SUB000820  
SUB000830  
SUB000840  
SUB000850  
SUB000860  
SUB000870  
SUB000880

SUB000890  
SUB000900  
SUB000910  
SUB000920  
SUB000930  
SUB000940



```

COMMON /IO/ CMS, IN1, IN2, IN4
DIMENSION G(IMAX,JMAX)
READ (IN1,39) NOF,IMAX,JMAX,ISYM,JSYM,IMS,JMS
READ (IN1,38) Z,XO,YO,PHISYM
READ (IN1,38) I(G1,J1)=1,IMS) J=1,JMS)
WRITE(6,37) NOF,Z,XO,YO,PHISYM,IMAX,JMAX,JSYM
JMAX=JMAX
MSYM=JSYM
IF (MSYM.EQ.0).OR.(MSYM.GT.JMAX)) MSYM=1
FCU=ISYM*JSYM*JMAX
IF (JSYM.GT.JMAX) FCU=JMAX
QSYM=FCU/RJMX
DO 4 J=1,JMS
  IF (ISYM.EQ.1) GO TO 2
  DO 1 I=1,IMS
    I1=IMAX+1-I
    G(I1,J)=G(I,J)
  GO TO 4
  J2=JMAX/2+1-J
  J3=JMAX/2+J
  J4=JMAX+1-J
  DO 3 I=1,IMAX
    I1=IMAX+1-I
    G(I1,J2)=G(I,J)
    G(I1,J3)=G(I,J)
    G(I1,J4)=G(I,J)
  CONTINUE
  FORMAT(10F5.3)
  FORMAT(10F7.3)
  1,1, XO=,F7.3,, PHISYM=,F7.3/,
  2,, JMAX=,I4,, JSYM=,I4//)
  RETURN
END
C000016
C

```

SUBROUTINE MAP (IM,JM,A,N,Z,BAND)

C MAP CALLS SUBROUTINE MIMPII AND PLOTS A CONTOUR MAP OF THE ARRAY

C DIMENSION A(IM,JM),T(24)

DATA BL/LH/

DO 1 I=1,24

T(I)=BL

ICON=1

IF(BAND.LT.O.) ICON=0

SUB01310  
SUB01320  
SUB01330  
SUB01340  
SUB01350  
SUB01360  
SUB01370  
SUB01380  
SUB01390  
SUB01400

SUB00950  
SUB00960  
SUB00970  
SUB00980  
SUB00990  
SUB01000  
SUB01010  
SUB01020  
SUB01030  
SUB01040  
SUB01050  
SUB01060  
SUB01070  
SUB01080  
SUB01090  
SUB01100  
SUB01110  
SUB01120  
SUB01130  
SUB01140  
SUB01150  
SUB01160  
SUB01170  
SUB01180  
SUB01190  
SUB01200  
SUB01210  
SUB01220  
SUB01230  
SUB01240  
SUB01250  
SUB01260  
SUB01270  
SUB01280  
SUB01290  
SUB01300

Z=,F7.3  
IMAX=,I4,





```

IF(BAND.LT.O.) BAND=-BAND
AMIN=0.
IJT=0
AZ=1.
BZ=0.
WRITE(6,49) N,Z
CALL MTMPII (A,IM,JM,T,BAND,AZ,BZ,AMIN,IJT,ICON)
FORMAT (1H1//, THE FUNCTION SURFACE, TEST NO.,I3, Z=F5.3//)
RETURN
END
C000017
C

SUBROUTINE GPLOT (G,GA,JMS)
C
C PLOT PRINTS A ROUGH PLOT OF THE LINE INTEGRAL FUNCTIONS IN GARRAY.
C
COMMON IMAX,JMAX,IHX,IJMX,IJMY,ALPHA,SIZE,EPS,MODE,BOX,SD,IX,Z
COMMON /TAB/ INDEX(7),JSYM,ISYM
COMMON /TAB2/ IPT,KPT,LPT,MPT,REST(5)
DIMENSION G(IMAX,JMAX),GA(IMAX,JMAX),ROW(101)
DIMENSION A(201),B(101),C(201),D(101)
JM=101
DATA BL,PL,ST,DH,EX/1H,1H*,1H*,1H-,1HX/
JMS2=JMAX/2+1
IF(ISYM.EQ.2)JMS2=1
JMS3=JMS2+JMS-1
DO 8 J=JMS2,JMS3
WRITE(6,67) (ST,I=1,120)
DO 1 I=1,IMAX
A(I)=G(I,J)
C(I)=GA(I,J)
AS=.5
BS=.0
CALL INTERP (A,IMAX,AS,B,JM,BS)
CALL INTERP (C,IMAX,AS,D,JM,BS)
WRITE (6,69) J
BIG=0.
SMALL=0.
DO 2 I=1,IMAX
IF(A(I).GT.BIG) BIG=A(I)
IF(C(I).GT.BIG) BIG=C(I)
IF(A(I).LT.SMALL) SMALL=A(I)
IF(C(I).LT.SMALL) SMALL=C(I)
RANGE=BIG-SMALL
RINK=RANGE/80.
TOP=BIG+RINK

```

SUB01410  
SUB01420  
SUB01430  
SUB01440  
SUB01450  
SUB01460  
SUB01470  
SUB01480  
SUB01490  
SUB01500  
SUB01510  
SUB01520  
  
SUB01530  
SUB01540  
SUB01550  
SUB01560  
SUB01570  
SUB01580  
SUB01590  
SUB01600  
SUB01610  
SUB01620  
SUB01630  
SUB01640  
SUB01650  
SUB01660  
SUB01670  
SUB01680  
SUB01690  
SUB01700  
SUB01710  
SUB01720  
SUB01730  
SUB01740  
SUB01750  
SUB01760  
SUB01770  
SUB01780  
SUB01790  
SUB01800  
SUB01810  
SUB01820  
SUB01830  
SUB01840  
SUB01850  
SUB01860



```

CEN=BIG
BOT=BIG-RINK
KC=0
DO 7 K=1,41
  IC=0
  DO 6 I=1,101
    ROW(I)=BL
    IF((I.EQ.1)).OR.(I.EQ.51)).OR.(I.EQ.101)) ROW(I)=PL
    IF((K.EQ.1)).OR.(K.EQ.41)) ROW(I)=PL
    IF((TOP.GE.0.))AND.(BOT.LE.0.)) ROW(I)=DH
    IF(IC.EQ.5) GO TO 3
    GO TO 4
  3
  IC=0
  IF(KC.EQ.10) ROW(I)=PL
  IF(KC.EQ.2) GO TO 5
  IF(KC.EQ.1).LE.2) .AND.(D(I).GE.BOT)) ROW(I)=ST
  IF((D(I).TOP).AND.(B(I).GE.BOT)) ROW(I)=EX
  IF((B(I).LE.TOP).AND.(B(I).GE.BOT)) ROW(I)=EX
  IC=IC+1
  IF(KC.EQ.5) KC=0
  IF(KC.NE.0) WRITE (6,65) (ROW(I),I=1,101)
  IF(KC.EQ.0) WRITE (6,68) CEN,(ROW(I),I=1,101)
  TOP = TOP-2.*RINK
  CEN=CEN-2.*RINK
  BOT=BOT-2.*RINK
  KC=KC+1
  WRITE (6,66) (ST,I=1,120)
  FORMAT (//,I3//)
  FORMAT (IX,F8.3,IX,TOTAL)
  FORMAT (//I1,/,I2I1//)
  FORMAT (//I2I1//)
  FORMAT (//I2I1//)
  RETURN
END
C000018

```

```

SUBROUTINE INTERP (A,IM,AS,B,JM,BS)
C
C   INTERP CONVERTS A REGULAR VECTOR A OF IM POINTS TO A REGULAR VECTOR
C   B OF JM POINTS. OS=.5 FOR A VECTOR WITH POINTS DEFINED IN THE
C   CENTER OF THE INTERVAL, AS AND BS ARE THE % OF AN INTERVAL FROM THE
C   EDGE OF THE FIELD TO THE FIRST POINT (.0 OR .5 FOR EDGE OR
C   DEFINED POINTS)
C
C   DIMENSION A(IM),B(JM)
C   RIM=IM
C   RJM=JM
C
C   SUB02220
C   SUB02230
C   SUB02240
C   SUB02250
C   SUB02260
C   SUB02270
C   SUB02280
C   SUB02290
C   SUB02300
C   SUB02310
C   SUB02320

```



```

RAT=(RIM-1.+2.*AS)/(RJM-1.+2.*BS)
DO 2 I=1,JM
  BI=I
  AI=RAT*(BI+BS)-AS
  IA=AI
  F=AI-FL0AT(IA)
  IF((IA.EQ.0).OR.(IA.EQ.JM)) GO TO 1
  B(I)=A(IA)+F*(A(IA+1)-A(IA))
  GO TO 2
  IF(IA.EQ.0) B(I)=A(I)*(F-AS)/(1.-AS)
  IF(IA.EQ.JM) B(I)=A(JM)*F/(1.-AS)
CONTINUE
RETURN
END

```

1  
2

CO00019

```

SUBROUTINE SPLINE
PURPOSE
  PROVIDES INTERPOLATED VALUE USING "CUBIC SPLINE FITTING"
USAGE
  FIRST CALL TO SUBROUTINE:
    CALL SPLINE(X,Y,M,XINT,YINT)
  SUBSEQUENT CALLS:
    CALL SPLIN(X,Y,M,XINT,YINT)
DESCRIPTION OF PARAMETERS
  X: MONOTONICALLY INCREASING ABSCISSA ARRAY
  Y: ONE-FOR-ONE CORRESPONDING ORDINATE ARRAY
  M: NUMBER OF X AND Y VALUES SUPPLIED < OR = 300
  XINT: VALUE OF ABSCISSA FOR WHICH CORRESPONDING ORDINATE
        IS TO BE INTERPOLATED (OR EXTRAPOLATED)
  YINT: INTERPOLATED (OR EXTRAPOLATED) ORDINATE VALUE
REMARKS
  IF SPECIFIED X FALLS OUTSIDE OF RANGE, AN EXTRAPOLATED
  VALUE WILL BE SUPPLIED
SUBROUTINES AND FUNCTION SUBPROGRAMS REQUIRED
  SUBROUTINE SPLICO IS INCLUDED IN SUBROUTINE SPLIN PACKAGE
MATHEMATICAL METHOD
  UPON FIRST ENTRY TO SPLIN, A CALL TO SPLICO IS MADE TO

```

SPL00010  
SPL00020  
SPL00030  
SPL00040  
SPL00050  
SPL00060  
SPL00070  
SPL00080  
SPL00090  
SPL00100  
SPL00110  
SPL00120  
SPL00130  
SPL00140  
SPL00150  
SPL00160  
SPL00170  
SPL00180  
SPL00190  
SPL00200  
SPL00210  
SPL00220  
SPL00230  
SPL00240  
SPL00250  
SPL00260  
SPL00270  
SPL00280  
SPL00290  
SPL00300  
SPL00310  
SPL00320  
SPL00330









```

      P(K)=D(K)/6.
2  E(K)=(Y(K+1)-Y(K))/D(K)
3  B(K)=E(K)-E(K-1)
   A(1,2)=-1.-D(1)/D(2)
   A(1,3)=D(1)/D(2)
   A(2,2)=P(2)-P(1)*A(1,3)
   A(2,3)=2.*(P(1)+P(2))-P(1)*A(1,2)
   A(2,1)=A(2,3)/A(2,2)
4  DO 4 K=3,MM
   A(K,2)=2.*(P(K-1)+P(K))-P(K-1)*A(K-1,3)
   A(K,3)=B(K)-P(K-1)*B(K-1)
   A(K,1)=P(K)/A(K,2)
   Q=D(M-2)/D(M-1)
   A(M,1)=1.+Q+A(M-2,3)
   A(M,2)=Q-A(M,1)*A(M-1,3)
   B(M)=B(M-2)-A(M,1)*B(M-1)
   Z(M)=B(M)/A(M,2)
   MN=M-2
6  I=1,MN
   K=M-I
   Z(K)=B(K)-A(K,3)*Z(K+1)
   Z(1)=-A(1,2)*Z(2)-A(1,3)*Z(3)
7  DO 7 K=1,MM
   Q=1./(6.*D(K))
   C(1,K)=Z(K)*Q
   C(2,K)=Z(K+1)*Q
   C(3,K)=Y(K)/D(K)-Z(K)*P(K)
   C(4,K)=Y(K+1)/D(K)-Z(K+1)*P(K)
7  RETURN
END

```

C000020

SPL00800  
 SPL00810  
 SPL00820  
 SPL00830  
 SPL00840  
 SPL00850  
 SPL00860  
 SPL00870  
 SPL00880  
 SPL00890  
 SPL00900  
 SPL00910  
 SPL00920  
 SPL00930  
 SPL00940  
 SPL00950  
 SPL00960  
 SPL00970  
 SPL00980  
 SPL00990  
 SPL01000  
 SPL01010  
 SPL01020  
 SPL01030  
 SPL01040  
 SPL01050  
 SPL01060  
 SPL01070  
 SPL01080  
 SPL01090  
 SPL01100  
 SPL01110  
 SPL01120

MET00010  
 MET00020  
 MET00030  
 MET00040  
 MET00050  
 MET00060  
 MET00070  
 MET00080  
 MET00090  
 MET00100  
 MET00110  
 MET00120

\*\*\*\*\*

SUBROUTINE MTMPII

PURPOSE

MTMPII WILL PRODUCE, ON THE PRINTER, A CONTOUR MAP  
OF ANY SINGLE PRECISION TWO DIMENSIONAL ARRAY.

USAGE

CALL MTMPII(Y,N,M,T,BND,AZ,BZ,AMIN,IJT,ICON)



```

CCCCCCCCCCCCCCCCCCCCCCCCCCCCCCCCCCCCCCCCCCCCCCCCCCCCCCCCCCCC
DESCRIPTION OF PARAMETERS
Y      - THE ARRAY TO BE CONTOURED. DIMENSIONED Y(N,M)
N      - NUMBER OF ROWS IN Y.
M      - NUMBER OF COLUMNS IN Y.
T      - ARRAY FOR PLOT TITLE. REAL*4 T(24).
BND    - BANDWIDTH FOR THE CONTOURING. IF BND IS ZERO
        - A BANDWIDTH WILL BE CALCULATED AS FOLLOWS
          BND=(MAX(Y)-MIN(Y))/15.
        - A LINEAR TRANSFORMATION MAYBE PERFORMED ON
          THE ARRAY Y OF THE FOLLOWING FORM AZ*Y+BZ.
          IF AZ=0 THEN AZ WILL BE COMPUTED SUCH THAT
          MAX((MAX(Y)),MIN(Y)) WILL BE LESS THAN 1,
          AND BZ WILL BE LEFT AS INPUT.
        - SEE UNDER AZ
BZ      -
AMIN    - THE LEVEL AT WHICH CONTOURING WILL BEGIN. IF
        - AMIN > MIN(Y) THEN AMIN WILL BE CALCULATED
        - TO BE, WITH REFERENCE AT ZERO, THE NEXT LOWER
        - CONTOUR LEVEL FROM MIN(Y) AS DETERMINED BY
        - BND.
IJT     - IF IJT=0 AMIN WILL BE CALCULATED AS DESCRIBED
        - ABOVE.
ICON    - IF ICON=0 NO CONTOURING WILL BE DONE BUT THE
        - ARRAY Y WILL BE PRINTED IN THE PLOT FORMAT.

REMARKS
MTMPLI REQUIRES A PRINTER WITH 132 PRINT POSITIONS.
IF NECESSARY THE MAP WILL BE SEGMENTED COLUMNWISE.
THE ROWS AND COLUMNS ARE NUMBERED ALONG THE EDGES.
THAT A SEGMENTED MAP MAYBE EASILY JOINED TOGETHER.
ONLY THREE SIGNIFICANT FIGURES WILL BE PRINTED AT
EACH POINT. THE POSITION OF THE FIRST SIGNIFICANT
DIGIT WILL BE DETERMINED BY MAX((MAX(Y)),MIN(Y)).
THE PLOT WILL BE PRODUCED ON A INCH INCH GRID. IT
WILL BE ASSUMED THAT THE SPACING BETWEEN POINTS IN
BOTH DIRECTIONS IS THE SAME AND EQUAL FOR ALL POINTS.

SUBROUTINES REQUIRED
NONE

METHOD
THE CONTOUR LEVELS ARE DETERMINED BY SIMPLE LINEAR
INTERPOLATION FROM THE FOUR SURROUNDING POINTS.

*****
MTMPLI SUBROUTINE FOR ONE-INCH GRID SPACING
*****

```

```

MET00130
MET00140
MET00150
MET00160
MET00170
MET00180
MET00190
MET00200
MET00210
MET00220
MET00230
MET00240
MET00250
MET00260
MET00270
MET00280
MET00290
MET00300
MET00310
MET00320
MET00330
MET00340
MET00350
MET00360
MET00370
MET00380
MET00390
MET00400
MET00410
MET00420
MET00430
MET00440
MET00450
MET00460
MET00470
MET00480
MET00490
MET00500
MET00510
MET00520
MET00530
MET00540
MET00550
MET00560
MET00570
MET00580
MET00590
MET00600

```



```

DESCRIPTION OF PARAMETERS
Y      - THE ARRAY TO BE CONTOURED. DIMENSIONED Y(N,M)
N      - NUMBER OF ROWS IN Y.
M      - NUMBER OF COLUMNS IN Y.
T      - ARRAY FOR PLOT TITLE. REAL*4 T(24).
BND    - BANDWIDTH FOR THE CONTOURING. IF BND IS ZERO
        A BANDWIDTH WILL BE CALCULATED AS FOLLOWS
        BND=(MAX(Y)-MIN(Y))/15.
AZ      - A LINEAR TRANSFORMATION MAYBE PERFORMED ON
        THE ARRAY Y OF THE FOLLOWING FORM AZ*Y+BZ.
        IF AZ=0 THEN AZ WILL BE COMPUTED SUCH THAT
        MAX((MAX(Y)),MIN(Y)) WILL BE LESS THAN 1,
        AND BZ WILL BE LEFT AS INPUT.
BZ      - SEE UNDER AZ
AMIN    - THE LEVEL AT WHICH CONTOURING WILL BEGIN. IF
        AMIN > MIN(Y) THEN AMIN WILL BE CALCULATED
        TO BE, WITH REFERENCE AT ZERO, THE NEXT LOWER
        CONTOUR LEVEL FROM MIN(Y) AS DETERMINED BY
        BND.
IJT     - IF IJT=0 AMIN WILL BE CALCULATED AS DESCRIBED
        ABOVE.
ICON    - IF ICON=0 NO CONTOURING WILL BE DONE BUT THE
        ARRAY Y WILL BE PRINTED IN THE PLOT FORMAT.

REMARKS
MTMPLI  REQUIRES A PRINTER WITH 132 PRINT POSITIONS.
        IF NECESSARY THE MAP WILL BE SEGMENTED COLUMNWISE.
        THE ROWS AND COLUMNS ARE NUMBERED ALONG THE EDGES.
        THAT A SEGMENTED MAP MAYBE EASILY JOINED TOGETHER.
        ONLY THREE SIGNIFICANT FIGURES WILL BE PRINTED AT
        EACH POINT. THE POSITION OF THE FIRST SIGNIFICANT
        DIGIT WILL BE DETERMINED BY MAX((MAX(Y)),MIN(Y)).
        THE PLOT WILL BE PRODUCED ON A INCH INCH GRID. IT
        WILL BE ASSUMED THAT THE SPACING BETWEEN POINTS IN
        BOTH DIRECTIONS IS THE SAME AND EQUAL FOR ALL POINTS.

SUBROUTINES REQUIRED
NONE

METHOD
THE CONTOUR LEVELS ARE DETERMINED BY SIMPLE LINEAR
INTERPOLATION FROM THE FOUR SURROUNDING POINTS.

*****
MTMPLI SUBROUTINE FOR ONE-INCH GRID SPACING

```



```

C      OAKES CODE 5105    15 JAN 69
C
SUBROUTINE MTMPII(Y,N,M,T,BND,AZ,BZ,AMIN,IJT,ICON)
  REAL*4 IH,KG,IT,JZ
  DIMENSION A(140),B(140),C(140),D(140),IH(20),Y(N,M),TP(10),TPX(10),
  Z,IPMI(10),XMT(10),BT(10),BX(10),BT(10),KG(10),Y(24)
  DIMENSION E(140),F(140),G(140),H(140)

  DATA DUE/4H /,EPL/4H+ /,EMI/4H- /,IH/1H0,1H ,1H1,1H ,1H2,
  11H ,1H3,1H ,1H4,1H ,1H5,1H ,1H6,1H7,1H8,1H9/,BLK/4H
  21H0,1H1,1H2,1H3,1H4,1H5,1H6,1H7,1H8,1H9/,BLK/4H

  YMIN=Y(1,1)
  YMAX=Y(1,1)
  DO 20 I=1,M
  DO 10 J=1,N
    YMIN=AMIN(YMIN,Y(J,I))
    YMAX=AMAX1(YMAX,Y(J,I))
  CONTINUE
  CONTINUE
  DELY=YMAX-YMIN
  IF(BND) 25,25,30
  BND=DELY/15.0
  25 IF (AMIN-YMIN) 31,31,32
  30 IF (I=1) 33,32,33
  31 PD=YMIN/BND
  PF=ABS(PD-INT(PD))
  IF(YMIN) 2,1,1
  1 AMIN=YMIN-PF*BND
  GO TO 33
  2 AMIN=YMIN-(1.0-PF)*BND
  33 AHLD=AZ
  35 SM=AMAX1(ABS(YMIN),ABS(YMAX))
  NS=0
  40 NS=NS+1
  SM=1.0*SM
  IF(SM-1.0) 40,50,45
  45 NS=NS-1
  SM=SM/10.0
  IF(SM-1.0) 50,50,45
  50 AHLD=BND/2.0
  55 PRINT 70
  PRINT 6,T

```

```

MET00610
MET00620
MET00630
MET00640
MET00650
MET00660
MET00670
MET00680
MET00690
MET00700
MET00710
MET00720
MET00730
MET00740
MET00750
MET00760
MET00770
MET00780
MET00790
MET00800
MET00810
MET00820
MET00830
MET00840
MET00850
MET00860
MET00870
MET00880
MET00890
MET00900
MET00910
MET00920
MET00930
MET00940
MET00950
MET00960
MET00970
MET00980
MET00990
MET01000
MET01010
MET01020
MET01030
MET01040
MET01050
MET01060

```





```

6  FORMAT(5X,2A4,/)
   PRINT 57,AHLD,BZ
57  FORMAT(1H0,65H THE FOLLOWING TRANSFORMATION WAS PERFORMED ON THE INPUT MATRIX /5X,1H,E12.5,8H*(I,J)+,E12.5,1H) //2X,73HAND THREE DIGITS TO THE RIGHT OF THE DECIMAL POINT ARE PRINTED IN THE MAP
   PRINT 54,YMAX,YMIN
54  FORMAT(/4X,5HYMAX=,E15.7,5X,5HYMIN=,E15.7)
   IF (ICON)5,58,5
5  PRINT 11,BND
11  FORMAT(2X,17H THE BAND WIDTH IS,E12.5,6H UNITS //4X,14H CONTOUR LEVELS
   I=0
   YTOP=AMIN
   IF (ABS(YMIN-YMAX)-100.0*BND)53,53,58
53  YB=YTOP
   YTOP=YTOP+BND
   I=I+1
   J=MOD(I,20)
   ITJZ=1H(J)
   IF (YB-YMAX)59,58,58
59  PRINT 61,YB,YTOP,ITJZ
61  FORMAT(/4X,E10.3,4H TO ,E10.3,2H =,1X,A1)
   GO TO 53
58  NCCP=0
   NCP=0
60  PRINT 70
70  FORMAT(1H1)
   PRINT 6,T
   NLINE=0
   NCCP=NCP+1
   NCP=NCP+13
73  IF (NCP-M)80,80,75
75  NCP=M
80  CONTINUE
   J=-2
   NLINE=NLINE+1
   LLINE=NLINE+1
   UP HEADING
   IF (NCCP-1) 85,85,90
85  J=-1
90  DO 100 I = 1,135
   A(I)=BLK
   B(I)=BLK
   H(I)=BLK
100 CONTINUE
110 DO 160 L=NCCP,NCP
   J = J+8

```



MET01550  
 MET01560  
 MET01570  
 MET01580  
 MET01590  
 MET01600  
 MET01610  
 MET01620  
 MET01630  
 MET01640  
 MET01650  
 MET01660  
 MET01670  
 MET01680  
 MET01690  
 MET01700  
 MET01710  
 MET01720  
 MET01730  
 MET01740  
 MET01750  
 MET01760  
 MET01770  
 MET01780  
 MET01790  
 MET01800  
 MET01810  
 MET01820  
 MET01830  
 MET01840  
 MET01850  
 MET01860  
 MET01870  
 MET01880  
 MET01890  
 MET01900  
 MET01910  
 MET01920  
 MET01930  
 MET01940  
 MET01950  
 MET01960  
 MET01970  
 MET01980  
 MET01990  
 MET02000  
 MET02010  
 MET02020

```

    KI=L
    IF(KI-100) 130,120,120
    120 LL=KI/100
        A(J)=KG(LL+1)
        KI=KI-100*LL
        GO TO 135
    130 A(J)=KG(1)
    135 J=J+1
    140 IF(KI-10) 150,140,140
        LL=KI/10
        A(J)=KG(LL+1)
        KI=KI-10*LL
        GO TO 155
    150 A(J)=KG(1)
    155 J=J+1
        A(J)=KG(KI+1)
    160 CONTINUE
    C SETUP FIRST ROW OF ARRAY
    170 GO TO 260 NE+1
        NLINE=N-NLINE+1
        IF(NLINE-N) 180,180,380
    180 DO 190 I=1,135
        A(I)=BLK
        B(I)=BLK
        C(I)=BLK
        D(I)=BLK
        E(I)=BLK
        F(I)=BLK
        G(I)=BLK
        H(I)=BLK
    190 CONTINUE
    195 IF (ICON) 195,260,195
        NCY=NCCP-1
        J=4
        IF(NCY) 200,200,210
        J=5
    200 NCY=NCY+1
    210 IF(NCY-NCP) 220,220,260
    220 IF(NCY-M) 230,260,260
    230 NLINE = NLINE - 1
        YDI = Y(NLINE,NCY) - Y(NLINE+1,NCY)
        YD2=Y(NLINE,NCY+1)-Y(NLINE+1,NCY+1)
        TP(1) = Y(NLINE,NCY)-0.125*YDI
        TPM(1)=Y(NLINE,NCY)-0.250*YDI
        XMT(1)=Y(NLINE,NCY)-0.375*YDI
        BT4(1)=Y(NLINE,NCY)-0.500*YDI
  
```



MET02030  
 MET02040  
 MET02050  
 MET02060  
 MET02070  
 MET02080  
 MET02090  
 MET02100  
 MET02110  
 MET02120  
 MET02130  
 MET02140  
 MET02150  
 MET02160  
 MET02170  
 MET02180  
 MET02190  
 MET02200  
 MET02210  
 MET02220  
 MET02230  
 MET02240  
 MET02250  
 MET02260  
 MET02270  
 MET02280  
 MET02290  
 MET02300  
 MET02310  
 MET02320  
 MET02330  
 MET02340  
 MET02350  
 MET02360  
 MET02370  
 MET02380  
 MET02390  
 MET02400  
 MET02410  
 MET02420  
 MET02430  
 MET02440  
 MET02450  
 MET02460  
 MET02470  
 MET02480  
 MET02490  
 MET02500

BTX(1)=Y(NLINE,NCY)-0.750\*YD1  
 BT(1)=Y(NLINE,NCY)-0.875\*YD1  
 TPX(10)=Y(NLINE,NCY+1)-0.125\*YD2  
 TPM(10)=Y(NLINE,NCY+1)-0.250\*YD2  
 XMT(10)=Y(NLINE,NCY+1)-0.375\*YD2  
 BTM(10)=Y(NLINE,NCY+1)-0.500\*YD2  
 BTX(10)=Y(NLINE,NCY+1)-0.625\*YD2  
 BT(10)=Y(NLINE,NCY+1)-0.750\*YD2  
 NLINE = NLINE + 1  
 D1=0.1 \* {TP(10)-TP(1)}  
 D2=0.1 \* {TPX(10)-TPX(1)}  
 D3=0.1 \* {TPM(10)-TPM(1)}  
 D4=0.1 \* {XMT(10)-XMT(1)}  
 D5=0.1 \* {BTM(10)-BTM(1)}  
 D6=0.1 \* {BTX(10)-BTX(1)}  
 D7=0.1 \* {BT(10)-BT(1)}  
 D0 240 I = 2,9  
 TP(1)=TP(I-1)+D1  
 TPX(1)=TPX(I-1)+D2  
 TPM(1)=TPM(I-1)+D3  
 XMT(1)=XMT(I-1)+D4  
 BTM(1)=BTM(I-1)+D5  
 BTX(1)=BTX(I-1)+D6  
 BT(1)=BT(I-1)+D7  
 CONTINUE  
 240 DO 250 I=1,10  
 J=J+1  
 I1=MOD(IFIX(TP(I)-AMIN)/BND),20)+1  
 I2=MOD(IFIX(TPX(I)-AMIN)/BND),20)+1  
 I3=MOD(IFIX(TPM(I)-AMIN)/BND),20)+1  
 I4=MOD(IFIX(XMT(I)-AMIN)/BND),20)+1  
 I5=MOD(IFIX(BTM(I)-AMIN)/BND),20)+1  
 I6=MOD(IFIX(BTX(I)-AMIN)/BND),20)+1  
 I7=MOD(IFIX(BT(I)-AMIN)/BND),20)+1  
 A(J)=IH(I1)  
 B(J)=IH(I2)  
 C(J)=IH(I3)  
 D(J)=IH(I4)  
 E(J)=IH(I5)  
 F(J)=IH(I6)  
 G(J)=IH(I7)  
 CONTINUE  
 250 GO TO 210  
 260 NCV=NCCP-1  
 J=-2  
 IF(NCY) 265,265,270  
 265 J=-1



```

270 GO TO 330
    NCY=NCY+1
    IF(NCY-NCP) 280,280,310
280 J=J+7
    THLD=AHLD*Y(INLINE,NCY)+BZ
    IF(THLD) 285,290,290
285 H(J)=EMI
    GO TO 295
290 H(J)=EPL
290 NUM=INT(ABS(THLD-INT(THLD))*1000.0+0.5)
295 NDS=100
    DO 300 KK=1,3
        J=J+1
        KI=NUM/NDS
        H(J)=KG(KI+1)
        NUM=NUM-KI*NDS
        NDS=NDS/10
300 CONTINUE
    GO TO 270
310 IF(NCP-M) 360,320,320
320 IF(J-127) 330,330,360
330 J=J+3
    KI=NLIN
    IF(KI-100) 340,335,335
335 LL=KI/100
    H(J)=KG(LL+1)
    KI=KI-100*LL
    GO TO 343
340 H(J)=KG(1)
343 J=J+1
    IF(KI-10) 350,345,345
345 LL=KI/10
    H(J)=KG(LL+1)
    KI=KI-10*LL
    GO TO 355
350 H(J)=KG(1)
355 J=J+1
    H(J)=KG(KI+1)
    J=J-5
360 IF(NCY-1) 270,270,360
362 IF(NLINE-1) 362,362,368
362 GO TO 370, (A(I), I=1,132), (8(IP1), IP1=1,132), (H(IP2), IP2=1,132)
368 PRINT 370, (A(I), I=1,132), (8(IP1), IP1=1,132), (C(IP2), IP2=1,132),
    1(D(IP3), IP3=1,132), (E(IP4), IP4=1,132), (F(IP5), IP5=1,132),
    2(G(IP6), IP6=1,132), (H(IP7), IP7=1,132)
370 FORMAT(132A1)
    GO TO 170

```

```

MET02510
MET02520
MET02530
MET02540
MET02550
MET02560
MET02570
MET02580
MET02590
MET02600
MET02610
MET02620
MET02630
MET02640
MET02650
MET02660
MET02670
MET02680
MET02690
MET02700
MET02710
MET02720
MET02730
MET02740
MET02750
MET02760
MET02770
MET02780
MET02790
MET02800
MET02810
MET02820
MET02830
MET02840
MET02850
MET02860
MET02870
MET02880
MET02890
MET02900
MET02910
MET02920
MET02930
MET02940
MET02950
MET02960
MET02970
MET02980
MET02990

```





```

380 DO 390 I=1,135
    A(I)=BLK
    B(I)=BLK
    C(I)=BLK
    D(I)=BLK
    CONTINUE
    J=-2
395 IF(NCCP-1) 395,395,400
400 J=-1
    DO 430 L=NCCP,NCP
        J=J+8
        KI=L
        IF(KI-100) 410,405,405
        LL=KI/100
        C(J)=KG(LL+1)
        KI=KI-100*LL
        GO TO 412
        C(J)=KG(I)
410 J=J+1
412 IF(KI-10) 420,415,415
415 LL=KI/10
        C(J)=KG(LL+1)
        KI=KI-10*LL
        GO TO 422
420 C(J)=KG(I)
422 J=J+1
430 C(J)=KG(KI+1)
        CONTINUE
        PRINT 370, (B(IP1),IP1=1,132),(C(IP2),IP2=1,132)
        IF(NCP-M)60,500,500
500 RETURN
    END

```

C000021

```

.....
SUBROUTINE GAUSS
PURPOSE
  COMPUTES A NORMALLY DISTRIBUTED RANDOM NUMBER WITH A GIVEN
  MEAN AND STANDARD DEVIATION
USAGE
  CALL GAUSS(IX,S,AM,V)
DESCRIPTION OF PARAMETERS
10 GAUS
20 GAUS
30 GAUS
40 GAUS
50 GAUS
60 GAUS
70 GAUS
80 GAUS
90 GAUS
100 GAUS
110 GAUS
120 GAUS
130 GAUS

```

MET02990  
 MET03000  
 MET03010  
 MET03020  
 MET03030  
 MET03040  
 MET03050  
 MET03060  
 MET03070  
 MET03080  
 MET03090  
 MET03100  
 MET03110  
 MET03120  
 MET03130  
 MET03140  
 MET03150  
 MET03160  
 MET03170  
 MET03180  
 MET03200  
 MET03210  
 MET03220  
 MET03230  
 MET03240  
 MET03250  
 MET03260  
 MET03270  
 MET03280  
 MET03290  
 MET03300







# AND PRODUCES A NEW INTEGER AND REAL RANDOM NUMBER.

## USAGE

CALL RANDU(IX,IY,YFL)

## DESCRIPTION OF PARAMETERS

IX - FOR THE FIRST ENTRY THIS MUST CONTAIN ANY ODD INTEGER NUMBER WITH NINE OR LESS DIGITS. AFTER THE FIRST ENTRY IX SHOULD BE THE PREVIOUS VALUE OF IY COMPUTED BY THIS SUBROUTINE.

ROUTINE - A RESULTANT INTEGER RANDOM NUMBER REQUIRED FOR THE NEXT ENTRY TO THIS SUBROUTINE. THE RANGE OF THIS NUMBER IS BETWEEN ZERO AND 2\*\*31

THE RESULTANT UNIFORMLY DISTRIBUTED, FLOATING POINT, RANDOM NUMBER IN THE RANGE 0 TO 1.0

REMARKS

THIS SUBROUTINE IS SPECIFIC TO SYSTEM/360 AND WILL PRODUCE  
TERMS BEFORE REPEATING. THE REFERENCE BELOW DISCUSSES  
22-29 (65539 HERE), RUN PROBLEMS, AND PROBLEMS CONCERNING  
RANDOM DIGITS USING THIS GENERATION SCHEME. MACLAREN AND  
MARSAGLIA, JACM 12, P. 83-89, DISCUSS CONGRUENTIAL  
GENERATION METHODS AND TESTS. THE USE OF TWO GENERATORS OF  
THE RANDU TYPE, ONE FILLING A TABLE AND ONE PICKING FROM THE  
TABLE, IS OF BENEFIT IN SOME CASES. 65549 HAS BEEN PROPERTIES  
SUGGESTED AS A SEED WHICH HAS BETTER STATISTICAL PROPERTIES  
FOR HIGH ORDER BITS OF THE GENERATED DEViate.  
SEEDS SHOULD BE CHOSEN IN ACCORDANCE WITH THE DISCUSSION  
GIVEN IN THE REFERENCE BELOW. ALSO, IT SHOULD BE NOTED THAT  
IF FLOATING POINT RANDOM NUMBERS ARE DESIRED, AS ARE  
AVAILABLE FROM RANDU, THE RANDOM CHARACTERISTICS OF THE  
FLOATING POINT DEViates ARE MODIFIED AND IN FACT THESE  
DEViates HAVE HIGH PROBABILITY OF HAVING A TRAILING LOW  
ORDER ZERO BIT IN THEIR FRACTIONAL PART.

## SUBROUTINES AND FUNCTION SUBPROGRAMS REQUIRED

NON

## METHOD

MOD POWER RESIDUE METHOD DISCUSSED IN IBM MANUAL C20-8011,  
RANDOM NUMBER GENERATION AND TESTING

```

AND PRODUCES A NEW INTEGER AND REAL RANDOM NUMBER.
USAGE
  CALL RANDU(IX,IY,YFL)
DESCRIPTION OF PARAMETERS
  IX - FOR THE FIRST ENTRY THIS MUST CONTAIN ANY ODD INTEGER
      NUMBER WITH NINE OR LESS DIGITS. AFTER THE FIRST ENTRY,
      IX SHOULD BE THE PREVIOUS VALUE OF IY COMPUTED BY THIS
      SUBROUTINE.
  IY - A RESULTANT INTEGER RANDOM NUMBER REQUIRED FOR THE NEXT
      ENTRY TO THIS SUBROUTINE. THE RANGE OF THIS NUMBER IS
      BETWEEN ZERO AND 2**31-1.
  YFL- THE RESULTANT UNIFORMLY DISTRIBUTED, FLOATING POINT,
      RANDOM NUMBER IN THE RANGE 0 TO 1.0
REMARKS
  THIS SUBROUTINE IS SPECIFIC TO SYSTEM/360 AND WILL PRODUCE
  2**29 TERMS BEFORE REPEATING. THE REFERENCE BELOW DISCUSSES
  SEEDS (65539 HERE), RUN PROBLEMS, AND PROBLEMS CONCERNING
  RANDOM DIGITS USING THIS GENERATION SCHEME. MACLAREN AND
  MARSAGLIA, JACM 12, P. 83-89, DISCUSS CONGRUENTIAL
  GENERATION METHODS AND TESTS. THE USE OF TWO GENERATORS OF
  THE RANDU TYPE, ONE FILLING A TABLE AND ONE PICKING FROM
  THE RANDU TYPE, ONE FILLING A TABLE, 65549 HAS BEEN
  SUGGESTED AS A SEED WHICH HAS BETTER STATISTICAL PROPERTIES
  FOR HIGH ORDER BITS OF THE GENERATED DEViate.
  SEEDS SHOULD BE CHOSEN IN ACCORDANCE WITH THE DISCUSSION
  GIVEN IN THE REFERENCE BELOW. ALSO, IT SHOULD BE NOTED THAT
  IF FLOATING POINT RANDOM NUMBERS ARE DESIRED, AS ARE
  AVAILABLE FROM RANDU, THE RANDOM CHARACTERISTICS OF THE
  FLOATING POINT DEViates ARE MODIFIED AND IN FACT THESE
  DEViates HAVE HIGH PROBABILITY OF HAVING A TRAILING LOW
  ORDER ZERO BIT IN THEIR FRACTIONAL PART.
SUBROUTINES AND FUNCTION SUBPROGRAMS REQUIRED
  NONE
METHOD
  POWER RESIDUE METHOD DISCUSSED IN IBM MANUAL C20-8011,
  RANDOM NUMBER GENERATION AND TESTING
.....

```

[illegible]



```

SUBROUTINE RANDU(IX,IY,YFL)
  IY=IX*65539
  IF(IY)5,8,9
5  IY=IY+2147483647+1
6  YFL=IY
  YFL=YFL*.4656613E-9
  RETURN
END

```

```

RAND 540
RAND 550
RAND 560
RAND 570
RAND 580
RAND 590
RAND 600

```









```

1  READ(5,10) U,V
   SU=(95*PIE)/180.
   Z=.95/TAN(SU/10)
   THETA=(29.677*PIE)/180.
   R2=Z*TAN(10*PIE)/180.
   R3=Z*TAN(SL)
   R1=Z*TAN(SU)
   R4=(1.0-R3)
   R5=(1.0-R2)
   R6=(1.0+R1)
   R7=(1.0+R1)
   DELR1=(R1-R2)/10.
   DELR2=(R3-R2)/10.
   DELR3=(1.0-R1)/25.
   DELR4=(1.0-R3)/25.
   DELR5=R2/12.5
   RHO(1)=0.
   READ(5,30) (RHO(I),I=2,14)
   READ(5,30) (RHO(I),I=15,27)
   RHO(28)=0.
   AX(1)=0.
   DO 2 I=2,26
     AX(I)=AX(I-1)+DELR4
     X(I)=0.
   X(2)=AX(26)
   DO 3 I=27,35
     AX(I)=AX(I-1)+DELR2
     J=I-24
   X(J)=AX(I)
   AX(36)=AX(35)+DELR2/2.
   X(12)=AX(36)
   DO 3 I=37,38
     AX(I)=AX(I-1)+DELR2/4.
     J=I-24
   X(J)=AX(I)
   DO 4 I=39,63
     AX(I)=AX(I-1)+DELR5
   X(15)=AX(63)
   DO 5 I=64,65
     AX(I)=AX(I-1)+DELR1/4.
     J=I-48
   X(J)=AX(I)
   AX(66)=AX(65)+DELR1/2.
   X(18)=AX(66)
   DO 32 I=67,75
     AX(I)=AX(I-1)+DELR1
     J=I-48

```



```

32 X(J)=AX(I)
X(28)=2.0
DO 6 I=1,28
6 CALL LSQPL2(28,-10,X,RHO,WI,RHOP,DELY,B,SB,TITLE)
WRITE(6,50)
50 FORMAT(///,LSQPL2 RETURNS)
10 FORMAT(2F10.7)
30 FORMAT(10F8.5/,3F8.5)
A1=B(1)
A2=B(2)
A3=B(3)
A4=B(4)
A5=B(5)
A6=B(6)
A7=B(7)
A8=B(8)
A9=B(9)
A10=B(10)
A11=B(11)
ARHO(1)=0.
DELY=2./200.
XP(1)=0.
DO 7 I=2,201
7 XP(I)=XP(I-1)+DELY
IF(XP(I).LT.R4) GO TO 9
IF(XP(I).GT.R7) GO TO 9
FORMAT(///,COMPUTING ARHO(I))
ARHO(I)=Y(A1,A2,A3,A4,A5,A6,A7,A8,A9,A10,A11,XP(I))
GO TO 7
9 ARHO(I)=0.
CONTINUE
WRITE(6,41)
41 X(I),RHO(I),I=1,28)
WRITE(6,40)
40 I,XP(I),ARHO(I),I=1,201)
WRITE(7,42)
42 (ARHO(I),I=1,201)
WRITE(7,43)
43 IF(W.EQ.1.) GO TO 1
FORMAT(//,XXXXXXXXXXXXXXXXXXXXXXXXXXXXXXXXXXXXXXXXXXXX)
60 FORMAT(F5.3)
39 FORMAT(//,//)
42 FORMAT(F8.5)
49 FORMAT(//,5X,I',10X,I',10X,XP(I)',10X,ARHO(I)',//)
40 FORMAT(5X,13,10X,F10.5,10X,F10.5)
41 FORMAT(//,5X,I',10X,I',10X,XP(I)',10X,ARHO(I)',//)
STOP

```









# COMPUTER PROGRAM 2

THIS COMPUTER PROGRAM IS DESIGNED TO INTERPOLATE THE DENSITY VALUES GIVEN IN AGARD 167 FOR MACH NUMBERS BETWEEN 2.5 AND 3.0. INTERPOLATION IS DONE BY CALLING ON SUBROUTINE LSQPL2 OF THE IBM SUBROUTINE PACKAGE TO PASS A CUBIC CURVE THROUGH THE FOUR INPUT VALUES OF DENSITY AT MACH NUMBERS 1.5, 2.0, 3.0 AND 4.0. THE VALUES OF THE DENSITY FOR MACH NUMBERS FROM 2.5 TO 3.0 IN INCREMENTS OF  $M=0.01$  ARE THEN EVALUATED AND PRINTED FOR EACH SET OF INPUT DATA VALUES.

## INPUT DATA...

EACH CARD HAS 4 DENSITY VALUES CORRESPONDING TO THE VALUES AT  $M=1.5, 2.0, 3.0$  AND  $4.0$  IN THAT ORDER, ACCORDING TO FORMAT 10. FOR EACH VALUE OF  $\phi$ , THERE ARE 14 SUCH CARDS, THE LAST ONE BEING THAT OF THE SHOCK ANGLE. CARDS ARE INPUT IN THE ORDER OF INCREASING  $\phi$ ,  $\phi$ , FOR EACH  $\phi$ , AND IN THE ORDER OF INCREASING  $\phi$ .

```
// EXEC, FORT, CLGP, TIME, GO=5, REGION, GO=100K
```

```
// FORT, SYSDIN, DD
```

```
10 DIMENSION AM(4), RO(4), WI(10), AROP(10), DELY(10), B(10), SB(10),
```

```
LAAM(50), ROP(50), PHI(10)
```

```
REAL*8 TITLE(10)/100, //
```

```
REAL*8 A1, A2, A3, A4, WI, AROP, DELY, SB, AAM, ROP, T, A1, A2, A3, A4
```

```
CALL ERRSET(209, 256, -1, 1, 0, 203)
```

```
PHI(1)=0
```

```
DELPHI=22.5
```

```
DO 2 K=1, 30
```

```
WRITE(6, 30) PHI(K)
```

```
FORMAT(//, //, 1X, PHI=, F10.5, //)
```

```
PHI(K+1)=PHI(K)+DELPHI
```

```
AXI=C
```

```
DELXI=C
```

```
AM(1)=1.5
```

```
AM(2)=2.0
```

```
AM(3)=3.0
```

```
AM(4)=4.0
```

```
DO 2 I=1, 14
```

```
READ(5, 10) (RO(M), M=1, 4)
```

```
FORMAT(4F10.5)
```

30

10



```

40 WRITE(6,40) AXI
   FORMAT(//,1X,'XI=',F10.5,///)
   AXI=AXI+DELXI
   DO 3 L=1,10
     WI(L)=1.000
     WRITE(6,10) (RO(II),II=1,4)
     WRITE(6,10) (AM(II),II=1,4)
     WRITE(6,10) (WI(II),II=1,10)
   CALL LSQPL2(4,-3,AM,RO,WI,AROP,DELY,B,SB,TITLE)
   A1=B(1)
   A2=B(2)
   A3=B(3)
   A4=B(4)
50 WRITE(6,50)
   FORMAT(//,3X,'MACH NO.',5X,'DENSITY',///)
   DLM=.01
   DO 2 J=1,50
     ROP(J)=FUN(A1,A2,A3,A4,AAM(J))
     WRITE(6,20) AAM(J),ROP(J)
     FORMAT(1X,F15.7,10X,F15.7)
     AAM(J+1)=AAM(J)+DLM
     CONTINUE
   STOP
   END

C C A TYPICAL DATA DECK .....
//GO,SYSIN DD SPACE=(CYL,(10,2))
1 0.0522 1.0490 2.6869 3.3792
1 0.0522 1.0479 2.6866 3.3790
1 0.0522 1.0437 2.6859 3.3784
1 0.0522 1.0437 2.6830 3.3760
1 0.0522 1.0437 2.6726 3.3669
1 0.0522 1.0437 2.6567 3.3533
1 0.0522 1.0437 2.6363 3.3332
1 0.0522 1.0437 2.6118 3.3094
1 0.0522 1.0437 2.5836 3.2813
1 0.0522 1.0437 2.5519 3.2491
1 0.0522 1.0437 2.5166 3.2171
1 0.0522 1.0437 2.4774 3.1852
1 0.0522 1.0437 2.4338 3.1536
1 0.0522 1.0437 2.3877 3.1229
1 0.0522 1.0437 2.3433 3.0923
1 0.0522 1.0437 2.2996 3.0617
1 0.0522 1.0437 2.2567 3.0311
1 0.0522 1.0437 2.2144 3.0006
1 0.0522 1.0437 2.1727 2.9700
1 0.0522 1.0437 2.1311 2.9394
1 0.0522 1.0437 2.0894 2.9088
1 0.0522 1.0437 2.0477 2.8782
1 0.0522 1.0437 2.0060 2.8476
1 0.0522 1.0437 1.9643 2.8170
1 0.0522 1.0437 1.9226 2.7864
1 0.0522 1.0437 1.8809 2.7558
1 0.0522 1.0437 1.8392 2.7252
1 0.0522 1.0437 1.7975 2.6946
1 0.0522 1.0437 1.7558 2.6640
1 0.0522 1.0437 1.7141 2.6334
1 0.0522 1.0437 1.6724 2.6028
1 0.0522 1.0437 1.6307 2.5722
1 0.0522 1.0437 1.5890 2.5416
1 0.0522 1.0437 1.5473 2.5110
1 0.0522 1.0437 1.5056 2.4804
1 0.0522 1.0437 1.4639 2.4498
1 0.0522 1.0437 1.4222 2.4192
1 0.0522 1.0437 1.3805 2.3886
1 0.0522 1.0437 1.3388 2.3580
1 0.0522 1.0437 1.2971 2.3274
1 0.0522 1.0437 1.2554 2.2968
1 0.0522 1.0437 1.2137 2.2662
1 0.0522 1.0437 1.1720 2.2356
1 0.0522 1.0437 1.1303 2.2050
1 0.0522 1.0437 1.0886 2.1744
1 0.0522 1.0437 1.0469 2.1438
1 0.0522 1.0437 1.0052 2.1132
1 0.0522 1.0437 0.9635 2.0826
1 0.0522 1.0437 0.9218 2.0520
1 0.0522 1.0437 0.8801 2.0214
1 0.0522 1.0437 0.8384 1.9908
1 0.0522 1.0437 0.7967 1.9602
1 0.0522 1.0437 0.7550 1.9296
1 0.0522 1.0437 0.7133 1.8990
1 0.0522 1.0437 0.6716 1.8684
1 0.0522 1.0437 0.6299 1.8378
1 0.0522 1.0437 0.5882 1.8072
1 0.0522 1.0437 0.5465 1.7766
1 0.0522 1.0437 0.5048 1.7460
1 0.0522 1.0437 0.4631 1.7154
1 0.0522 1.0437 0.4214 1.6848
1 0.0522 1.0437 0.3797 1.6542
1 0.0522 1.0437 0.3380 1.6236
1 0.0522 1.0437 0.2963 1.5930
1 0.0522 1.0437 0.2546 1.5624
1 0.0522 1.0437 0.2129 1.5318
1 0.0522 1.0437 0.1712 1.5012
1 0.0522 1.0437 0.1295 1.4706
1 0.0522 1.0437 0.0878 1.4400
1 0.0522 1.0437 0.0461 1.4094
1 0.0522 1.0437 0.0044 1.3788
1 0.0522 1.0437 0.0000 1.3482
1 0.0522 1.0437 0.0000 1.3176
1 0.0522 1.0437 0.0000 1.2870
1 0.0522 1.0437 0.0000 1.2564
1 0.0522 1.0437 0.0000 1.2258
1 0.0522 1.0437 0.0000 1.1952
1 0.0522 1.0437 0.0000 1.1646
1 0.0522 1.0437 0.0000 1.1340
1 0.0522 1.0437 0.0000 1.1034
1 0.0522 1.0437 0.0000 1.0728
1 0.0522 1.0437 0.0000 1.0422
1 0.0522 1.0437 0.0000 1.0116
1 0.0522 1.0437 0.0000 0.9810
1 0.0522 1.0437 0.0000 0.9504
1 0.0522 1.0437 0.0000 0.9198
1 0.0522 1.0437 0.0000 0.8892
1 0.0522 1.0437 0.0000 0.8586
1 0.0522 1.0437 0.0000 0.8280
1 0.0522 1.0437 0.0000 0.7974
1 0.0522 1.0437 0.0000 0.7668
1 0.0522 1.0437 0.0000 0.7362
1 0.0522 1.0437 0.0000 0.7056
1 0.0522 1.0437 0.0000 0.6750
1 0.0522 1.0437 0.0000 0.6444
1 0.0522 1.0437 0.0000 0.6138
1 0.0522 1.0437 0.0000 0.5832
1 0.0522 1.0437 0.0000 0.5526
1 0.0522 1.0437 0.0000 0.5220
1 0.0522 1.0437 0.0000 0.4914
1 0.0522 1.0437 0.0000 0.4608
1 0.0522 1.0437 0.0000 0.4302
1 0.0522 1.0437 0.0000 0.3996
1 0.0522 1.0437 0.0000 0.3690
1 0.0522 1.0437 0.0000 0.3384
1 0.0522 1.0437 0.0000 0.3078
1 0.0522 1.0437 0.0000 0.2772
1 0.0522 1.0437 0.0000 0.2466
1 0.0522 1.0437 0.0000 0.2160
1 0.0522 1.0437 0.0000 0.1854
1 0.0522 1.0437 0.0000 0.1548
1 0.0522 1.0437 0.0000 0.1242
1 0.0522 1.0437 0.0000 0.0936
1 0.0522 1.0437 0.0000 0.0630
1 0.0522 1.0437 0.0000 0.0324
1 0.0522 1.0437 0.0000 0.0018
1 0.0522 1.0437 0.0000 0.0000

```



[illegible]













# BIBLIOGRAPHY

1. Heflinger, L. O., Wuerker, R. F., and Brooks, R. F., "Holographic Interferometry," Journal of Applied Physics, Vol. 37, No. 2, pp. 642-649, February 1966.
2. Brooks, R. E., Heflinger, L. O., and Wuerker, R. F., "9A9-Pulsed Laser Holograms," IEEE Journal of Quantum Electronics, Vol. EQ-2, No. 8, pp. 275-299, August 1966.
3. Matulka, R. D., "The Application of Holographic Interferometry to the Determination of Asymmetric Three-dimensional Density Fields in Free Jet Flow," PhD Thesis, Naval Postgraduate School, June 1970.
4. Maldonado, C. D., Caron, A. P., and Olsen, H. N., "New Method for Obtaining Emission Coefficients from Emitted Spectral Intensities. Part I - Circularly Symmetric Light Sources," Journal of the Optical Society of America, Vol. 55, No. 10, pp. 1247-1254, October 1965.
5. Maldonado, C. D., and Olsen, H. N., "New Method for Obtaining Emission Coefficients from Emitted Spectral Intensities. Part II - Asymmetric Sources," Journal of the Optical Society of America, Vol. 56, No. 10, pp. 1305-1312, October 1966.
6. Jones, D. J., "Tables of Inviscid Supersonic Flow About Circular Cones at Incidence, Part I and II," Advisory Group for Aerospace Research and Development, November 1969.
7. Liepmann, H. W., and Roshko, A., "Elements of Gas Dynamics," pp. 165, John Wiley and Sons, Inc., 1957.
8. Olsen, H. N., Maldonado, C. D., and Duckworth, G. D., "A Numerical Method for Obtaining Internal Emission Coefficients from Externally Measured Spectral Intensities of Asymmetric Plasmas," Journal of Quantum Spectroscopy and Radiation Transfer, Vol. 8, pp. 1419-1439, 1968.
9. Olsen, H. N., Maldonado, C. D., Duckworth, G. D., and Caron, A. P., "Investigation of the Interaction of an External Magnetic Field with an Electric Arc," Aerospace Research Laboratories Report ARL66-0016, January, 1966.



10. Sullivan, J. B., "An Investigation of Three-Dimensionality in Holographic Interferometry," Masters Thesis, Naval Postgraduate School, 1968.
11. Matulka, R. D., and Collins, D. J., "The Application of Holographic Interferometry to the Determination of Asymmetric Three-Dimensional Density Field in Free Jet Flow."
12. Taylor, G. I., and Maccoll, J. W., "The Air Pressure on a Cone Moving at High Speed," Proceedings of the Royal Society, London, Series A, Vol. 139, 1933.
13. Stone, A. H., "On Supersonic Flow Past a Slightly Yawing Cone," Journal of Mathematics and Physics, Vol. 27, 1948.
14. Staff of the Computing Section of Analysis (under the direction of Zdenek Kopal), "Tables of Supersonic Flow Around Cones," Technical Report No. 1, NORD Contract No. 9169, M.I.T., 1947.
15. Staff of the Computing Section, Centre of Analysis (under the direction of Zdenek Kopal), "Tables of Supersonic Flow Around Yawing Cones," Technical Report No. 3, NORD Contract No. 9169, M.I.T., 1949.
16. Staff of the Computing Section (under the direction of Zdenek Kopal), "Tables of Supersonic Flow Around Cones of Large Yaw," NORD Contract No. 8555 and 9169, M.I.T., 1949.
17. Jones, D. J., "Numerical Solutions of the Supersonic Flow Field for Conical Bodies in a Supersonic Stream," National Research Council of Canada National Aeronautical Establishment, Aeronautical Report LR-507, 1968.
18. Ladenburg, R., Van Voorhis, C. C., and Winckler, J., "Interferometric Study of Supersonic Phenomena - Part II," NAVORD Report 93-46, September, 1946.



# INITIAL DISTRIBUTION LIST

	No. Copies
1. Defense Documentation Center Cameron Station Alexandria, Virginia 22314	2
2. Library, Code 0212 Naval Postgraduate School Monterey, California 93940	2
3. Professor D. J. Collins Department of Aeronautics Naval Postgraduate School Monterey, California 93940	1
4. LCDR R. C. Jagota, I.N. Engineer Officer I.N.S. "Trishul" c/o Fleet Mail Office Bombay, India	1





UNCLASSIFIED

Security Classification

## DOCUMENT CONTROL DATA - R &amp; D

(Security classification of title, body of abstract and indexing annotation must be entered when the overall report is classified)

ORIGINATING ACTIVITY (Corporate author)

Naval Postgraduate School  
Monterey, California 93940

2a. REPORT SECURITY CLASSIFICATION

Unclassified

2b. GROUP

REPORT TITLE

THE APPLICATION OF HOLOGRAPHIC INTERFEROMETRY TO THE DETERMINATION  
OF THE FLOW FIELD AROUND A RIGHT CIRCULAR CONE AT ANGLE OF ATTACK

DESCRIPTIVE NOTES (Type of report and, inclusive dates)

Aeronautical Engineer's Thesis

AUTHOR(S) (First name, middle initial, last name)

Ravi Chandar Jagota, Lieutenant Commander, Indian Navy

REPORT DATE

December 1970

7a. TOTAL NO. OF PAGES

150

7b. NO. OF REFS

18

8. CONTRACT OR GRANT NO.

9a. ORIGINATOR'S REPORT NUMBER(S)

9. PROJECT NO.

9b. OTHER REPORT NO(S) (Any other numbers that may be assigned  
this report)

10. DISTRIBUTION STATEMENT

This document has been approved for public release and sale;  
its distribution is unlimited.

11. SUPPLEMENTARY NOTES

12. SPONSORING MILITARY ACTIVITY

Naval Postgraduate School  
Monterey, California 93940

13. ABSTRACT

The successful application of holography to the study of three dimensional flow fields due to phase objects has been reported in the literature. The present report extends this technique to the study of density fields around opaque bodies as would normally be encountered in wind tunnel experiments. The density field around a 10 degree half-angle cone at zero and ten degree angle of attack has been investigated in the Naval Postgraduate School supersonic wind tunnel. In these experiments, the finite fringe method for the production of interferograms has, for the first time, been applied to holographic interferometry. The density field obtained from the reduction of the interferograms was found to agree with that obtained from an analytical solution of the governing equations as reported by D. J. Jones in Reference 1. The computer program used for the reduction of the interferograms has been evaluated for the effect of the presence of the cone and the shock wave and has been found to yield stable and accurate results.

DD FORM 1473  
1 NOV 65

(PAGE 1)

S/N 0101-807-6811

149

UNCLASSIFIED  
Security Classification

A-31408





### KEY WORDS

LINK A

LINK B

LINK C

ROLE

WT

ROLE

WT

ROLE

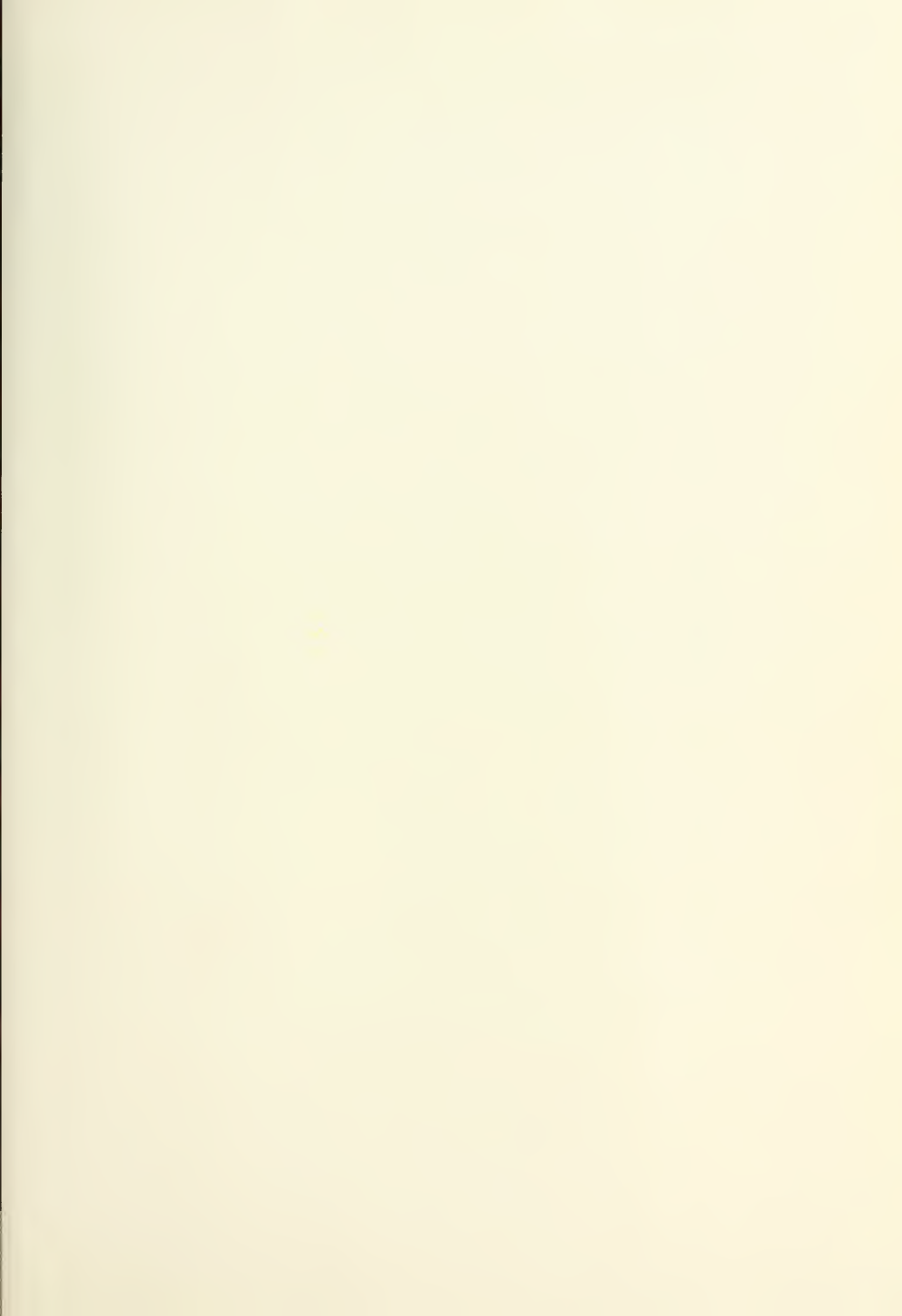
WT

## CONICAL FLOW













31 JUL 71

19944

SECRET 77

20223

Thesis

125861

J239

Jagota

c.1

The application of  
helographic inter-  
ferometry to the  
determination of the  
flow field around a  
right circular cone  
at angle of attack.

31 JUL 71

19944

SECRET 77

SECRET 77

SECRET 77

Thesis

125861

J239

Jagota

c.1

The application of  
helographic inter-  
ferometry to the  
determination of the  
flow field around a  
right circular cone  
at angle of attack.

thesJ239

The application of holographic interferem



3 2768 002 10002 6

DUDLEY KNOX LIBRARY